

INTENTIONALLY LEFT BLANK

CONTENTS

	Page
1. PURPOSE	7
2. METHOD	8
3. ASSUMPTIONS	9
4. USE OF COMPUTER SOFTWARE AND MODELS	11
4.1 SOFTWARE	11
4.1.1 MCNP	11
5. CALCULATION	12
5.1 WASTE PACKAGE COMPONENTS DESCRIPTION	12
5.1.1 TMI-2 Spent Nuclear Fuel	13
5.1.2 TMI-2 Fuel Canisters	14
5.1.3 Description of DOE SNF Canister	17
5.1.4 High-Level Waste Glass Pour Canister	19
5.1.5 Chemical Description of Borosilicate Glass	19
5.1.6 Waste Package Description	19
5.2 MATERIALS DESCRIPTION	21
5.3 FORMULAS	26
5.4 INTACT MODE CRITICALITY CALCULATIONS	27
5.4.1 Treatment of TMI Fuel and Canisters	27
5.4.2 TMI Fuel Pellet and Other Modeling Details	29
5.5 DEGRADED MODE	32
5.5.1 Components Degrades Within the Intact SNF Canister	34
5.5.2 Internal Components of the Waste Package Outside SNF Canister Degrade	35
5.5.3 All Components Have Degraded	40
6. RESULTS	41
6.1 INTACT MODE	42
6.1.1 Loose TMI Fuel Pellets in TMI Fuel Canisters and Other Modeling Details ...	42
6.2 DEGRADED MODE	54
6.2.1 Inner Components of the SNF Canister Degrade First	55
6.2.2 Outer Components of the Waste Package are Degraded (Outside SNF Canister)	58
6.2.3 TMI Fuel Surrounded by Post-breach Clay in the Waste Package	69
6.3 SUMMARY	70
7. REFERENCES	71
7.1 DOCUMENTS CITED	71
7.2 CODES, STANDARDS, REGULATIONS, AND PROCEDURES	72
7.3 SOURCE DATA	73
8. ATTACHMENTS	74

TABLES

	Page
Table 1. TMI Maximum Uranium Mass (both Total Uranium and U-235).	17
Table 2. Waste Package Dimensions ^a and Material Specifications.	20
Table 3. Composition and Density of Stainless Steel 304L.....	21
Table 4. Composition and Density of Savannah River Site High-Level Waste Glass	22
Table 5. Composition and Density of Stainless Steel 316L.....	23
Table 6. Composition and Density of Alloy 22	23
Table 7. Composition and Density of Carbon Steel 516 Grade 70.....	23
Table 8. Composition and Density of Dry Tuff.....	24
Table 9. Pre-Breach Clay Compositions ^{a,b}	24
Table 10. Post-Breach Clay Compositions	25
Table 11. Alternative Post-Breach Clay Composition.....	25
Table 12. Cylindrical TMI Fuel Pellets in the Knockout (KO) Canister.....	42
Table 13. Spherical TMI Fuel Pellets in the Knockout (KO) Canister ^a without Internals.....	45
Table 14. Spherical TMI Fuel Pellets in the Knockout (KO) Canister ^a with Internals.....	47
Table 15. Spherical TMI Fuel Pellets in Dry Knockout (KO) Canister ^a without Internals	49
Table 16. Variations of Cases with Spherical Fuel Pellets in the Knockout (KO) Canister.....	50
Table 17. Cylindrical TMI Fuel Pellets in the Fuel Canister (D-type).....	53
Table 18. Homogenized TMI Fuel in the Knockout (KO) Canister (without Internals)	54
Table 19. TMI Fuel Pellets in SNF Canister (Degraded Sleeve and KO Canister).....	56
Table 20. TMI Fuel Pellets in Intact SNF and TMI Canisters Surrounded by Pre-breach Clay	60
Table 21. TMI Fuel Pellets in Intact SNF Canister Surrounded by Dry Pre-breach Clay (Degraded TMI Canister and Sleeve).....	61
Table 22. TMI Fuel in Intact SNF Canister Containing Goethite Mixed with Water Surrounded by Dry Pre-breach Clay.....	63
Table 23. TMI Fuel in Intact KO Canister with Degraded SNF Canister Surrounded by Pre-breach Clay	65
Table 24. TMI Fuel Pellets Form Array Surrounded by Layers of Goethite and Pre-breach Clay in the Waste Package	66
Table 25. TMI Fuel Pellets are Surrounded with the Post-breach Clay	69
Table 26. Degraded TMI Fuel Mixed with Post-breach Clay	70

FIGURES

	Page
Figure 1. Typical Pressurized Water Reactor Fuel Assembly	14
Figure 2. Schematic Cross-section of Three Mile Island Unit 2 Canister Types.	15
Figure 3. Cross-sectional Schematic of the Fuel Canister (D-type) Inserted in an Outer Can.	16
Figure 4. DOE Spent Nuclear Fuel Standard Canister	18
Figure 5. Cross-sectional View of Typical Waste Package.....	21
Figure 6. Cross-sectional View of Knockout (KO) Canister at Different Elevations.	29
Figure 7. Pellet Array Partially Fills KO Canister's Cross-section.	30
Figure 8. Canisters Are in a Gravity Position in the waste package.....	31
Figure 9. Sleeve Is Collapsed in the SNF Canister.....	31
Figure 10. Cross-sectional View of the TMI Fuel Canister.....	32
Figure 11. Cross-sectional View of the SNF Canister.....	35
Figure 12. Cross-sectional View of an Intact SNF Canister Centered in Clay Formed from the Degradation of Components External to the Canister	36
Figure 13. Intact TMI Canister Surrounded by Goethite Trapped in Pre-breach Clay in the Waste Package.....	38
Figure 14. Fuel Pellets Surrounded by Goethite and Pre-breach Clay from Completely Degraded Components in the Waste Package	39
Figure 15. Similar Configuration as Shown in Figure 14 but Fewer Pellet Stacks in Fuel Array 40	

INTENTIONALLY LEFT BLANK

1. PURPOSE

The objective of these calculations is to perform intact and degraded mode criticality evaluations of the Department of Energy's (DOE) Three Mile Island – Unit 2 (TMI-2) spent nuclear fuel (SNF) in canisters. This analysis evaluates codisposal in a 5-Defense High-Level Waste (5-DHLW/DOE SNF) Long Waste Package (Civilian Radioactive Waste Management System Management and Operating Contractor [CRWMS M&O] 2000b, Attachment V), which is to be placed in a potential monitored geologic repository (MGR). The scope of this calculation is limited to the determination of the effective neutron multiplication factor (k_{eff}) for both intact and degraded mode internal configurations of the waste package.

These calculations will support the analysis that will be performed to demonstrate the technical viability for disposing of low-enriched spent nuclear fuel at yucca mountain. There are no limitations on the use of the results of this calculation.

This calculation is subject to the *Quality Assurance Requirements and Description* (DOE 2003a) as it addresses the codisposal viability of TMI-2 SNF at Yucca Mountain. This document is prepared in accordance with AP-3.12Q, *Design Calculations and Analyses*, and AP-3.15Q, *Managing Technical Product Inputs*.

2. METHOD

The method to perform the criticality calculations consists of using MCNP Version 4B2LV (CRWMS M&O 1998a, CRWMS M&O 1998b) to calculate the effective neutron multiplication factor of the waste package. The calculations are performed using the continuous-energy cross section libraries, which are part of the qualified code system MCNP 4B2LV (CRWMS M&O 1998a, CRWMS M&O 1998b). All calculations are performed with the most reactive fissile concentration that bounds the beginning-of-life (BOL) and end-of-life (EOL) TMI fuels.

3. ASSUMPTIONS

- 3.1 For the degraded mode criticality calculations, it is assumed that the iron in the stainless steel degrades to goethite (FeOOH) rather than hematite (Fe_2O_3). The basis of this assumption is that it is conservative to consider goethite rather than hematite since hydrogen (a moderator) is a component of goethite. All the other constituents of stainless steel are neglected since they are neutron absorbers, and hence their absence provides a conservative (higher) value for the k_{eff} of the system. This assumption is used throughout Section 5.
- 3.2 Ba-138 cross sections are used instead of Ba-137 cross sections in the MCNP input since the cross sections of Ba-137 are not available in the MCNP 4B2LV cross section libraries. The basis of this assumption is that it is conservative since the thermal neutron capture cross section and the resonance integral of Ba-137 (5.1 and 4 barn, respectively [Parrington et al. 1996, p. 34]) are greater than the thermal neutron capture cross section and the resonance integral of Ba-138 (0.43 and 0.3 barn, respectively [Parrington et al. 1996, p. 34]). This assumption is used throughout Section 5.
- 3.3 The most reactive fissile enrichment of 3 wt% is used for the TMI fuel to bound the enrichment of the most highly loaded fuel canister. This selected fuel enrichment (3 wt.%) is larger than the enrichments used in any intact fuel assembly. The basis of this assumption is that the selected enrichment is conservative since it maximizes the fissile isotope (U-235) content while minimizing the effect of neutron absorption (U-238). This assumption is used throughout Section 5.
- 3.4 Al cross sections are used instead of Zn cross sections in the MCNP input since the cross sections of Zn are not available in the MCNP 4B2LV cross-section libraries. The basis of this assumption is that it is conservative since the thermal neutron capture cross section and the resonance integral of Zn (Parrington et al., 1996, p. 24) are greater than the thermal neutron capture cross section and the resonance integral of Al (Parrington et al., 1996, p. 21). This assumption is used throughout Section 5.
- 3.5 Water is always assumed present and is assumed to fill void spaces in the fuel pellet arrays and canisters. The basis of this assumption is that it is conservative since this allows optimal moderation and therefore more reactive configurations. This assumption is used throughout Section 5.
- 3.6 An interim critical limit of 0.97 is assumed. The basis for this assumption is that once the criticality model has been validated for TMI-2 SNF, the critical limit is expected to be higher than 0.97. This value is used in determining whether the criticality concerns of any scenario are satisfied but is not used directly in the calculations. This assumption is used throughout Section 6.
- 3.7 The composition of the Hanford HLW glass is assumed to be the same as the Savannah River Site glass composition. The basis for this assumption is that the predicted composition of

Savannah River Site glass is known (CRWMS M&O 1999a, p. 7). This assumption is used throughout Section 5.

4. USE OF COMPUTER SOFTWARE AND MODELS

4.1 SOFTWARE

The commercial off-the-shelf software MS EXCEL Version 2000 SR-1 installed on a personal computer (PC) Dell Optiplex GX260 operating under Windows 2000 operating system, was used for performing arithmetical manipulations in a spreadsheet type environment. Microsoft EXCEL Version 2000 SR-1 is an exempt software application in accordance with LP-SI.11Q-BSC, Section 2.1.1. The developed spreadsheet files are included in Attachment I. The spreadsheets contain sufficient information to allow an independent check to reproduce or verify the results.

4.1.1 MCNP

The MCNP code is used to calculate the k_{eff} of the waste package. The software specifications are as follow:

- Program Name: MCNP
- Version/Revision Number: Version 4B2LV
- Status/Operating System: Qualified/HP-UX B.10.20
- Computer Software Configuration Item Number: 30033 V4B2LV
- Computer Type: Hewlett Packard (HP) 9000 Series Workstations
- Computer processing unit number: Software is installed on the INEEL workstation "bigdog" whose INEEL Tag number is 336829

The input and output files for the various MCNP calculations are included in Attachment I, (Attachment II gives the list of the files on Attachment I). The calculation files described in Sections 5 and 6 are such that an independent repetition of the software use may be performed.

The MCNP software used is: (a) appropriate for the application of research and commercial reactor k_{eff} calculations, (b) used only within the range of validation as documented in CRWMS M&O (1998a), (c) obtained from the Software Configuration Management in accordance with Administrative Procedure AP-SI.1Q, *Software Management*.

5. CALCULATION

This section describes the calculations performed to calculate the k_{eff} of an intact and a degraded waste package containing high-level waste material and TMI spent nuclear fuel. Section 5.1 describes the waste package and its contents. Section 5.2 gives the composition of the materials used in this calculation. The basic formulas used in this calculation are listed in Section 5.3. The different intact configurations of a waste package are outlined in Section 5.4. Section 5.5 describes calculations performed to characterize the degraded configurations of a waste package. The MCNP input and output files developed for this section are presented in Attachment I. The spreadsheet used to prepare the MCNP input files is given in Attachment I, file "tmi_calcs.xls." The results of the calculations are presented in Section 6.

The Savannah River Site high-level waste glass degraded (pre-breach clay) compositions are from CRWMS M&O (2000a) and BSC (2001a). The composition from CRWMS M&O (2000a) is for the Shippingport LWBR fuel. Since these fuels (Shippingport and TMI) share the same waste package externals, i.e., components external to the SNF canister, the pre-breach compositions would be the same. The Savannah River Site high-level waste glass composition and density are from CRWMS M&O (1999a) and Stout and Leider (1991), respectively. The Savannah River Site high-level waste glass canister dimensions are from Taylor (1997).

Avogadro's number is from Parrington et al. (1996). Atomic weights are from Parrington et al. (1996) and Audi and Wapstra (1995).

The description of the TMI fuel and canisters is from the *TMI Fuel Characteristics for Disposal Criticality Analysis* report (DOE 2003b). All fuel and canister-related information is from this reference unless otherwise noted.

The tuff composition and the tuff density are taken from a previous calculation (CRWMS M&O 2001, Attachment II, spreadsheet "Tuff Composition.xls").

This calculation is based in part on technical information given in DOE (2003b). The fuel group is identified by the National Spent Nuclear Fuel Program, and a 'representative' fuel type within that group is used to establish limits, e.g. burnup, fissile content, weights, dimensions.

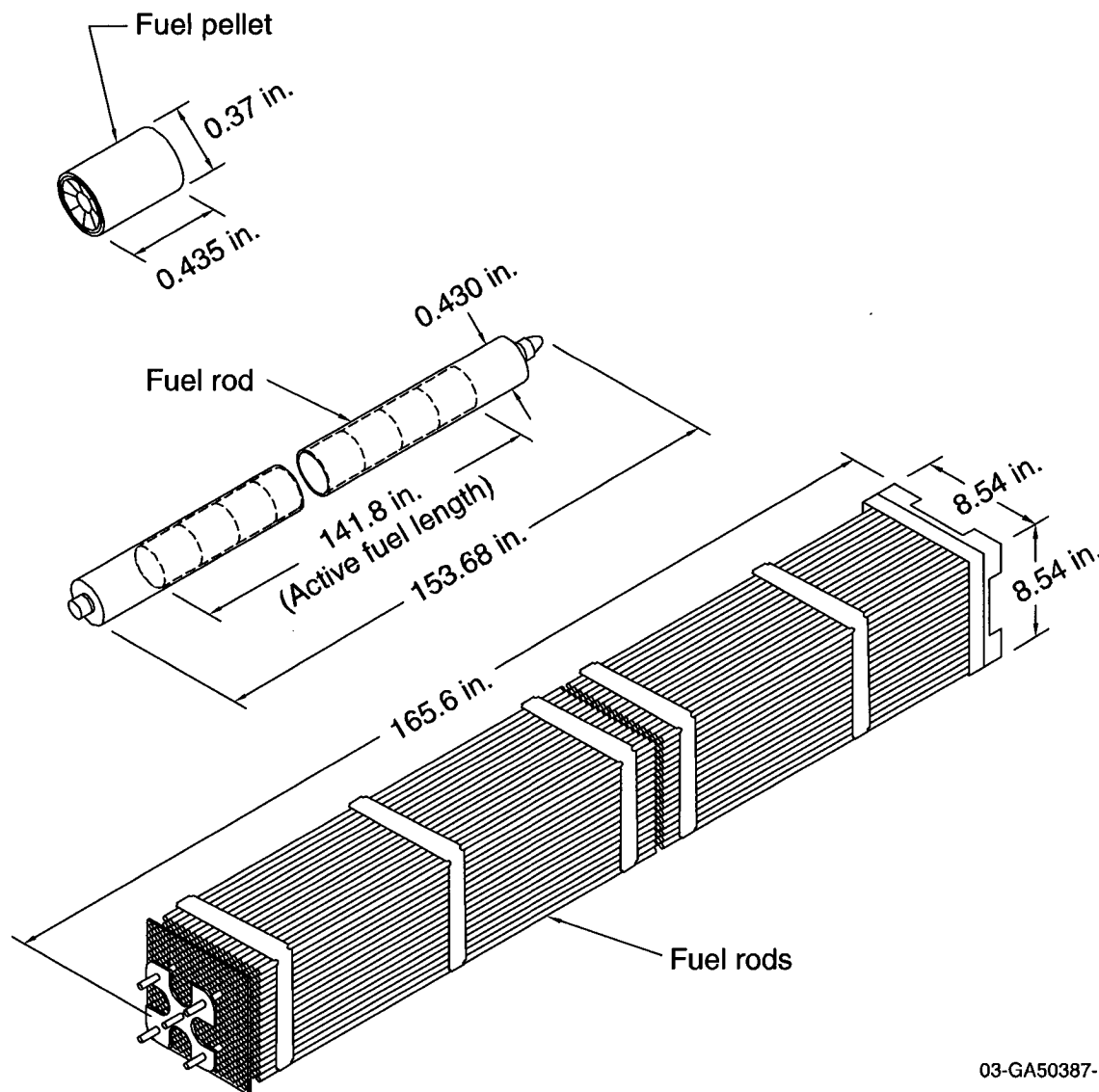
The number of digits in the values cited herein may be the result of a calculation or may reflect the input from another source; consequently, the number of digits should not be interpreted as an indication of accuracy.

The metric units used in this document are calculated using the English units as given in DOE (2003b). The differences that might exist between the metric units calculated and the metric units cited in DOE (2003b) have no effect on the calculation and should not be interpreted as an indication of accuracy.

5.1 WASTE PACKAGE COMPONENTS DESCRIPTION

5.1.1 TMI-2 Spent Nuclear Fuel

The typical fuel assembly used in the TMI-2 reactor was a Babcock & Wilcox 15 × 15-rod array inside a 216.81 mm (8.536 in.) square envelope (see Figure 1 for a depiction of a typical pressurized water reactor [PWR] assembly). Although this array gives a total count of 225 rods per assembly, the manufacturer specification indicates that typically only 208 of the rods are filled with uranium oxide pellets. While the total assembly is 4206.88 mm (165.625 in.) long, and the individual rod lengths are 3903.47 mm (153.68 in.), the active rod length is listed as 3601.72 mm (141.8 in.). The uranium oxide pellets stack constitutes the active rod length. The uranium fuel matrix is contained in pellets that are 9.398 mm (0.37 in.) in diameter and 11.049 mm (0.435 in.) long. If the active length is divided by this pellet length of 11.049 mm (0.435 in.), this gives almost 326 pellets per rod, which is reduced to 325 pellets to give a (conservative) slightly larger fissile mass per pellet. This gives a total number of $(208 \times 325 =)$ 67,600 pellets per assembly. The maximum beginning-of-life (BOL) U-235 content of 13.72 kg in any TMI-2 assembly provides the basis for the criticality analysis. The maximum enrichment of the uranium fuel is given as 2.96 wt%. Enrichments of 2.64 wt% and 1.98 wt% are reported for pellets in some of the PWR assemblies. The void fraction in the fuel matrix is given as 7.5%. (The terms "TMI-2" and "TMI" are used inter-changeably in this report.)



03-GA50387-13

Figure 1. Typical Pressurized Water Reactor Fuel Assembly

(overall dimensions may differ slightly based on manufacturer and are not necessarily those used in this analysis).

5.1.2 TMI-2 Fuel Canisters

The TMI-2 canisters were fabricated for use in recovery and cleanup of the reactor core after the TMI-2 accident. The design of the TMI-2 canisters is such that not more than a single commercial 15 × 15 Babcock & Wilcox PWR assembly could be installed in any one canister. The highest reported fissile loading in any TMI-2 canister is only 73.3% of a BOL fissile load for the most highly loaded PWR assembly. The defueling operations of the TMI-2 core used three types of canisters (see Figure 2), each with its own particular designation and numerical code.

The canisters with the “D” designator (defueling) were used to contain the bulk of core materials of a size that enabled grappling, could be picked up, or remotely handled. The “K” designator relates to the knockout (KO) canisters that were used in association with wet-vacuuming operations to remove loose debris that did not lend itself to physical grappling. There are only a total of 12 KO canisters, though one is reported to contain the highest total uranium loading of any TMI-2 canister. Subsequent and downstream collection of the vacuumed debris stream then passed through a filter canister with an “F” designator. These filter canisters represent the least heavily loaded for either total uranium or U-235 per package and, in several cases, are reported to have no reportable uranium. A schematic representation of each type TMI-2 canister is shown in Figure 2.

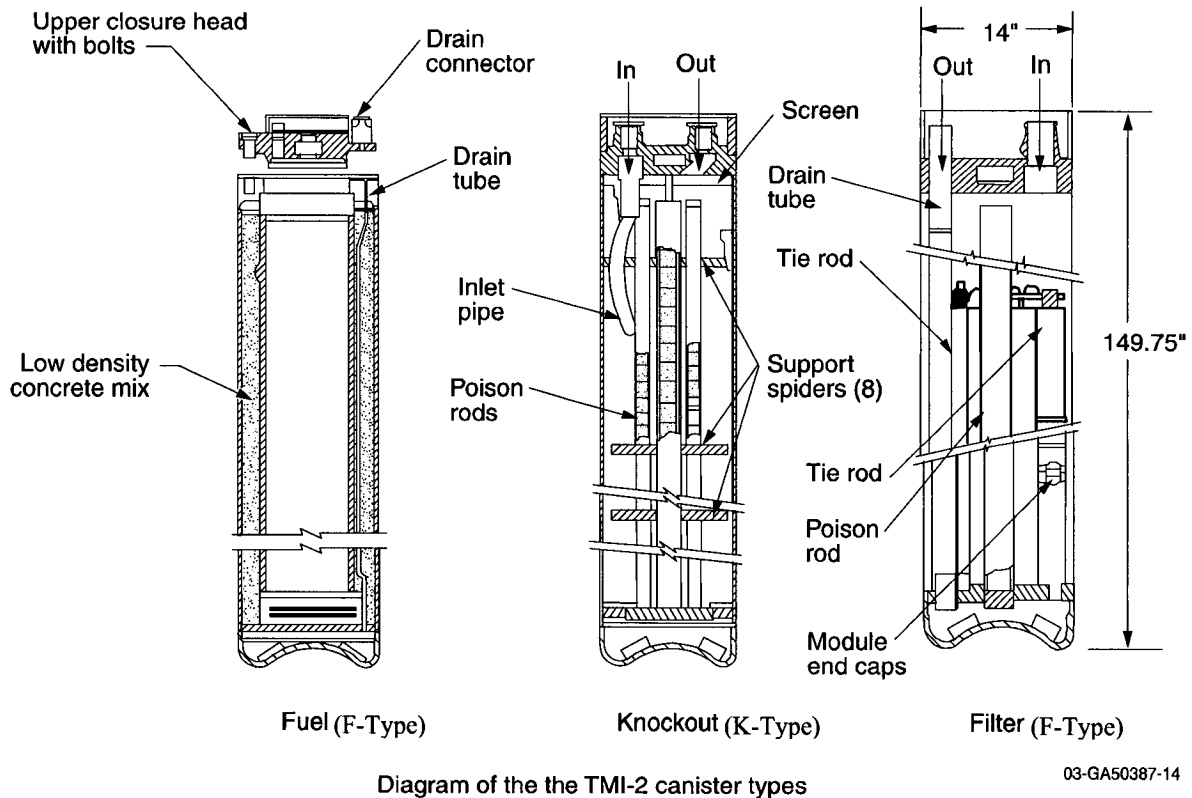


Figure 2. Schematic Cross-section of Three Mile Island Unit 2 Canister Types.

The basic structure of the TMI canister centers on a 14-in. Schedule 10 (0.25-in. wall thickness) pipe. The bottom of the canister is a reversed-dish head with a 0.375-in. thickness. The top of the canister is a 4-in.-thick metal plate with penetrations suitable for hydraulic loading and dewatering. All structural canister materials used Type 304L stainless steel for canister construction.

The D-type canisters, also referred to as “fuel canisters,” have a box structure located in the center of the canister that has internal dimensions of 231.78 mm (9.125 in.) square and 3465.51 mm (136 7/16 in.) long. The chord sections between the internal box and the inside of the TMI canister are filled with LiCon™. This is a low density (1 g/cm³) concrete mixture consisting of 60% Alcoa

CA-25C refractory cement, 11% glass microspheres, and 29% water by weight. This mixture was intended to create a solid filler with an approximate density of 1 g/cm^3 . Its composition is given in Attachment I, spreadsheet "tmi_calcs.xls," sheet "Materials." A cross-sectional schematic of the canister is seen in Figure 3.

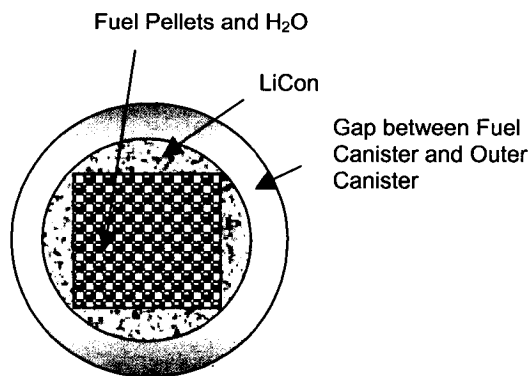


Figure 3. Cross-sectional Schematic of the Fuel Canister (D-type) Inserted in an Outer Can.

Materials of construction employ a variety of the 300 series stainless steels, and those in turn are dominated by the use of 304L type stainless. The internal sleeve is a seal-welded sandwich of 304L stainless steel that completely encompasses the Boral™ (boron aluminide) layer.

For the K-type canisters the internal assembly is designed to support five internal tubes with B_4C poisoning. The larger center "A" tube consists of a 73-mm (2.875 in.) diameter tube with a 7.9-mm (0.312 in.) wall thickness and a length of 3371.85 mm (132.75 in.). This center tube has an internal tube of 53.975 mm (2.125 in.) with a 1.6-mm (0.063 in.) wall thickness and is filled with B_4C pellets. The four outer "B" rods are centered approximately 63.50 mm (2.50 in.) each way on an X-Y plane from the canister centerline. These peripheral tubes have a 33.35-mm (1.313-in.) outer diameter with a 6.35-mm (0.25-in.) wall thickness with a minimum length of 3327.4 mm (131 in.). The seven intermediate support plates (referred to as "spiders" in Figure 2) are held in place by the poison rods, and the plates are spaced approximately 406.4 mm (16 in.) apart with a 12.7-mm (0.5-in.) plate thickness. The single, bottom support plate has a 340.52-mm (13-13/32-in.) diameter and a 31.75-mm (1.25-in.) thickness.

From shipping data, the five canisters with the highest reported uranium and U-235 weights are given in Table 1. From this data, the nominal enrichments of the canisters containing the highest uranium and U-235 masses are 2.13 wt% (K506) and 2.67 wt% (D119), respectively. The total debris mass at time of packaging and the corresponding masses for a new assembly are also listed. The loading of a new assembly (BOL) is also included in the table.

Table 1. TMI Maximum Uranium Mass (both Total Uranium and U-235).

Canister ID Number	Nine Highest Uranium Masses, kg ^a	Interim Storage Uranium Mass, kg ^b	Nine Highest U-235 Masses, kg ^a	Interim Storage U-235 Mass, kg ^b	Total Pu, kg	Corresponding Debris Mass, kg
K506	441.9 ± 99.9 ^c	441.90	9.42 ± 2.13 ^d	9.42	0.900	842.18 ± 168.3
D330	402.7 ± 42.7 ^c	402.70	8.58 ± 0.92	8.58	0.820	767.35 ± 9.1
D283	400.5 ± 103 ^c	400.50	7.57 ± 1.95	7.57	0.898	0 ± 0
D331	399.3 ± 42.3 ^c	399.30	8.51 ± 0.91	8.51	0.813	761.00 ± 9.1
D361	398.8 ± 42.3 ^c	398.80	8.50 ± 0.91	8.50	0.812	760.09 ± 9.1
D119	376.5 ± 97.3	376.50	10.06 ± 2.6 ^d	10.06	0.539	0 ± 0
D260	373.8 ± 96.4	373.80	9.66 ± 2.42 ^d	9.66	0.571	115.64 ± 102.9
D299	353.9 ± 104.0	353.90	9.37 ± 2.60 ^d	9.37	0.516	0 ± 0
D193	351.9 ± 93.0	351.90	9.41 ± 2.49 ^d	9.41	0.504	0 ± 0
New assembly ^e	463.63 ^f	—	13.72 ^f	—	—	—

SOURCE: DOE 2003b, Table 4.

NOTES: ^a Reported masses at time of shipment from TMI to the INEEL.

^b Masses reported for TMI-2 canisters transferred to interim, dry storage; these values provide the basis for criticality safety analysis for up to 12 TMI-2 canisters (per position) in Nuclear Regulatory Commission-licensed dry storage.

^c Five highest uranium masses.

^d Five highest U-235 masses.

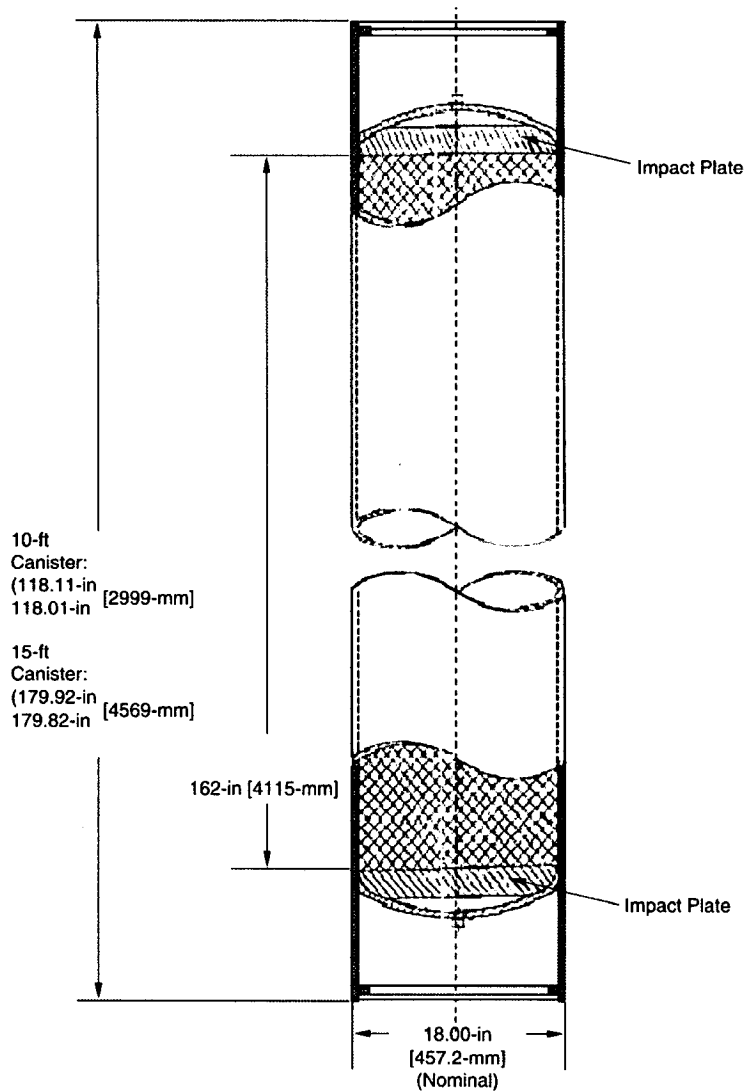
^e Comparison masses are for an intact, beginning-of-life fuel loading.

^f Due to the rounding up of the conversion factor from pounds to kilograms, a slightly smaller total uranium mass of 463.55 kg was used in these calculations. The calculations are still conservative since the enrichment was rounded up to 3 wt% giving a larger than actual U-235 mass of 13.906 kg.

A discussion of previous criticality analyses done to support various systems or conditions is presented in DOE (2003b), which highlights the differences in assumptions and/or values used in the various TMI-2 models. There are differences in modeling assumptions because of the different conditions expected in storage and transportation versus those expected in monitored geologic repository disposal.

5.1.3 Description of DOE SNF Canister

The description of the 15-ft DOE SNF canister (also referred to as the 18 in.-diameter DOE SNF canister) is taken from DOE design specifications (DOE 1999, p. 5, A-2 and A-3). The DOE SNF canister is a right circular cylinder made of stainless steel pipe (Type 316L or UNS S31603) with an outside diameter of 457.2 mm (18 in.) and a wall thickness of 9.525 mm (0.375 in.). A nominal internal length of the DOE SNF canister used for fuel loading is 4117.086 mm (162.09 in.); minimum length dimension is 4114.8 mm (162 in.). (This nominal length is insignificantly different from the minimum length.) A sketch of the canister is shown in Figure 4.



03-GA50387-15

Figure 4. DOE Spent Nuclear Fuel Standard Canister

A sleeve of 16 in. (40.64 cm) outside diameter and 0.5 in. (1.27 cm) thickness is used as a spacer inside the SNF canister. The sleeve could be made of either stainless or carbon steel depending on desired structural and corrosion properties. The sleeve would utilize some sort of standoff structure that would center it in the SNF canister, though this detail is not modeled. The TMI canister is placed directly in the sleeve.

5.1.4 High-Level Waste Glass Pour Canister

There is no long Savannah River Site high-level waste (HLW) glass canister. Therefore, the expected Hanford 15-foot HLW glass canister is used in the TMI canister waste package. Because the specific composition of the Hanford HLW glass has not yet been specified, it is assumed to be the same as the Savannah River Site glass composition. The Hanford 15-foot HLW glass canister is a 4,572-mm (180-in.)-long stainless steel Type 304L canister with an outer diameter of 610 mm (24 in.) (Taylor 1997). The wall thickness is 10.5 mm (0.4134 in.). These parameters are the same as the Savannah River Site canister, except that it is longer. The maximum loaded canister weight is 4,200 kg, and the fill volume is 87% (Taylor 1997).

5.1.5 Chemical Description of Borosilicate Glass

The borosilicate glass intended for the Hanford canister has yet to be specified in terms of composition, physical properties, etc. However, given similar characteristics of the waste produced in the fuel dissolution and neutralization before tank farm storage, the resulting glass composition should be similar to that produced at Savannah River. Trace quantities of these materials provide a minimal impact on overall chemistry behavior and mobilization of fissile materials.

5.1.6 Waste Package Description

The waste package contains five HLW glass pour canisters spaced radially around an 18 in. DOE SNF canister (CRWMS M&O 2000b, pp. 30-32 and Attachment V). The waste package description used to generate the calculated results in this report is based on recent design changes (unless noted otherwise), where the dimensions are slightly different than those given in this section. For example, there is now a 5 mm gap between the inner and outer shells resulting in a 10 mm increase in the outer shell diameter, and the details of the closure lids have also changed slightly. These dimensional changes have an insignificant effect on the calculated results based on a selected number of cases evaluated with the dimensions given in this section. The waste package barrier materials are typical of those used for commercial spent nuclear fuel waste containers. The waste package is designed to accommodate five HLW canisters surrounding a single SNF canister in the center position. The length of the waste package varies depending on whether it is to accommodate a 10 or 15-ft HLW/DOE SNF canister. Figure 5 depicts a cross-sectional view of the waste package and its internals.

The barrier materials of the waste package are typical of those used for commercial SNF waste packages. The inner barrier is composed of 50-mm (1.969-in.)-thick Type 316 NG stainless steel. The outer barrier comprises 25 mm (0.984 in.) of high-nickel alloy (Alloy 22). The SNF canister support tube and basket plates are constructed out of carbon steel (ASTM A 516). A summary of pertinent dimensions and material specifications is provided in Table 2.

Table 2. Waste Package Dimensions^a and Material Specifications.

Component	Material	Parameter	Dimension (mm)
Outer barrier shell	SB-575 (Alloy 22)	Thickness	25
		Outer diameter	2030
Inner barrier shell	SS 316 NG	Thickness	50
		Inner length	4618
Extended outer shell lid	SB-575 (Alloy 22)	Thickness	25
Outer shell flat closure lid	SB-575 (Alloy 22)	Thickness	10
Inner shell lid	SS 316 NG	Thickness	105
Closure lid to extended outer lid gap	Air	Thickness	30
Inner shell lid to closure lid gap	Air	Thickness	30
Support tube	ASTM A 516 Grade 70	Outer diameter	565
		Inner diameter	501.5
		Length	4607
Inner bracket	ASTM A 516 Grade 70	Thickness	25.4
		Length	4607
Outer bracket	ASTM A 516 Grade 70	Thickness	12.7
		Length	4607

SOURCE: CRWMS M&O 2000b, pp. 30-32 and Attachment V

NOTE: ^a More recent, proposed dimensions (used to generate the MCNP results) are: outer diameter of outer barrier shell is 2040 mm; inner length of inner barrier shell is 4617 mm; thickness of outer shell lid is 25.4 mm; thicknesses of inner shell lids are 50.8 mm (top) and 50 mm (bottom); thickness of gap between inner shell lid and closure lid is 47.23 mm; and thickness of gap between bottom inner and outer shell lids is 70 mm.

The outside diameter of the waste package is 2,030 mm (79.92 in.), and the inside cavity length is 4,618 mm (181.8 in.), which is designed to accommodate Hanford 15-ft HLW glass canisters. The lids of the inner barrier are 105 mm (4.134 in.) thick; those of the outer barrier are 25 mm (0.984 in.) thick. There is a 30-mm (1.181-in.) gap between the inner and outer barrier upper lids. Each end of the waste package has a 225-mm-long (8.858-in.) skirt. Note that some of the details concerning the lids are simplified, e.g., a 1 cm flat closure lid and 3 cm gap are neglected for the upper lid.

The DOE SNF canister is placed in a 31.75-mm (1.250-in.)-thick support tube with a nominal outer diameter of 565 mm (22.244 in.). The support tube is connected to the inside wall of the waste package by a web-like structure of basket plates to support five long HLW glass canisters. The support tube and the plates are 4,607 mm (181.378 in.) long.

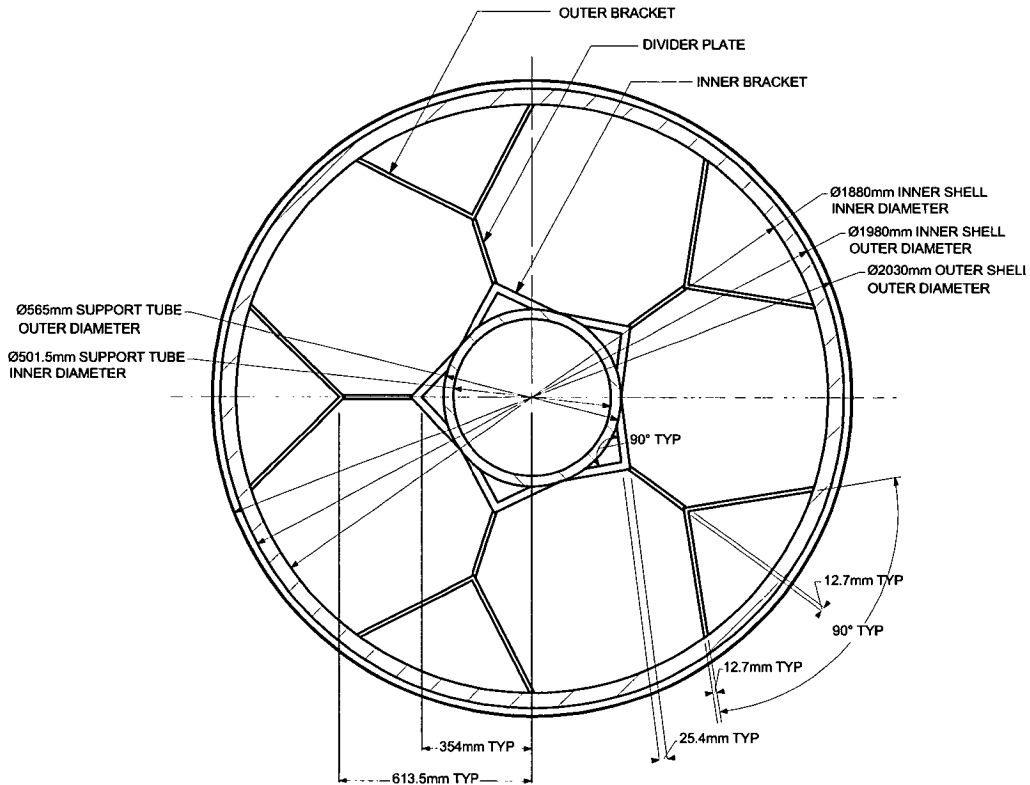


Figure 5. Cross-sectional View of Typical Waste Package.

5.2 MATERIALS DESCRIPTION

Tables 3 through 11 give the composition of the materials used in this calculation. The number densities used in the inputs are calculated in Attachment I, spreadsheet “tmi_calcs.xls.”

Table 3. Composition and Density of Stainless Steel 304L.

Element	Composition (wt %) ^a	Value Used (wt %)
C	0.030 (max)	0.030
Mn	2.000 (max)	2.000
P	0.045 (max)	0.045
S	0.030 (max)	0.030
Si	0.750 (max)	0.750
Cr	18-20	19.000
Ni	8-12	10.000
N	0.100 (max)	0.100
Fe	Balance	68.045
Density ^b = 7.94 g/cm ³		

NOTES: ^a ASTM A 240/A 240M-99b, p. 2.

^b ASTM G 1-90, Table X1.1.

Table 4. Composition and Density of Savannah River Site High-Level Waste Glass

Element / Isotope	Composition ^a (wt %)	Element / Isotope	Composition ^a (wt %)
O	4.4770E+01	Ni	7.3490E-01
U-234	3.2794E-04	Pb	6.0961E-02
U-235	4.3514E-03	Si	2.1888E+01
U-236	1.0415E-03	Th	1.8559E-01
U-238	1.8666E+00	Ti	5.9676E-01
Pu-238	5.1819E-03	Zn ^d	6.4636E-02
Pu-239	1.2412E-02	B-10	5.9176E-01
Pu-240	2.2773E-03	B-11	2.6189E+00
Pu-241	9.6857E-04	Li-6	9.5955E-02
Pu-242	1.9168E-04	Li-7	1.3804E+00
Cs-133	4.0948E-02	F	3.1852E-02
Cs-135	5.1615E-03	Cu	1.5264E-01
Ba-137 ^c	1.1267E-01	Fe	7.3907E+00
Al	2.3318E+00	K	2.9887E+00
S	1.2945E-01	Mg	8.2475E-01
Ca	6.6188E-01	Mn	1.5577E+00
P	1.4059E-02	Na	8.6284E+00
Cr	8.2567E-02	Cl	1.1591E-01
Ag	5.0282E-02	—	—
Density ^b at 25 °C = 2.85 g/cm ³			

- NOTES:
- ^a CRWMS 1999a, p. 7.
 - ^b Stout and Leider 1991, p. 2.2.1.1-4.
 - ^c See Assumption 3.2.
 - ^d See Assumption 3.4

Table 5. Composition and Density of Stainless Steel 316L

Element	Composition ^a (wt %)	Value Used
C	0.03 (max)	0.0300
N	0.10 (max)	0.1000
Si	1.00 (max)	1.0000
P	0.045 (max)	0.0450
S	0.03 (max)	0.0300
Cr	16-18	17.0000
Mn	2.00 (max)	2.0000
Ni	10-14	12.0000
Mo	2-3	2.5000
Fe	Balance	65.2950
Density ^b = 7.98 g/cm ³		

NOTES: ^aASTM A 276-91a, p. 2.
^bASTM G 1-90, Table X1.1.

Table 6. Composition and Density of Alloy 22

Element	Composition (wt %)	Value Used
C	0.015 (max)	0.015
Mn	0.50 (max)	0.5
Si	0.08 (max)	0.08
Cr	20-22.5	21.25
Mo	12.5-14.5	13.5
Co	2.50 (max)	2.5
W	2.5-3.5	3.0
V	0.35 (max)	0.35
Fe	2.0-6.0	4.0
P	0.02 (max)	0.02
S	0.02 (max)	0.02
Ni	Balance	54.765
Density = 8.69 g/cm ³		

SOURCE: DTN: MO0003RIB00071.000

Table 7. Composition and Density of Carbon Steel 516 Grade 70

Element	Composition (wt %)	Value Used
C	0.28	0.30
Mn	0.85-1.20	1.025
P	0.035 (max)	0.035
S	0.035 (max)	0.035
Si	0.15-0.40	0.275
Fe	Balance	98.33
Density = 7.85 g/cm ³		

SOURCE: DTN: MO0003RIB00072.000

Table 8. Composition and Density of Dry Tuff

Mineral	Composition (wt %)	Element	Composition (wt %)
SiO ₂	76.83	Si	0.359
Al ₂ O ₃	12.74	Al	0.067
FeO	0.84	Fe	0.007
MgO	0.25	Mg	0.002
CaO	0.56	Ca	0.004
Na ₂ O	3.59	Na	0.027
K ₂ O	4.93	K	0.041
TiO ₂	0.1	Ti	0.001
P ₂ O ₅	0.02	P	0.0001
MnO	0.07	Mn	0.001
—	—	H	0.000
—	—	O	0.492
Density=2.245 g/cm ³			

NOTE: CRWMS M&O (2001, Attachment II spreadsheet "Tuff composition.xls")

Table 9. Pre-Breach Clay Compositions^{a,b}

Element	Mass of Element after 59473 Years of Emplacement ^c (kg)	Mass of Element after 53241 Years of Emplacement (kg)
O	1.55E+04	9.67E+03
H	8.07E+01	7.14E+01
Fe	1.98E+04	1.07E+04
Al	3.46E+02	3.36E+02
Ba	2.16E+01 ^d	2.15E+01 ^d
Ca	1.69E+02	8.11E+01
F	2.60E+00	1.04E+00
P	1.27E+01	5.09E+00 ^d
K	1.62E+01	0.00E+00
Mg	5.81E+01	9.05E+01
Mn	4.46E+02	1.67E+02
Na	1.39E+01	0.00E+00
Ni	1.85E+03	3.87E+02 ^d
Si	4.47E+03	3.42E+03
Cr	8.14E+00	8.10E+00
U	2.69E+02	0.00E+00
Total (kg)	4.31E+04	2.50E+04
Density (g/cm³)	4.23^e	3.88

NOTES: ^a Clay is formed from DHLW glass degradation.

^b BSC 2001a, p. 56 and CRWMS M&O 2000a, p. 41

^c Composition same as used for Shippingport LWBR, (CRWMS M&O 2000a, p. 41).

^d Values vary by one digit in least significant decimal place since masses are calculated from number of moles from reference using isotopic rather than elemental atomic masses.

^e Value listed in reference is 4.235 which is insignificantly different from value used.

Table 10. Post-Breach Clay Compositions

Element	Mass of Element after 72689 Years of Emplacement (kg)	Mass of Element after 378240 Years of Emplacement (kg)
O	9.93E+03	1.24E+04
Al	3.35E+02	3.35E+02
Ba	2.14E+01	2.13E+01
Ca	6.58E+01	7.02E+01
Cr	8.09E+00	8.08E+00
F	5.51E-01	0.00E+00
Fe	1.13E+04	1.65E+04
H	6.94E+01	7.10E+01
C	0.00E+00	0.00E+00
P	5.41E+00	8.80E+00
Mg	9.93E+01	9.99E+01
Mn	1.82E+02	3.43E+02
Mo	1.60E+01	2.51E+01
Ni	4.18E+02	4.10E+02
Si	3.43E+03	3.53E+03
Th	3.23E+00 ^a	5.39E+01 ^a
U-235	4.48E-01 ^a	7.25E+00 ^a
Total (kg)	2.59E+04	3.39E+04
Density (g/cm³)	3.98^b	4.16^b

SOURCE: BSC (2001a, p. 59 and Attachment III, file fm2t1011.6o)

NOTES: ^a These thorium and U-235 masses are not used since they are for Fort Saint Vrain SNF; uranium masses from one TMI assembly and the plutonium from the HLW glass (see Table 4) are included in the post-breach composition used here, see Attachment I, spreadsheet "tmi_calcs.xls," sheet "Materials."

^b Densities of 4.05 and 4.21 g/cm³ are used for the clay compositions at 72689 and 378240 years, respectively.

Table 11. Alternative Post-Breach Clay Composition

Element	Mass of Element after 74818 Years of Emplacement (kg)
O	9.96E+03
Al	3.35E+02
B	0.00E+00
Ba	2.14E+01
Ca	6.58E+01
Cr	8.09E+00
F	4.80E-01
Fe	1.13E+04
H	6.94E+01
P	5.44E+00
Mg	9.93E+01
Mn	1.84E+02
Mo	1.77E+01
Ni	4.19E+02
Si	3.43E+03
Th	5.39E-01 ^a

Table 11. Alternative Post-Breach Clay Composition (Continued)

Element	Mass of Element after 74818 Years of Emplacement (kg)
U-235	7.18E-02 ^a
Total (kg)	2.59E+04
Density (g/cm³)	3.92^b

SOURCE: BSC 2001a, p. 62 and file fm2i1021.6o.

NOTES: ^a These thorium and U-235 masses are not used since they are for Fort Saint Vrain SNF; uranium masses from one TMI assembly and the plutonium from the HLW glass (see Table 4) are included in the post-breach composition used here, see Attachment I, spreadsheet "tmi_calcs.xls," sheet "Materials."

^b A density of 3.99 g/cm³ is used.

5.3 FORMULAS

The basic equation used to calculate the number density values for materials composed of one or more elements/isotopes is shown below. It is used in the spreadsheet included in Attachment I, and in the cases described throughout Section 5:

$$N_i = (m_i / m) * \rho * N_a / M_i = (V_i / V) * \rho_i * N_a / M_i = (af)_i * \rho * N_a / M$$

where: N_i is the number density in atoms/cm³ of the i^{th} element/isotope, note that in Attachment I, N_i is multiplied by 10^{-24} cm²/barn and is therefore in units of atoms/(barn*cm)
 m_i is the mass in grams of the i^{th} element/isotope in the material
 m is the mass in grams of the material; note that $m = \Sigma m_i$
 N_a is the Avogadro's number (6.022 E+23 atoms/mole, Parrington et al. 1996, p. 59)
 M_i is the atomic mass in g/mole of the i^{th} element (Parrington et al., 1996)/isotope (Audi and Wapstra, 1995)
 M is the atomic mass in g/mole of the material
 V_i is the volume in cm³ of the i^{th} element/isotope in the material
 V is the volume in cm³ of the material; note that $V = \Sigma V_i$
 ρ_i is the density of the i^{th} element/isotope
 ρ is the *density* of the material; note that $\rho = \Sigma \rho_i * (V_i / V)$
 $(af)_i$ is the atom fraction of the i^{th} isotope of the element; note that $M = \Sigma (af)_i M_i$

Volumes of horizontal, cylinder segments (volume = area of circle segment × length of the cylinder) are also calculated throughout Attachment I. Given a specified volume of material in a cylinder, the following equation is solved iteratively for the material height (h) inside the package. These calculations are based on the equation for the segment of a circle shown below (Beyer 1987, p. 125):

$$\text{Area of a segment of a circle} = \left(R^2 \cos^{-1} \left(\frac{R-h}{R} \right) - (R-h) \sqrt{2Rh-h^2} \right)$$

where: R is the cylinder radius, and
 h is the height of the segment.

Alternatively, the height of the material in a degraded waste package can be calculated with the following parametric formula for the area of the segment and the angle θ (Beyer 1987, p. 125), which is defined such that $h=R*[1-\cos(\theta)]$ and $0 \leq \theta \leq \pi$

$$\text{Area of a segment of a circle} = R^2 \left(\theta - \frac{1}{2} \sin(2\theta) \right).$$

The equation to calculate the fuel array void fraction, V_f , for each fuel array is shown below. For example, if the pellet array fills the entire cross-section of the canister then A_{cs} is the canister cross-sectional area.

$$V_f = 1 - (N_s V_p) / (A_{cs} p_{axial})$$

where: p_{axial} is the axial pitch,
 N_s is the number of pellet stacks,
 V_p is the volume of the fuel pellet, and
 A_{cs} is the effective cross-sectional area of the pellets (in the plane perpendicular to the axis of the cylinder).

5.4 INTACT MODE CRITICALITY CALCULATIONS

In this section, the intact mode of the DOE SNF canister is analyzed. These configurations represent a waste package, which has been breached allowing inflow of water, but the internal components of the waste package are as-loaded, i.e., intact. Though, unless noted otherwise, unoccupied spaces in the SNF canister and waste package are modeled as void, but the TMI canister is water flooded. Modeling of the end structure of the DOE SNF canister treats both the impact plate and the dished head as a single piece that serves as an end reflector. The curved gap between the two pieces is conservatively modeled as filled with carbon steel. A sleeve is positioned between the SNF and TMI canisters and reduces the amount of "rattle-room" in the SNF canister. The waste package is reflected by tuff. Variations of the intact configurations are examined to identify the configuration that results in the highest calculated k_{eff} value within the range of possible conditions.

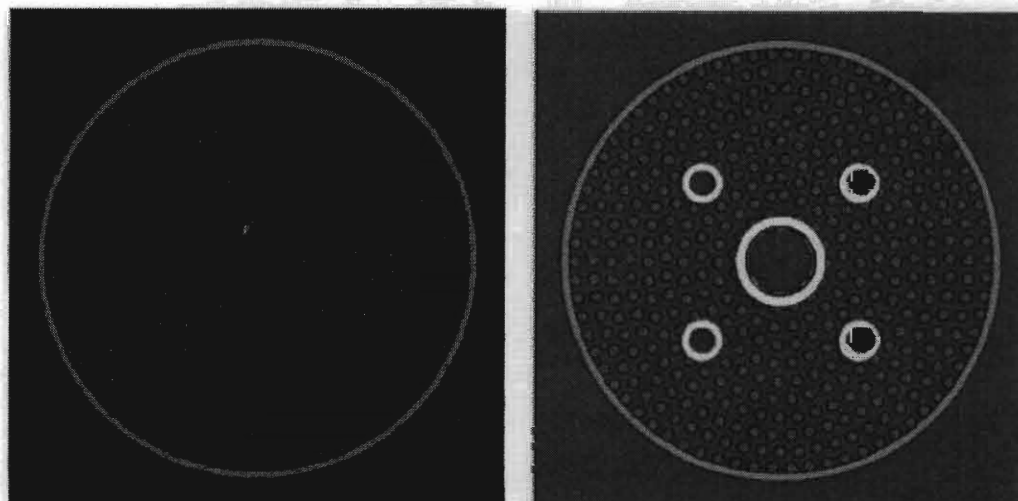
5.4.1 Treatment of TMI Fuel and Canisters

A single PWR fuel assembly is used as the basis for criticality scenarios associated with the TMI canisters. The enrichment of the fuel is assumed to be 3 wt% (Assumption 3.3), giving a U-235 mass of 13.906 kg per assembly for the new assembly total uranium mass given in Table 1. These values of enrichment and fissile mass are in excess of those values for the actual fuel in the canisters since they contain, in general, a blend of the three different enrichments given in Section

5.1.1 (all less than 3 wt%). (See DOE 2003b [Table C-1] for a detailed accounting of uranium and plutonium content for each TMI canister.) The void fraction inside the fuel (7.5%) is assumed saturated with water (Assumption 3.5). The fuel is modeled as individual pellets with the dimensions given in Section 5.1.1 though spherical pellets with different diameters are also investigated. The individual fuel pellets (either cylindrical or spherical) remain axially aligned in what are referred to here as "pellet stacks." Most results given below are for cylindrical pellets.

In many cases intact TMI canisters are modeled completely filled with pellets. Depending on the spacing of the pellets this is typically more than one assembly's worth of fuel pellets or 67,600 pellets, unless stated otherwise. No zirconium is included in the canisters, but if present would act as a moderator displacer. The B_4C is replaced by water in the poison tubes of the KO canister, and the annular gap in the center tube contains a mixture of fuel and water. The canisters are assumed water flooded (Assumption 3.5). While Boral[™] was installed as an integral part of the box liner for the fuel type canisters, no credit is taken for its presence.

Only a portion all of the KO canister internals are modeled. The fuel sits on a bottom plate inside the canister, and this is always modeled. The B_4C in the poison tubes is replaced with water; and the annulus between the central (larger) poison tube and its support tube is assumed to contain fuel and water. Since the poison tubes do not extend over the entire inner length of the canister, this upper portion of the canister is open (no other internals are modeled in this portion of the canister). The pellets in the pellet stacks that happen to partially intersect with the poison tubes are modeled as partial pellets; the MCNP code allows a partial pellet to be modeled. In other words, the partial pellets consist of that portion of the intersecting pellets that are external to the poison tube. Because no internals are modeled in the upper portion of the canister, the fuel pellets always completely fill this upper (open) portion, unless noted otherwise. These details are shown in Figure 6 at different elevations of the canister. In some cases, as identified in the tables, the poison tubes in the KO canister are neglected (this is referred to as simply "without internals").



A) The Upper Portion of the KO Canister Above the Poison Tubes

B) Lower Portion of the KO Canister Showing Poison Tubes

Figure 6. Cross-sectional View of Knockout (KO) Canister at Different Elevations.

5.4.2 TMI Fuel Pellet and Other Modeling Details

In this section, an exhaustive study of the spacing of cylindrical (same dimensions as intact TMI pellets) and spherical pellets in the KO canister is conducted to determine the most reactive KO canister configuration. As part of this study, the diameter of the spherical pellets is also varied. The two most obvious choices for the spherical radius, R , are: (1) the diameter of the sphere equal to the smallest cylindrical pellet dimension, in this case the cylindrical diameter; and (2) the radius chosen such that the volume of the sphere and cylinder are equal. The former and latter choices give the smallest and largest radii, respectively, that are considered here. A total of four values of radius are investigated, these are 0.46990 cm, 0.52000 cm, 0.54500 cm and 0.56772 cm, the two intermediate values are chosen to be about midway between the minimum and maximum radii, and then again about midway between this value and the maximum. For modeling convenience, the pellets (spherical and cylindrical) are aligned with the axial direction of the canister to form pellet stacks. The pellet stacks are arranged in a circular array in the canister. The array is referred to as being circular, because it is generated by positioning the centers of the pellet stacks on concentric circles (each a row) while maintaining as uniform a spacing (a pitch) as possible between all adjacent rods (not just those on the same row). This produces an irregular lattice that is neither completely triangular nor square. In practice, circular arrays have been shown to be as or more reactive than triangular arrays with the same pitch and number of rods (DOE 2002, p. 41). This spacing between stacks is referred to as a "radial" pitch, and the axial spacing is characterized by the gap between pellets (cylindrical pellets) or an axial pitch (spherical pellets). (Note that an axial pitch could also be used for the cylindrical pellets and is equal to the sum of the pellet length and gap.) In actuality, the pellets in the canisters are generally not axially aligned or uniformly spaced. If the localized pellet orientation and separation are reasonably uniform throughout the fuel, then the actual pellet spacing may be better characterized by the array void fraction as calculated in Section 5.3.

Results for the spacing study of cylindrical pellets are given in Table 12. The radial and axial spacing is increased from the pellets touching until the most reactive configuration is found. In the first set of cases, the canister contains one assembly's worth of pellets, and the poison tubes are neglected. In the second set, the canister internals (poison tubes) are modeled, and the internal canister length is filled with pellets. In all cases, this is more pellets than are in an assembly (67,600 pellets).

Similar cases studying pellet spacing but for spherical pellets are studied in Tables 13 and 14 for the canister without and with internals, respectively. Each table is divided into four sets, one for each value of spherical radius. As for the cylindrical pellet cases, the canister contains either an assembly's worth or greater of pellets for the internals neglected or modeled, respectively. Cases with no water in the KO canister are investigated in Table 15. For these cases the canister contains an assembly's worth of spherical fuel pellets with the maximum radius, and the canister internals are neglected. The pellets are touching in the radial and axial directions since this configuration is anticipated to be most reactive for a dry canister. To confirm this, a limited number of cases with increased radial and axial separation are also considered.

In the next table, Table 16, the fuel loading in the canisters (with internals) and other details are investigated. These cases are variations of cases in Tables 13 and 14. In the first four sets of results (one for each value of spherical radius), the canister contains an assembly's worth of fuel. Since this only partially fills the canister length, the pellets are modeled in the upper part of the canister since this end is open above the poison tubes. This is done to maximize the pellet array cross-sectional area even though this open volume is not sufficient to contain all the fuel. In the first set of the table, the effect of reducing the cross-sectional area of the pellet array, i.e., reducing the number of pellet stacks, is investigated. For cases with reduced cross-section, the canister is rotated 45° in order to change the relative positioning of the poison tubes and pellet array as shown in Figure 7. Similar cases in the fourth and sixth sets investigate different fuel loadings (both sets) and reduced array cross-sectional area (sixth set) for a canister with and without internals, respectively. Other details investigated in this table are: water replaces the void between the SNF and TMI canister; location of these canisters in the waste package; fuel located in the bottom rather than top portion of KO canister; variations in the thickness and composition of the sleeve surrounding the TMI canister; no water saturation of voids in the fuel pellets; all canisters (including HLW canister) in the waste package have shifted downward due to the effect of gravity, see Figure 8; the sleeve between the SNF and TMI canisters is no longer centered in the SNF canister, see Figure 9; the earlier design dimensions of the waste package are used, see Section 5.1.6; and the enrichment and plutonium content of the fuel are varied. The enrichment and fuel mass used here must be shown to bound the effective enrichment of the most highly loaded KO canister given in Table 1 (2.13 wt% enrichment) and its plutonium content which is less than one kg of total plutonium.

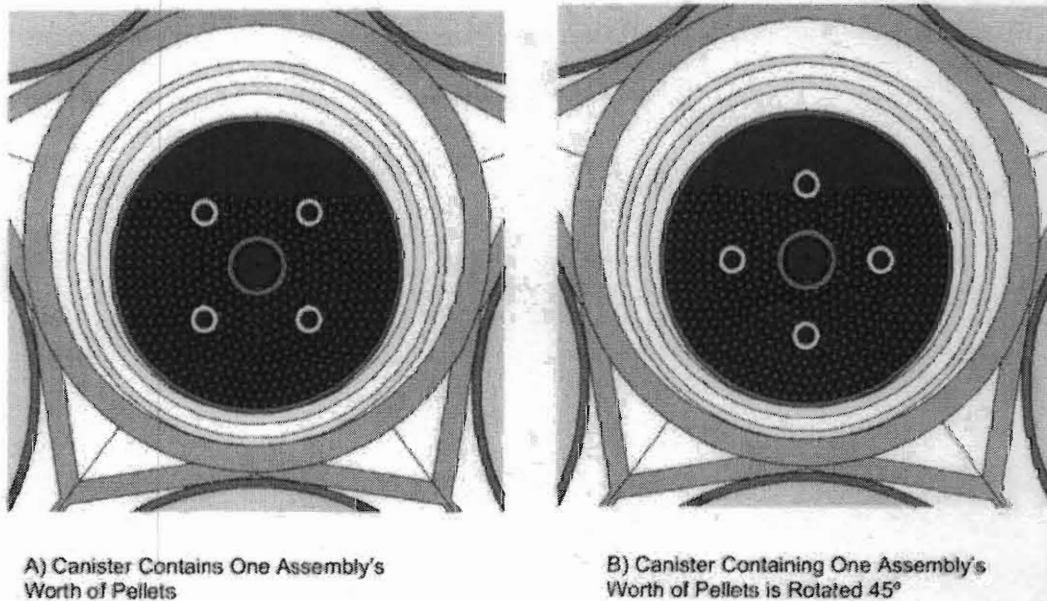


Figure 7. Pellet Array Partially Fills KO Canister's Cross-section.

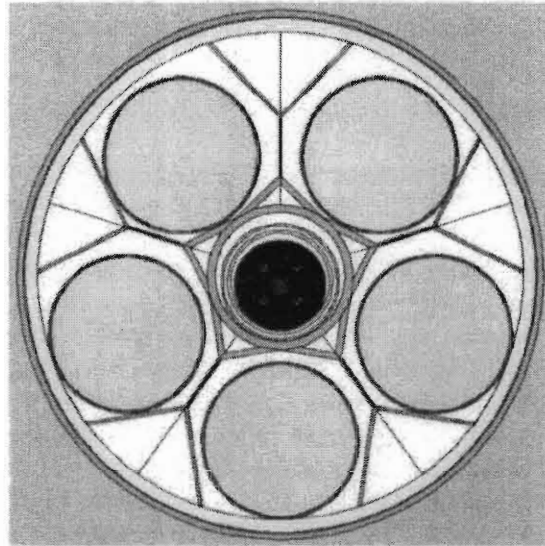


Figure 8. Canisters Are in a Gravity Position in the waste package.

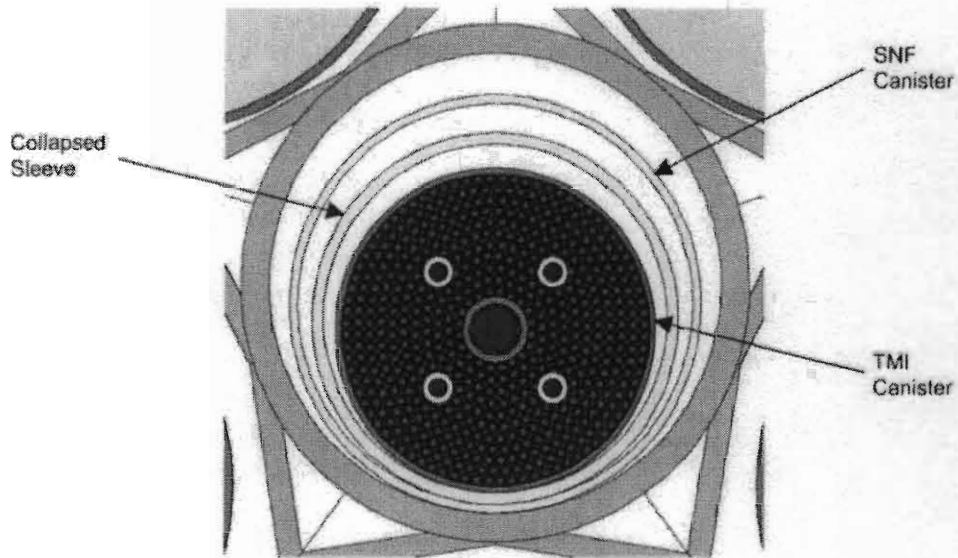


Figure 9. Sleeve Is Collapsed in the SNF Canister.

A spacing study of cylindrical pellets in a TMI fuel canister (D-type) is given in Table 17. This is done to determine which canister is the most reactive. In the first set of the table, the canister contains an assembly's worth of fuel pellets that are in a hexagonal array. In these cases only whole pellets are modeled in the canister. In the second set of cases if there is sufficient space around the inside perimeter of the canister, then partial pellets are positioned in these array positions as shown in Figure 10. Since these cases contain the same number of whole pellets, the number of partial

pellets is the amount of fuel in excess of one assembly's worth. For all cases, the Boral™ layer is replaced by water, and the inner square box structure remains intact.

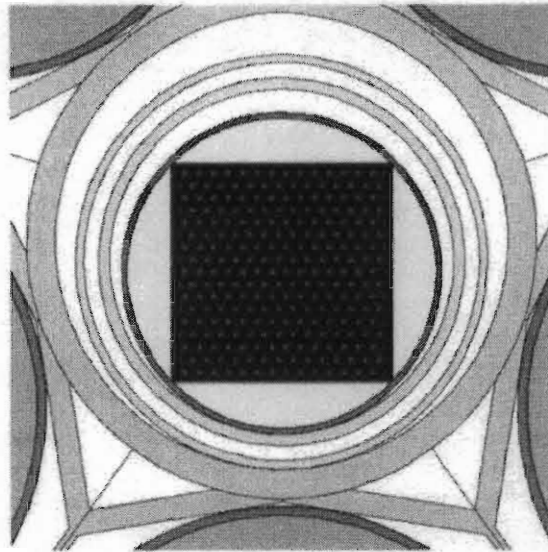


Figure 10. Cross-sectional View of the TMI Fuel Canister.

In the final table of results of this section, cases are considered where the KO canister contains one assembly's worth of fuel homogenized with varying amounts of water. This is done to demonstrate that modeling heterogeneous fuel pellets is more reactive than a homogeneous mixture for TMI fuel (i.e., low-enriched fuel). For simplicity the canister internals are neglected, and the water volume fraction (wvf) in the fuel is increased from completely dry until the most reactive fuel mixture is found. The remainder of the canister is assumed (Assumption 3.5) to contain water (Assumption 3.5) except for a couple of cases where it is dry. These results are given in Table 18, and the most reactive case can be compared to the equivalent heterogeneous cases given in Tables 12 and 13.

5.5 DEGRADED MODE

The criticality calculations conducted for the degraded cases are discussed in the following sections. Several configurations are considered. Detailed descriptions of these configurations are given on pages 27 through 37 of CRWMS M&O (1999b). In Section 5.5.1, configurations are analyzed resulting from the degradation scenarios in which the components inside the SNF canister (sleeve and TMI-2 canister) degrade (CRWMS M&O 1999b, pp. 27-29). In Section 5.5.2, configurations resulting from the degradation of the high-level waste glass are investigated (see Attachment I, spreadsheet "tmi_calcs.xls," sheet "WP" for detailed description of cases) for sensitivity to changing waste package parameters. Configurations where all the internal components of the waste package have degraded are discussed in Section 5.5.3 (see Attachment I, spreadsheet "tmi_calcs.xls" sheet "WP" for detailed description of cases), and are also investigated for different waste package conditions. In configurations resulting from water flowing through the waste package, it has been shown (BSC 2001a, p. 64) that the fissile material will likely be flushed out of the waste package. As the amount of fissile material decreases, the risk of internal criticality is diminished.

The degraded configurations are analyzed as a sequence of progressing degradation rather than an immediate transition from intact to completely degraded. These degraded configurations are expected to be more reactive than intact configurations. Water is always assumed present and is responsible for the degradation considered here. The details of this process depend on degradation rates and how the water enters the waste package and interacts with its contents. Except for the scenario where everything is degraded in the waste package, no degradation of the fuel pellets is considered since low-enriched (less than approximately 5 wt%) uranium fuel is more reactive when in a heterogeneous configuration (DOE 2003b, p. 50). Typically the first components to degrade would be the HLW canisters, the waste package basket and the inner lining of the waste package. The degraded components form pre-breach clay which surrounds the intact SNF canister. The sleeve inside the SNF canister could also be degraded at this time, or might degrade prior to the formation of the pre-breach clay. Details of the degradation process would determine whether the SNF or TMI canister degrade first leaving fuel pellets in the surviving canister surrounded by pre-breach clay and the other degradation products. A near final configuration is all components degraded and the fuel pellets surrounded by layers of different materials with little mixing between layers. The presence of water in the layers is an added complication that must be considered. A possible final configuration, though uninteresting from a criticality point of view (as shown below in Table 26), would be for the entire contents of the waste package to be completely degraded and mixed together. There may be no identified mechanism for such complete homogenization of the degraded waste package contents.

For degraded mode calculations, the iron content of stainless steel degrades to goethite (FeOOH) (Assumption 3.1), and the degradation products from the other steel constituents are neglected. In determining the amount of goethite formed, only the canister walls are considered, and the internal canister components are neglected. The void fraction in the degradation products is expected to be around 40% though in some cases values of 60% and larger are used. In an aqueous environment, water can saturate the material filling these voids.

The TMI pellets remain intact except for the scenario of complete internal degradation. At least one assembly's worth of pellets is used in the analysis. The loose pellet arrays are modeled as stacks of axially aligned pellets with a uniform separation between stacks and pellets, i.e., characterized by radial and axial pitches (two parameters), respectively. In actuality, the loose, randomly positioned pellets are not, in general, axially aligned or uniformly spaced. If the pellet separation is reasonably uniform throughout the array, then the pellet spacing can be characterized by (one parameter) an array void fraction (see definition in Section 5.4.2) which is also listed in the results. Degradation products and/or water can fill these voids between fuel pellets.

While this addresses the spacing of the pellets, the axial loading of the pellets must also be addressed. For an un-breached TMI canister, the maximum loading is limited by the maximum number of pellets that would fit in the canister and is determined here for whichever canister type has the largest cross-sectional area, i.e., the KO canister. Once the TMI canister is breached and if there is no axial redistribution of fuel, the axial fuel loading is also limited by the canister's maximum loading. Another consideration is that there is no identifiable mechanism to elevate any pellet against gravity. This means that each pellet should be located somewhere between its intact position and the bottom of the medium containing the entire array. For a realistic array, this imposes an upper limit on the radial pitch for any given axial fuel loading.

In these cases, the terms "fraction of water" or "percent of water" refer to a volume fraction (vf) or to a percentage of volume, respectively. The percentages listed for the other components of the degradation products are volume fractions. As was done for the intact cases, the waste package is reflected by tuff.

5.5.1 Components Degrades Within the Intact SNF Canister

In this section, cases are investigated where components inside the SNF canister degrade while it remains intact. This most closely corresponds to scenario IP-1A from YMP (2000, pp.3-13 and 3-14) and from CRWMS M&O 1999b, p. 27). Results for this section are given in Section 6.2.1.

For this scenario, the sleeve and TMI canister have degraded leaving the fuel pellets inside the intact SNF canister surrounded by goethite and/or water. Unless noted otherwise, the SNF canister contained a stainless steel sleeve. Components external to the SNF canister are also intact. Cylindrical pellets are considered and the results examine a range of pellet pitches and axial fuel loadings. This includes cases where the entire cross-section of the SNF canister is filled as shown in Figure 11. This case is unrealistic because some of the pellets at the top of the array have been moved against gravity (gravity is downward in the plane of the figure) from their intact positions that can be seen in Figure 8. Results are shown in Table 19. In the first set of the table, goethite is neglected and the pellets are surrounded by water. In the next two sets, water is above dry goethite that is at the bottom of the canister, see Figure 11. The level of goethite is determined by the amount produced and by the number of pellet stacks that are displaced. Cases in these sets examine the effects of increased goethite from a carbon steel sleeve and of completely filling the canister with dry goethite. This latter case is done solely as a comparison. In the third set, the number of pellet stacks is decreased giving a reduced axial fuel loading for some of the more reactive cases of the second set. This is accomplished by maintaining the radial pitch and axial spacing between pellets while decreasing the number of pellets stacks and appropriately increasing the number of pellets per stack so as to maintain the same total amount of fuel. In the last two sets of the table, goethite is mixed with sufficient water to completely fill the SNF canister except for the last case of the fourth set which has a smaller wvf. This case illustrates the effect of decreasing the amount of water in the surrounding goethite mixture. Other cases in this set show the effect of changing pitch in the array. Cases in the last set show the effect of decreasing the number of pellet stacks for some of the more reactive cases of the previous set.

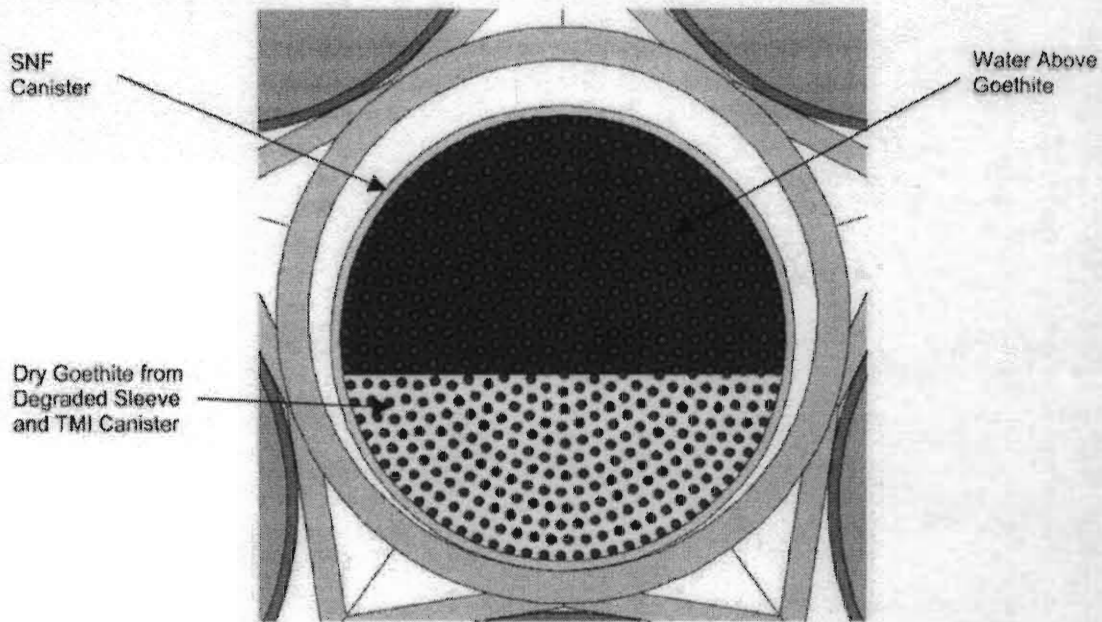


Figure 11. Cross-sectional View of the SNF Canister.

5.5.2 Internal Components of the Waste Package Outside SNF Canister Degrade

This section describes configurations resulting from the scenario IP-3 (YMP 2000, p. 3-13). The internal components of the waste package outside the SNF canister are completely degraded, including the inner barrier shell of the waste package. The compositions of the slurry resulting from this degradation are given in CRWMS M&O (2000a, p. 41) and BSC (2001a, p. 56) and are referred to as the pre-breach clay (Table 9). The amount of water mixed with this clay is varied. There is U-238 present in the slurry from the degraded glass, but it is (conservatively) neglected in these calculations since it is a neutron absorber. The cases in this section can be further divided into 2 categories depending upon whether the SNF canister is treated as being intact or degraded. In the first category, described in Section 5.5.2.1, the SNF canister is intact and its contents can either be intact, partially or completely degraded. In the second category, described in Section 5.5.2.2, the SNF canister has degraded, but the degradation products from the canister and its contents remain separate and have not yet chemically reacted with the pre-breach clay.

5.5.2.1 Intact SNF Canister with Contents Either Intact or Degraded

The SNF canister configurations studied include intact and degraded cases and are derived from the most reactive cases identified in the previous sections (Sections 5.4 and 5.5.1). For the cases given in Table 20, the intact SNF canister containing intact components is surrounded by pre-breach clay. The KO canister and sleeve are intact, except as noted below, and the canister (with internals) is filled with spherical pellets. This configuration is not the most reactive case of Section 5.4, but it is typical of the most reactive cases of interest. In the first set of this table, the vertical height of the SNF canister in dry clay is varied from just under the clay layer to resting on the bottom of the

waste package. A variation of the case with the SNF canister resting on the waste package bottom but with earlier waste package design dimensions is investigated. Other cases in this set examine the effect of filling the void between the sleeve and the canisters with clay mixed with varying amounts of water and of a carbon steel sleeve degraded to goethite. Figure 12 shows this configuration where the sleeve has degraded to goethite, and the SNF canister is centered in the pre-breach clay. In the second set, the water content of the clay is increased until the waste package is completely filled. The composition of the clay with the various volume fractions of water is determined in Attachment I, spreadsheet "tmi_calcs.xls," sheet "WP".

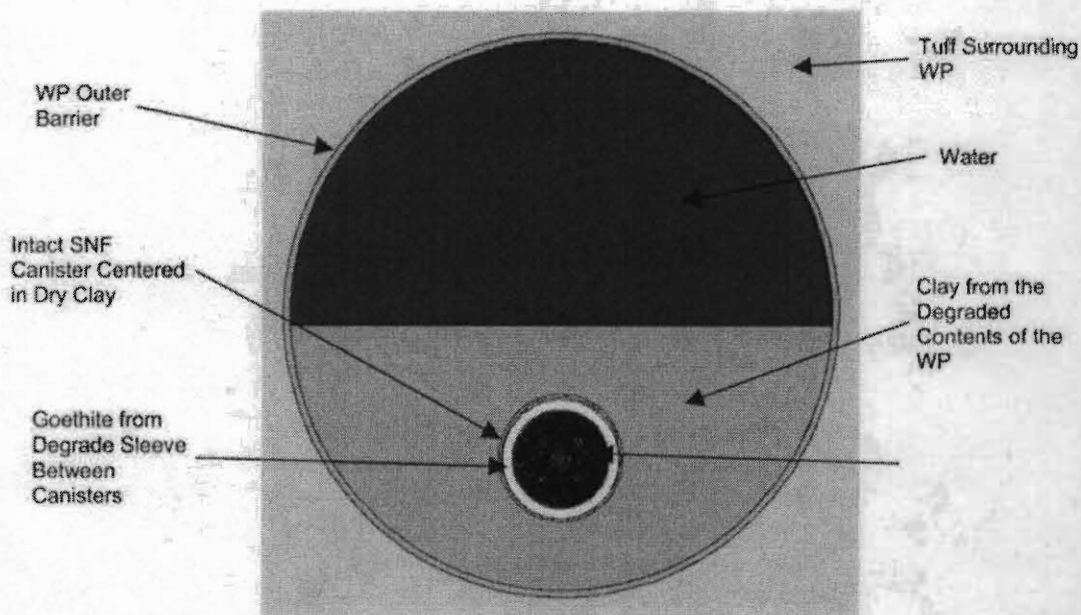


Figure 12. Cross-sectional View of an Intact SNF Canister Centered in Clay Formed from the Degradation of Components External to the Canister

The next table of results, Table 21, considers cases where the TMI canister and sleeve have degraded leaving fuel pellets and goethite in the SNF canister. The description of these cases very closely parallels those in Section 5.5.1. Summarizing, variations in pellet spacing and material composition in the canister are investigated. In the first set, the goethite is neglected leaving only water in the canister. Cases with fuel pellets surrounded by dry goethite covered with water are given in the second and third sets. A case in the second set evaluates the effect of using the earlier design waste package dimensions. In the third set of the table the number of pellet stacks is reduced for some of the more reactive cases of the second set. The remaining results for this section are given in Table 22. Here goethite mixed with sufficient water to completely fill the SNF canister surrounds the fuel pellets. These cases investigate the effects of pellet spacing, reducing the wvf in the goethite and reducing the number of pellet stacks while increasing the number of pellets per stack, and maintaining the same radial pitch and axial spacing between pellets.

5.5.2.2 Degraded SNF Canister with Non-reacted Pre-breach Clay

For these configurations the SNF canister and sleeve have degraded to goethite, but the TMI canister is intact (Section 5.5.2.2.1) or fully degraded (Section 5.5.2.2.2). The goethite formed from the sleeve and canister walls has not yet chemically reacted with the pre-breach clay. The configurations in this section are similar to those in Sections 5.4 and 5.5.1, but now pre-breach clay and goethite, in separate layers, can surround the fuel pellets. The positioning of these configurations in the waste package is varied, and any unoccupied space in the waste package is filled with water. The results of these cases can be found in Section 6.2.2.2.

5.5.2.2.1 Intact TMI Canister with Degraded SNF Canister and Pre-breach Clay in the Waste Package

In these configurations, the TMI canister is intact and surrounded by unmixed layers of pre-breach clay and goethite. The volume fraction of water in the materials is varied. Results for the cases described here are presented in Table 23. For these cases the KO canister contains spherical pellets with identical canister details as that described in Section 5.4. In the first set of the table, the goethite is neglected leaving the canister surrounded by dry pre-breach clay. Cases in this set investigate the effect of reducing the number of pellet stacks in the canister. The first few cases of the second set investigate the effect of changing the position of the canister in the dry clay, and of changing the wvf in the clay. In the next few cases the goethite forms an annulus surrounding the canister which in turn is surrounded by clay. This type of configuration could occur if the SNF canister and sleeve degrade to goethite after being trapped in the pre-breach clay and is shown in Figure 13. Several variations of this case are investigated by changing the volume fraction of water in the goethite surrounding the canister. In the last two cases of the table, the effect of homogeneously mixing pre-breach clay with the water inside of the canister is determined.

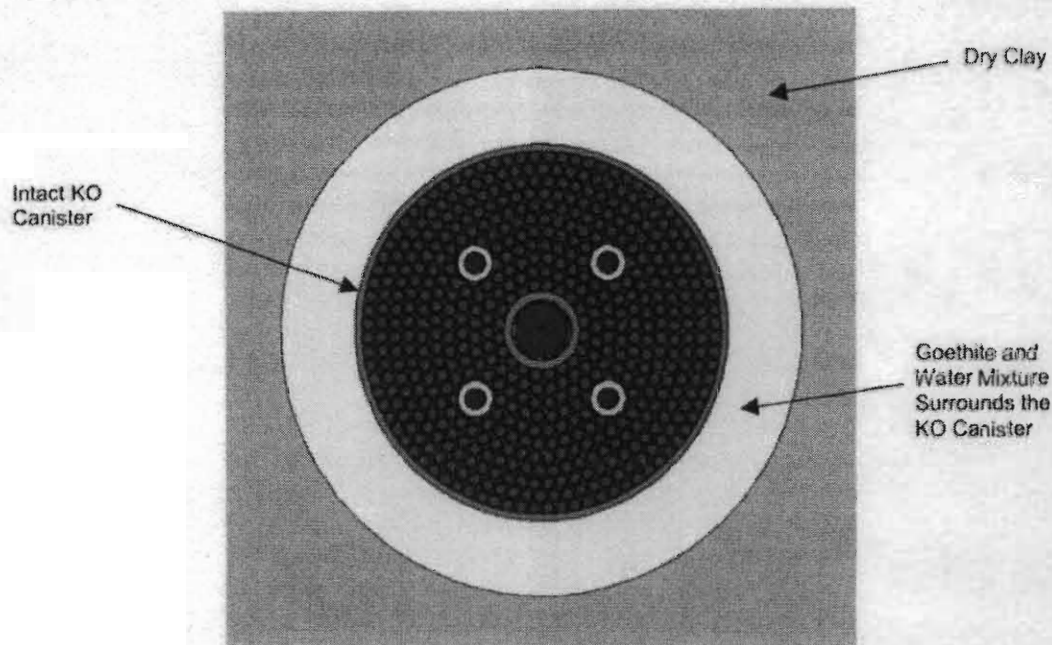


Figure 13. Intact TMI Canister Surrounded by Goethite Trapped in Pre-breach Clay in the Waste Package

5.5.2.2.2 Degraded TMI Canister, Sleeve and SNF Canister with Pre-breach Clay in the Waste Package

These configurations are a continuation of those in Section 5.5.2.1 where the sleeve and TMI canister have degraded, but now the SNF canister is also degraded. These materials can form separate or mixed layers covering the fuel pellets at the bottom of the waste package. Since water is available in the waste package, different wvf in the layers must also be investigated. Figure 14 shows an example of these materials forming different layers in the waste package. Fuel pellets heaped at the bottom of the waste package and are mostly surrounded by a layer of goethite and water. The next layer composed of pre-breach clay and water covers the uppermost pellets. The rest of the waste package is filled with water. Configurations with these materials at least partially mixed together would be more realistic, though due to the high iron content of the pre-breach clay (see Table 9) even complete mixing of these materials would not significantly alter the composition of the clay. The results for these cases are shown in Table 24.

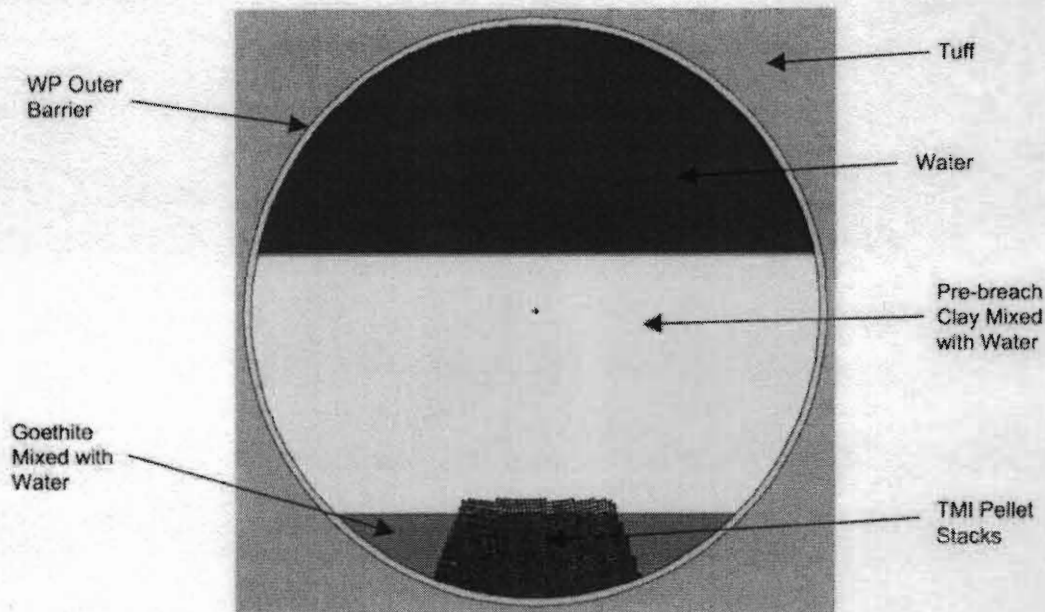


Figure 14. Fuel Pellets Surrounded by Goethite and Pre-breach Clay from Completely Degraded Components in the Waste Package

Variations of the water volume fraction in these materials (goethite and pre-breach clay) and the spacing (pitch) of the pellet stacks are investigated. Different pellet configurations with the same pitch and covered with the same or similar material layers are also considered. For example, the configuration shown in Figure 15 has the same pitch and goethite/water composition for the bottom layer as that shown in Figure 14, but since there are fewer pellet stacks (the number of pellets per stack is appropriately increased) the pellets are almost completely covered by the goethite layer. A case also compares the effect of modeling the earlier design waste package dimensions. Cases with a reduced number of pellet stacks are considered in the second set of the table.

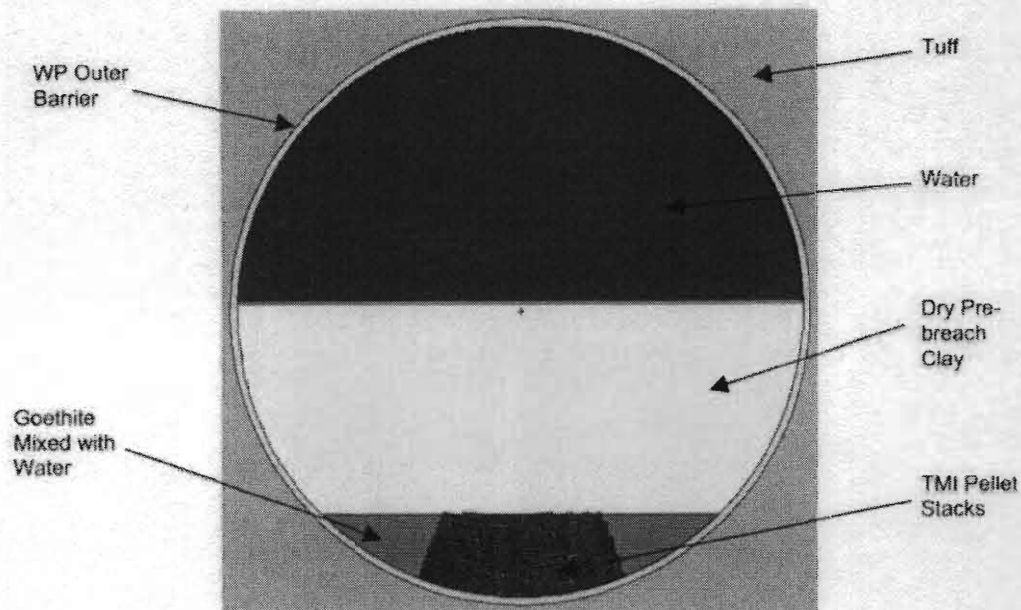


Figure 15. Similar Configuration as Shown in Figure 14 but Fewer Pellet Stacks in Fuel Array

5.5.3 All Components Have Degraded

These configurations represent the final stage of degradation that would occur after the scenario described in Section 5.5.2.2.2. The composition of the clay resulting from the degradation of all components inside the waste package is taken from Tables 10 and 11, which comes from BSC (2001a, pp. 59 and 62). This clay is referred to as post-breach clay and is the clay from the Fort Saint Vrain HTGR SNF analysis. It is used here after neglecting the thorium and uranium content but includes the plutonium from the HLW glass, see Table 9. Compositions for the clay, fuel and/or water mixed in various proportions are determined in Attachment I, spreadsheet "tmi_calcs.xls" sheet "WP." Results for the cases described here are presented in Table 25 where the fuel pellets remain intact and are surrounded by post-breach clay. The pellet configurations are similar to those described in Section 5.5.2.2.2, but only post-breach clay and water are in the waste package. Cases investigate varying pitches, water volume fraction in the clay and pellet configurations. A case also compares the effect of using the earlier design waste package dimensions.

For the next cases, results given in Table 26, one assembly's worth of fuel pellets are assumed to be completely degraded and the fuel is homogenized with the post-breach clay. Three cases are considered, one for each of the compositions given in Tables 10 and 11, so as to determine the most reactive composition. The clay is homogenized with varying amounts of water, and any remaining space in the waste package is filled with water. The percentage of water in the clay is increased until the entire volume available in the waste package is filled with the clay mixture. The effect of neglecting the U-238 content of the fuel is also examined.

6. RESULTS

This report documents the various calculations for intact and degraded mode configurations of the TMI-2 canister waste package. Sections 6.1 and 6.2 present the k_{eff} for the intact and the degraded configurations, respectively. The k_{eff} results represent the average collision, absorption, and track length estimator from the MCNP calculations. The standard deviation (σ) represents the standard deviation of k_{eff} about the average combined collision, absorption, and track length estimate due to Monte Carlo calculation statistics. The average energy of a neutron causing fission (AENCF) is the energy per source particle lost to fission divided by the weight per source neutron lost to fission from the "problem summary section" of the MCNP output. The MCNP input and output files developed for this calculation are included in ASCII format in Attachment I. (The output file name is derived by appending ".o" to the input file name.) The H/X ratio is the ratio of moles of hydrogen to moles of fissile materials (U-235) and is determined on the basis of a fuel pellet unit cell. Since the fuel pellets are typically in an irregular array, the ratio is the simple average of the values of H/X for square and hexagonal unit cells. The array void fraction is also listed for all cases that involve fuel pellets and is determined from the expression for V_f given in Section 5.4.2 using the effective cross-sectional area of the array, unless noted otherwise.

For convenience in referring to cases in a given table, groups of cases may be referred to as a "set," where the set of cases examine variations to a single or limited number of parameters. A preceding header (in bold type) within each table denotes the set. In all discussions of k_{eff} in the text, it is implied that k_{eff} is $k_{\text{eff}} + 2\sigma$. For example, if it states that " k_{eff} for the system is greater than 0.95," it is to be interpreted as " $k_{\text{eff}} + 2\sigma$ for the system is greater than 0.95." Values of k_{eff} in the tables are as labeled in the column headings.

A single PWR fuel assembly is used as the basis for criticality scenarios associated with the TMI canisters. The enrichment of the fuel is assumed to be 3 wt% (Assumption 3.3), giving a U-235 mass of 13.906 kg per assembly. The void fraction inside the fuel is assumed saturated with water (Assumption 3.5). The fuel is modeled as individual pellets with the dimensions given in Section 5.1.1 though spherical pellets with different diameters are investigated. The individual fuel pellet remain axially aligned in what are referred to as "pellet stacks." This applies for either cylindrical or spherical pellets. The results given below are for cylindrical pellets unless otherwise stated. While Boral[™] was installed as an integral portion of the box liner for the fuel assembly, no credit is taken for its presence.

For many cases intact TMI canisters are modeled completely filled with pellets. This is typically more than one assembly's worth of intact fuel pellets or 67,600 pellets. No zirconium is included in the canisters. Zirconium would act as a moderator displacer. The B_4C is replaced by water in the poison tubes of the KO canister, and the annular gap in the center tube contains a mixture of fuel and water. The canisters are assumed water flooded (Assumption 3.5).

For degraded mode calculations, the iron content of stainless steel degrades to goethite ($FeOOH$), and the other steel constituents are neglected. For this process, only the canister walls are considered, and the internal canister components are neglected. The TMI pellets remain intact even

for the completely degraded scenarios. For degraded TMI canisters, one assembly's worth of pellets is used in the analysis.

The interim critical limit (ICL) is assumed to be 0.97 (Assumption 3.6).

6.1 INTACT MODE

This section gives the results of the calculations described in Section 5.4. For these cases intact means that the canisters (both TMI and SNF) and waste package internals (external to the SNF canister) are intact, but the TMI fuel is modeled as being most reactive. For low enrichment, this means the fuel is heterogeneous, i.e., pellets, but not necessarily with the same dimensions as the intact assembly fuel pellets. The following results are for TMI fuel in the KO canister inside an SNF canister in the center basket position of the waste package surrounded by five HLW canisters in the outer basket positions. The KO canister is water flooded, and the empty space in the SNF canister (between canisters and sleeve) is void. The internals of the waste package are intact, empty spaces in the waste package are modeled as void, and the waste package is reflected by dry tuff.

6.1.1 Loose TMI Fuel Pellets in TMI Fuel Canisters and Other Modeling Details

Before evaluating details for TMI fuel, it is necessary to develop a conservative yet realistic model for the fuel in the TMI canister. This is also useful because the characteristics important to the criticality of the fuel can be learned. The first step is to find the most reactive fuel pellet by investigating fuel pellet shape, size and spacing. Here only spherical and cylindrical fuel pellets are considered though it is generally expected that spherical pellets would be as or more reactive than any other shape.

The results shown in Table 12 are for cylindrical pellets in a KO canister. The dimensions of the pellets are the same as those of an intact fuel assembly, i.e., 0.9398 cm diameter and 1.1049 cm length. The spacing between pellet stacks is characterized by a (radial) pitch, and the axial separation between pellets in the stack is characterized by a gap or axial pitch which is simply equal to the length of the pellet plus gap.

Table 12. Cylindrical TMI Fuel Pellets in the Knockout (KO) Canister

Radial Pitch, cm	Axial Pellets Gap, cm	Void Fraction, V_f	$k_{eff} \pm \sigma$	$k_{eff} + 2\sigma$	AENCF, keV	H/X Ratio	File Name
Cylindrical Pellets (R = 0.4699 cm) in Canister^a without Internals							
0.94 ^b	0.	0.188	0.6790 ± 0.0009	0.6808	607.5	25.6	cy-l_0.94.o
1.1	0.	0.400	0.8915 ± 0.0011	0.8936	328.6	68.3	cy-l_1.1.o
1.2	0.	0.494	0.9749 ± 0.0011	0.9771	253.1	98.4	cy-l_1.2.o
1.3	0.	0.570	1.0256 ± 0.0010	1.0276	205.0	131.1	cy-l_1.3.o
1.4	0.	0.623	1.0536 ± 0.0009	1.0555	175.2	166.4	cy-l_1.4.o
1.5	0.	0.669	1.0703 ± 0.0010	1.0722	151.7	204.3	cy-l_1.5.o
1.6	0.	0.710	1.0724 ± 0.0009	1.0742	134.7	244.9	cy-l_1.6.o

Table 12. Cylindrical TMI Fuel Pellets in the Knockout (KO) Canister (Continued)

Radial Pitch, cm	Axial Pellets Gap, cm	Void Fraction, V_f	$k_{eff} \pm \sigma$	$k_{eff} + 2\sigma$	AENCF, keV	H/X Ratio	File Name
1.7	0.	0.739	1.0683 ± 0.0010	1.0704	123.6	288.0	cy-l_1.7.o
1.8	0.	0.767	1.0582 ± 0.0011	1.0603	113.2	333.8	cy-l_1.8.o
1.9	0.	0.789	1.0462 ± 0.0010	1.0482	105.4	382.2	cy-l_1.9.o
2.0	0.	0.809	1.0250 ± 0.0010	1.0269	98.4	433.2	cy-l_2.o
0.94 ^b	0.5	0.441	0.9303 ± 0.0011	0.9324	297.4	77.9	cy-l_94_5.o
0.94 ^b	1.0	0.574	1.0238 ± 0.0010	1.0258	209.3	130.2	cy-l_94_1.o
0.94 ^b	1.25	0.619	1.0415 ± 0.0010	1.0436	186.6	156.4	cy-l_94_1.25.o
0.94 ^b	1.5	0.656	1.0505 ± 0.0010	1.0525	170.1	182.5	cy-l_94_1.5.o
0.94 ^b	1.75	0.686	1.0485 ± 0.0009	1.0503	157.0	208.7	cy-l_94_1.75.o
0.94 ^b	2.0	0.711	1.0398 ± 0.0010	1.0417	148.2	234.8	cy-l_94_2.o
0.94 ^b	2.5	0.751	1.0167 ± 0.0009	1.0186	138.0	287.1	cy-l_94_2.5.o
1.2	0.2	0.571	1.0187 ± 0.0009	1.0205	203.3	132.5	cy-l_1.2_2.o
1.2	0.4	0.628	1.0492 ± 0.0010	1.0512	172.8	166.6	cy-l_1.2_4.o
1.2	0.6	0.672	1.0636 ± 0.0010	1.0655	151.3	200.7	cy-l_1.2_6.o
1.2	0.8	0.706	1.0695 ± 0.0009	1.0713	136.7	234.8	cy-l_1.2_8.o
1.2	1.0	0.734	1.0673 ± 0.0009	1.0691	126.1	268.9	cy-l_1.2_1.o
1.2	1.2	0.757	1.0617 ± 0.0009	1.0635	116.3	303.0	cy-l_1.2_1.2.o
1.3	0.2	0.636	1.0527 ± 0.0011	1.0548	167.5	171.1	cy-l_1.3_2.o
1.3	0.4	0.684	1.0680 ± 0.0010	1.0700	143.5	211.1	cy-l_1.3_4.o
1.3	0.6	0.721	1.0726 ± 0.0010	1.0747	129.2	251.1	cy-l_1.3_6.o
1.3	0.8	0.750	1.0682 ± 0.0009	1.0701	118.3	291.1	cy-l_1.3_8.o
1.4	0.2	0.681	1.0672 ± 0.0010	1.0692	145.5	212.8	cy-l_1.4_2.o
1.4	0.4	0.723	1.0718 ± 0.0010	1.0738	128.2	259.2	cy-l_1.4_4.o
1.4	0.6	0.756	1.0691 ± 0.0010	1.0711	115.0	305.6	cy-l_1.4_6.o
1.5	0.1	0.697	1.0712 ± 0.0010	1.0731	138.9	231.0	cy-l_1.5_1.o
1.5	0.2	0.720	1.0732 ± 0.0010	1.0751	128.5	257.6	cy-l_1.5_2.o
1.5	0.3	0.740	1.0699 ± 0.0010	1.0718	120.3	284.2	cy-l_1.5_3.o
1.5	0.5	0.772	1.0633 ± 0.0010	1.0653	107.9	337.5	cy-l_1.5_5.o
1.6	0.1	0.734	1.0705 ± 0.0009	1.0724	123.4	275.2	cy-l_1.6_1.o
1.6	0.2	0.754	1.0680 ± 0.0010	1.0699	114.9	305.5	cy-l_1.6_2.o
1.6	0.3	0.772	1.0625 ± 0.0010	1.0644	107.4	335.8	cy-l_1.6_3.o
Cylindrical Pellets (R = 0.4699 cm) in Canister^c with Internals							
1.3	0.	0.570	0.9489 ± 0.0010	0.9509	203.3	131.1	cy_1.3.o
1.4	0.	0.623	0.9545 ± 0.0009	0.9563	175.4	166.4	cy_1.4.o
1.5	0.	0.669	0.9605 ± 0.0010	0.9625	156.1	204.3	cy_1.5.o
1.6	0.	0.710	0.9586 ± 0.0010	0.9606	139.3	244.9	cy_1.6.o
1.7	0.	0.739	0.9429 ± 0.0009	0.9447	127.9	288.0	cy_1.7.o
1.3	0.2	0.636	0.9606 ± 0.0010	0.9625	170.1	171.1	cy_1.3_2.o
1.3	0.3	0.661	0.9646 ± 0.0009	0.9665	158.3	191.1	cy_1.3_3.o
1.3	0.4	0.684	0.9649 ± 0.0009	0.9667	147.5	211.1	cy_1.3_4.o
1.3	0.5	0.704	0.9615 ± 0.0011	0.9637	139.5	231.1	cy_1.3_5.o
1.3	0.6	0.721	0.9585 ± 0.0009	0.9604	133.8	251.1	cy_1.3_6.o
1.4	0.1	0.654	0.9555 ± 0.0010	0.9575	162.0	189.6	cy_1.4_1.o
1.4	0.2	0.681	0.9560 ± 0.0010	0.9580	149.0	212.8	cy_1.4_2.o
1.4	0.3	0.703	0.9535 ± 0.0009	0.9554	140.2	236.0	cy_1.4_3.o
1.4	0.4	0.723	0.9514 ± 0.0011	0.9536	130.5	259.2	cy_1.4_4.o

Table 12. Cylindrical TMI Fuel Pellets in the Knockout (KO) Canister (Continued)

Radial Pitch, cm	Axial Pellets Gap, cm	Void Fraction, V_f	$k_{eff} \pm \sigma$	$k_{eff} + 2\sigma$	AENCF, keV	H/X Ratio	File Name
1.4	0.6	0.756	0.9381 ± 0.0010	0.9400	119.8	305.6	cy_1.4_.6.o
1.5	0.1	0.697	0.9575 ± 0.0010	0.9595	143.6	231.0	cy_1.5_.1.o
1.5	0.2	0.720	0.9552 ± 0.0010	0.9571	132.9	257.6	cy_1.5_.2.o
1.5	0.3	0.740	0.9516 ± 0.0010	0.9535	125.1	284.2	cy_1.5_.3.o

NOTES: ^a Canister contains one assembly's worth of pellets.

^b Pellets are essentially touching in the radial direction.

^c Pellet stacks fill the entire length of the canister.

In the first set of Table 12, the pellet array is positioned in the KO canister where the internal poison tubes are neglected (referred to as "without internals"). The pitch of the pellet array and the gap between pellets are varied. For a given pitch, the pellet stacks are positioned so as to best fill the cross-section of the KO canister. The number of pellets per stack (length of stack) is adjusted to give one assembly's worth of pellets per KO canister. The results show the effect of these variations. For the first several cases of the first set, the pellets are axially touching (0 cm gap) and the pitch is varied whereas in the remaining cases of the set the pitch is fixed and the gap is varied.

Similar results are given in the second set, but the internals of the KO canister are included. The portion of any pellet stack that intersects a poison tube is represented as being a partial (incomplete) pellet. In this set, unlike the previous set, the pellet stacks fill the entire length of the KO canister. This models more than one assembly's worth of pellets in the KO canister, with the exact number depending on the pitch and gap. Because no internals are in the upper portion of the canister, i.e., the poison tubes do not extend over the entire inner length of the canister, the fuel pellets always fill this upper (open) portion. Cross-sectional views of the canister at these different elevations are shown in Figure 6.

For cases without canister internals, the results show that for a fixed value of pitch a most reactive case occurs at a specific value of gap. As the pitch increases, these most reactive cases occur at a decreasing value of gap. The largest k_{eff} , 1.0751, occurs for pitch and gap equal to 1.5 cm and 0.2 cm, respectively, though statistically identical values also occur for other values of pitch and gap. For example, k_{eff} for a gap of 0 cm and pitch of 1.7 cm is just a few σ smaller than this largest value. It is interesting to note that these values all have an array void fraction of about 0.72. Any increase in gap and/or pitch causes k_{eff} to further decrease. These values of $k_{eff} > 1$ show that the degraded canister internals are needed for reactivity control. In the second set, the most reactive case, $k_{eff} = 0.9667$, occurs for a pitch and gap of 1.3 cm and 0.4 cm, respectively, though statistically equivalent results also occurs for other values of pitch and gap. The results show similar behavior as the previous set, though the most reactive cases occur for an array void fraction of about 0.68.

The results in the remainder of this section are for spherical pellets and are investigated to insure that the most reactive pellet configuration is modeled. A radial pitch characterizes the spacing of the fuel stacks, but a dimensionless axial pitch is used instead of an axial gap. This dimensionless

pitch is defined to be $(p_{axial} - p_{min}) / (p_{radial} - p_{min})$, where p_{axial} is the axial pitch, p_{min} is the minimum pitch given by $p_{min} = 2R$ (R is the pellet radius) and p_{radial} is the radial pitch. This is a relative measure of the axial to radial spacing between pellets.

The results in Table 13 are for spherical pellets in a KO canister with the poison tubes neglected. The number of pellets is chosen to give an assembly's worth of fuel. The table is divided into four sets, one for each value of radius, and the cases within each set are organized with varying radial pitches for fixed values of the dimensionless axial pitch. Values of k_{eff} for the most reactive case of each set are, 1.0742, 1.0749, 1.0756 and 1.0759 and occur for an array void fraction of about 0.73. These values are statistically identical to each other and to the value for the cylindrical pellets.

Table 13. Spherical TMI Fuel Pellets in the Knockout (KO) Canister^a without Internals

Radial Pitch, cm	Dimensionless Axial Pitch	Void Fraction, V_f	$k_{eff} \pm \sigma$	$k_{eff} + 2\sigma$	AENCF, keV	H/X Ratio	File Name
Spherical Pellets (R = 0.4699 cm)							
1.1	0.	0.600	1.0324 ± 0.0011	1.0345	187.9	147.4	wp1ae-l_1.1t.o
1.2	0.	0.662	1.0605 ± 0.0010	1.0624	156.0	192.6	wp1ae-l_1.2t.o
1.3	0.	0.713	1.0711 ± 0.0010	1.0732	132.0	241.6	wp1ae-l_1.3t.o
1.4	0.	0.749	1.0720 ± 0.0010	1.0739	116.7	294.6	wp1ae-l_1.4t.o
1.5	0.	0.780	1.0608 ± 0.0010	1.0627	104.4	351.5	wp1ae-l_1.5t.o
1.1	0.5	0.631	1.0473 ± 0.0011	1.0496	171.0	167.7	wp1ae-l_1.1h.o
1.2	0.5	0.704	1.0694 ± 0.0010	1.0714	135.1	231.7	wp1ae-l_1.2h.o
1.3	0.5	0.759	1.0706 ± 0.0010	1.0725	112.3	305.2	wp1ae-l_1.3h.o
1.4	0.5	0.798	1.0549 ± 0.0010	1.0569	97.1	388.7	wp1ae-l_1.4h.o
1.1	1.0	0.658	1.0577 ± 0.0010	1.0597	156.8	187.9	wp1ae-l_1.1.o
1.2	1.0	0.736	1.0722 ± 0.0010	1.0742	121.4	270.8	wp1ae-l_1.2.o
1.3	1.0	0.793	1.0586 ± 0.0010	1.0606	99.1	368.7	wp1ae-l_1.3.o
1.4	1.0	0.831	1.0247 ± 0.0009	1.0266	85.5	482.9	wp1ae-l_1.4.o
1.1	1.5	0.681	1.0671 ± 0.0010	1.0690	146.3	208.1	wp1ae-l_1.1+h.o
1.2	1.5	0.762	1.0682 ± 0.0010	1.0701	110.8	309.9	wp1ae-l_1.2+h.o
1.3	1.5	0.818	1.0393 ± 0.0009	1.0410	90.7	432.2	wp1ae-l_1.3+h.o
1.0	2.0	0.577	1.0186 ± 0.0011	1.0209	202.7	131.4	wp1ae-l_1.0+2h.o
1.1	2.0	0.702	1.0708 ± 0.0010	1.0727	137.1	228.4	wp1ae-l_1.1+2h.o
1.2	2.0	0.783	1.0617 ± 0.0011	1.0638	103.1	349.0	wp1ae-l_1.2+2h.o
1.3	2.0	0.838	1.0176 ± 0.0009	1.0195	83.9	495.8	wp1ae-l_1.3+2h.o
Spherical Pellets (R = 0.5200 cm)							
1.2	0.	0.590	1.0310 ± 0.0010	1.0329	193.1	140.8	wp1ac-l_1.2t.o
1.3	0.	0.649	1.0596 ± 0.0010	1.0615	163.0	180.8	wp1ac-l_1.3t.o
1.4	0.	0.697	1.0700 ± 0.0011	1.0721	139.3	224.1	wp1ac-l_1.4t.o
1.5	0.	0.734	1.0718 ± 0.0010	1.0737	123.9	270.5	wp1ac-l_1.5t.o
1.2	0.5	0.619	1.0445 ± 0.0011	1.0467	177.6	158.5	wp1ac-l_1.2h.o
1.3	0.5	0.688	1.0696 ± 0.0010	1.0715	142.9	214.6	wp1ac-l_1.3h.o
1.4	0.5	0.742	1.0720 ± 0.0009	1.0738	119.1	278.4	wp1ac-l_1.4h.o
1.5	0.5	0.783	1.0616 ± 0.0010	1.0636	104.7	350.2	wp1ac-l_1.5h.o
1.2	1.0	0.644	1.0554 ± 0.0010	1.0574	163.9	176.2	wp1ac-l_1.2.o
1.3	1.0	0.719	1.0730 ± 0.0009	1.0749	130.1	248.5	wp1ac-l_1.3.o

Table 13. Spherical TMI Fuel Pellets in the Knockout (KO) Canister^a without Internals (Continued)

Radial Pitch, cm	Dimension-less Axial Pitch	Void Fraction, V _f	k _{eff} ± σ	k _{eff} + 2σ	AENCF, keV	H/X Ratio	File Name
1.4	1.0	0.775	1.0656 ± 0.0010	1.0676	107.3	332.8	wp1ac-l_1.4.o
1.5	1.0	0.816	1.0404 ± 0.0010	1.0423	91.7	430.0	wp1ac-l_1.5.o
1.2	1.5	0.667	1.0623 ± 0.0010	1.0644	154.1	194.0	wp1ac-l_1.2+h.o
1.3	1.5	0.744	1.0713 ± 0.0010	1.0733	119.2	194.0	wp1ac-l_1.3+h.o
1.4	1.5	0.801	1.0492 ± 0.0009	1.0511	97.8	194.0	wp1ac-l_1.4+h.o
1.5	1.5	0.840	1.0137 ± 0.0009	1.0156	84.2	194.0	wp1ac-l_1.5+h.o
1.2	2.0	0.686	1.0680 ± 0.0010	1.0700	144.1	211.7	wp1ac-l_1.2+2h.o
1.3	2.0	0.766	1.0676 ± 0.0010	1.0695	110.0	211.7	wp1ac-l_1.3+2h.o
1.4	2.0	0.821	1.0321 ± 0.0010	1.0340	90.5	211.7	wp1ac-l_1.4+2h.o
Spherical Pellets (R = 0.5450 cm)							
1.1	0.	0.472	0.9514 ± 0.0011	0.9535	271.8	86.5	wp1ab-l_1.1t.o
1.2	0.	0.555	1.0115 ± 0.0010	1.0135	215.1	120.1	wp1ab-l_1.2t.o
1.3	0.	0.615	1.0460 ± 0.0010	1.0479	179.9	156.5	wp1ab-l_1.3t.o
1.4	0.	0.668	1.0665 ± 0.0011	1.0687	153.3	195.9	wp1ab-l_1.4t.o
1.5	0.	0.709	1.0724 ± 0.0009	1.0742	135.3	238.2	wp1ab-l_1.5t.o
1.6	0.	0.741	1.0720 ± 0.0009	1.0739	121.6	283.4	wp1ab-l_1.6t.o
1.1	0.5	0.474	0.9534 ± 0.0010	0.9555	269.5	87.3	wp1ab-l_1.1h.o
1.2	0.5	0.577	1.0227 ± 0.0010	1.0248	202.2	130.7	wp1ab-l_1.2h.o
1.3	0.5	0.649	1.0570 ± 0.0010	1.0591	162.8	180.3	wp1ab-l_1.3h.o
1.4	0.5	0.709	1.0736 ± 0.0010	1.0756	133.4	236.6	wp1ab-l_1.4h.o
1.5	0.5	0.755	1.0711 ± 0.0011	1.0732	115.0	299.9	wp1ab-l_1.5h.o
1.6	0.5	0.790	1.0560 ± 0.0009	1.0578	101.9	370.8	wp1ab-l_1.6h.o
1.1	1.0	0.477	0.9529 ± 0.0012	0.9552	267.4	88.1	wp1ab-l_1.1.o
1.2	1.0	0.596	1.0300 ± 0.0010	1.0319	189.8	141.3	wp1ab-l_1.2.o
1.3	1.0	0.677	1.0669 ± 0.0010	1.0689	148.1	204.0	wp1ab-l_1.3.o
1.4	1.0	0.741	1.0722 ± 0.0010	1.0742	120.0	277.2	wp1ab-l_1.4.o
1.5	1.0	0.789	1.0570 ± 0.0010	1.0589	101.9	361.6	wp1ab-l_1.5.o
1.6	1.0	0.823	1.0298 ± 0.0009	1.0316	89.4	458.1	wp1ab-l_1.6.o
1.2	1.5	0.614	1.0426 ± 0.0011	1.0447	181.5	151.9	wp1ab-l_1.2+h.o
1.3	1.5	0.701	1.0715 ± 0.0010	1.0735	138.1	227.8	wp1ab-l_1.3+h.o
1.4	1.5	0.767	1.0676 ± 0.0010	1.0696	110.6	317.9	wp1ab-l_1.4+h.o
1.5	1.5	0.814	1.0388 ± 0.0010	1.0407	93.4	423.4	wp1ab-l_1.5+h.o
1.2	2.0	0.630	1.0486 ± 0.0011	1.0508	173.0	162.5	wp1ab-l_1.2+2h.o
1.3	2.0	0.722	1.0737 ± 0.0009	1.0755	129.6	251.5	wp1ab-l_1.3+2h.o
1.4	2.0	0.788	1.0575 ± 0.0010	1.0594	103.0	358.5	wp1ab-l_1.4+2h.o
Spherical Pellets (R = 0.56772cm)							
1.136	0.	0.462	0.9438 ± 0.0011	0.9461	280.5	83.5	wp1a-l_tt.o
1.2	0.	0.519	0.9860 ± 0.0010	0.9880	239.9	103.6	wp1a-l_1.2t.o
1.3	0.	0.582	1.0257 ± 0.0010	1.0278	199.3	137.2	wp1a-l_1.3t.o
1.4	0.	0.640	1.0563 ± 0.0011	1.0585	167.0	173.5	wp1a-l_1.4t.o
1.5	0.	0.685	1.0699 ± 0.0009	1.0717	145.9	212.5	wp1a-l_1.5t.o
1.6	0.	0.719	1.0716 ± 0.0010	1.0735	131.1	254.1	wp1a-l_1.6t.o
1.7	0.	0.751	1.0691 ± 0.0009	1.0708	117.7	298.5	wp1a-l_1.7t.o
1.2	0.5	0.532	0.9933 ± 0.0011	0.9954	230.8	109.1	wp1a-l_1.2h.o

Table 13. Spherical TMI Fuel Pellets in the Knockout (KO) Canister^a without Internals (Continued)

Radial Pitch, cm	Dimension-less Axial Pitch	Void Fraction, V _f	k _{eff} ± σ	k _{eff} + 2σ	AENCF, keV	H/X Ratio	File Name
1.3	0.5	0.610	1.0413 ± 0.0010	1.0433	183.0	153.7	wp1a-l_1.3h.o
1.4	0.5	0.677	1.0699 ± 0.0010	1.0720	147.5	204.2	wp1a-l_1.4h.o
1.5	0.5	0.729	1.0724 ± 0.0010	1.0744	127.2	261.0	wp1a-l_1.5h.o
1.6	0.5	0.766	1.0683 ± 0.0010	1.0702	110.5	324.5	wp1a-l_1.6h.o
1.2	1.0	0.544	1.0022 ± 0.0010	1.0042	222.7	114.6	wp1a-l_1.2.o
1.3	1.0	0.635	1.0546 ± 0.0009	1.0565	170.0	170.1	wp1a-l_1.3.o
1.4	1.0	0.708	1.0719 ± 0.0010	1.0739	134.7	234.9	wp1a-l_1.4.o
1.5	1.0	0.762	1.0683 ± 0.0009	1.0701	112.6	309.6	wp1a-l_1.5.o
1.6	1.0	0.800	1.0493 ± 0.0009	1.0511	98.7	394.9	wp1a-l_1.6.o
1.2	1.5	0.556	1.0111 ± 0.0010	1.0131	215.2	120.1	wp1a-l_1.2+h.o
1.3	1.5	0.657	1.0637 ± 0.0010	1.0657	158.9	186.6	wp1a-l_1.3+h.o
1.4	1.5	0.733	1.0740 ± 0.0010	1.0759	124.8	265.6	wp1a-l_1.4+h.o
1.5	1.5	0.787	1.0568 ± 0.0009	1.0587	104.0	358.1	wp1a-l_1.5+h.o
1.2	2.0	0.567	1.0193 ± 0.0011	1.0214	208.3	125.6	wp1a-l_1.2+2h.o
1.3	2.0	0.676	1.0658 ± 0.0010	1.0678	150.6	203.0	wp1a-l_1.3+2h.o
1.4	2.0	0.754	1.0700 ± 0.0010	1.0721	116.6	296.3	wp1a-l_1.4+2h.o
1.5	2.0	0.808	1.0428 ± 0.0010	1.0447	95.5	406.7	wp1a-l_1.5+2h.o

NOTE: ^a Canister contains one assembly's worth of pellets.

The results in Table 14 are for spherical pellets in the KO canister with internal poison tubes. The pellet stacks extend the entire length of the KO canister. As was done with the cylindrical pellets, this models more than one assembly's worth of pellets, with the exact number depending on the axial and radial pitches. The table is divided into sets, one for each value of the four radii of interest. Values of k_{eff} for the most reactive case of each set are 0.9662, 0.9668, 0.9662 and 0.9665, and they occur for an array void fraction of about 0.67. These values are again statistically identical to each other and to the value of k_{eff} for the most reactive case with cylindrical pellets.

Table 14. Spherical TMI Fuel Pellets in the Knockout (KO) Canister^a with Internals

Radial Pitch, cm	Dimension-less Axial Pitch	Void Fraction, V _f	k _{eff} ± σ	k _{eff} + 2σ	AENCF, keV	H/X Ratio	File Name
Spherical Pellets (R = 0.4699 cm)							
1.0	0.	0.523	0.9188 ± 0.0010	0.9208	232.9	106.2	wp1ae_1.0t.o
1.1	0.	0.600	0.9521 ± 0.0010	0.9540	188.4	147.4	wp1ae_1.1t.o
1.2	0.	0.662	0.9643 ± 0.0009	0.9662	157.7	192.6	wp1ae_1.2t.o
1.3	0.	0.713	0.9610 ± 0.0009	0.9628	134.1	241.6	wp1ae_1.3t.o
1.0	0.5	0.538	0.9246 ± 0.0010	0.9265	224.3	112.5	wp1ae_1.0h.o
1.1	0.5	0.631	0.9574 ± 0.0010	0.9594	173.3	167.7	wp1ae_1.1h.o
1.2	0.5	0.704	0.9640 ± 0.0010	0.9660	139.3	231.7	wp1ae_1.2h.o
1.3	0.5	0.759	0.9448 ± 0.0009	0.9467	116.7	305.2	wp1ae_1.3h.o
1.0	1.0	0.551	0.9304 ± 0.0010	0.9324	215.1	118.8	wp1ae_1.0.o
1.1	1.0	0.658	0.9624 ± 0.0010	0.9644	159.0	187.9	wp1ae_1.1.o
1.2	1.0	0.736	0.9584 ± 0.0010	0.9604	125.2	270.8	wp1ae_1.2.o
1.3	1.0	0.793	0.9264 ± 0.0009	0.9282	104.2	368.7	wp1ae_1.3.o
1.0	1.5	0.565	0.9343 ± 0.0011	0.9364	207.3	125.1	wp1ae_1.0+h.o
1.1	1.5	0.681	0.9620 ± 0.0010	0.9640	148.8	208.1	wp1ae_1.1+h.o

Table 14. Spherical TMI Fuel Pellets in the Knockout (KO) Canister^a with Internals (Continued)

Radial Pitch, cm	Dimension-less Axial Pitch	Void Fraction, V _f	k _{eff} ± σ	k _{eff} + 2σ	AENCF, keV	H/X Ratio	File Name
1.2	1.5	0.762	0.9493 ± 0.0009	0.9511	115.7	309.9	wp1ae_1.2+h.o
1.3	1.5	0.818	0.9029 ± 0.0010	0.9048	96.2	432.2	wp1ae_1.3+h.o
Spherical Pellets (R = 0.520 cm)							
1.1	0.	0.520	0.9249 ± 0.0010	0.9269	234.3	103.9	wp1ac_1.1t.o
1.2	0.	0.590	0.9494 ± 0.0010	0.9514	196.0	140.8	wp1ac_1.2t.o
1.3	0.	0.649	0.9622 ± 0.0010	0.9642	163.5	180.8	wp1ac_1.3t.o
1.4	0.	0.697	0.9565 ± 0.0009	0.9584	143.0	224.1	wp1ac_1.4t.o
1.1	0.5	0.533	0.9300 ± 0.0010	0.9320	225.9	109.5	wp1ac_1.1h.o
1.2	0.5	0.619	0.9573 ± 0.0010	0.9592	179.5	158.5	wp1ac_1.2h.o
1.3	0.5	0.688	0.9648 ± 0.0010	0.9668	145.1	214.6	wp1ac_1.3h.o
1.4	0.5	0.742	0.9481 ± 0.0010	0.9501	124.5	278.4	wp1ac_1.4h.o
1.1	1.0	0.546	0.9358 ± 0.0009	0.9376	219.9	115.1	wp1ac_1.1.o
1.2	1.0	0.644	0.9619 ± 0.0009	0.9636	167.8	176.2	wp1ac_1.2.o
1.3	1.0	0.719	0.9599 ± 0.0011	0.9620	133.8	248.5	wp1ac_1.3.o
1.4	1.0	0.775	0.9300 ± 0.0009	0.9319	112.6	332.8	wp1ac_1.4.o
Spherical Pellets (R = 0.5450 cm)							
1.2	0.	0.555	0.9404 ± 0.0010	0.9423	214.2	120.1	wp1ab_1.2t.o
1.3	0.	0.615	0.9571 ± 0.0010	0.9592	181.9	156.5	wp1ab_1.3t.o
1.4	0.	0.668	0.9588 ± 0.0009	0.9606	156.0	195.9	wp1ab_1.4t.o
1.5	0.	0.709	0.9555 ± 0.0010	0.9574	139.0	238.2	wp1ab_1.5t.o
1.2	0.5	0.577	0.9481 ± 0.0009	0.9500	201.1	130.7	wp1ab_1.2h.o
1.3	0.5	0.649	0.9634 ± 0.0010	0.9654	163.4	180.3	wp1ab_1.3h.o
1.4	0.5	0.709	0.9562 ± 0.0009	0.9580	137.9	236.6	wp1ab_1.4h.o
1.2	1.0	0.596	0.9517 ± 0.0009	0.9535	192.1	141.3	wp1ab_1.2.o
1.3	1.0	0.677	0.9643 ± 0.0010	0.9662	151.3	204.0	wp1ab_1.3.o
1.4	1.0	0.741	0.9470 ± 0.0010	0.9490	125.2	277.2	wp1ab_1.4.o
1.2	1.5	0.614	0.9555 ± 0.0009	0.9573	183.6	151.9	wp1ab_1.2+h.o
1.3	1.5	0.701	0.9628 ± 0.0010	0.9647	141.5	227.8	wp1ab_1.3+h.o
1.4	1.5	0.767	0.9362 ± 0.0010	0.9381	115.3	317.9	wp1ab_1.4+h.o
1.1	2.0	0.481	0.9072 ± 0.0011	0.9094	258.9	89.8	wp1ab_1.1+2h.o
1.2	2.0	0.630	0.9596 ± 0.0010	0.9615	175.6	162.5	wp1ab_1.2+2h.o
1.3	2.0	0.722	0.9595 ± 0.0009	0.9614	132.2	251.5	wp1ab_1.3+2h.o
1.4	2.0	0.788	0.9207 ± 0.0009	0.9225	108.2	358.5	wp1ab_1.4+2h.o
Spherical Pellets (R = 0.56772cm)							
1.2	0.	0.519	0.9258 ± 0.0009	0.9277	232.9	103.6	wp1a_1.2t.o
1.3	0.	0.582	0.9483 ± 0.0010	0.9504	198.9	137.2	wp1a_1.3t.o
1.4	0.	0.640	0.9587 ± 0.0010	0.9606	169.5	173.5	wp1a_1.4t.o
1.5	0.	0.685	0.9571 ± 0.0010	0.9590	150.5	212.5	wp1a_1.5t.o
1.6	0.	0.719	0.9620 ± 0.0009	0.9638	133.8	254.1	wp1a_1.6t.o
1.2	0.5	0.532	0.9317 ± 0.0009	0.9336	226.2	109.1	wp1a_1.2h.o
1.3	0.5	0.610	0.9569 ± 0.0009	0.9588	183.3	153.7	wp1a_1.3h.o
1.4	0.5	0.677	0.9602 ± 0.0010	0.9621	152.9	204.2	wp1a_1.4h.o
1.5	0.5	0.729	0.9523 ± 0.0009	0.9541	131.2	261.0	wp1a_1.5h.o
1.2	1.0	0.544	0.9351 ± 0.0010	0.9372	220.6	114.6	wp1a_1.2.o
1.3	1.0	0.635	0.9622 ± 0.0009	0.9640	171.7	170.1	wp1a_1.3.o
1.4	1.0	0.708	0.9576 ± 0.0010	0.9596	139.0	234.9	wp1a_1.4.o
1.5	1.0	0.762	0.9363 ± 0.0009	0.9382	117.9	309.6	wp1a_1.5.o
1.2	1.5	0.556	0.9400 ± 0.0010	0.9419	213.0	120.1	wp1a_1.2+h.o
1.3	1.5	0.657	0.9645 ± 0.0010	0.9665	161.6	186.6	wp1a_1.3+h.o

Table 14. Spherical TMI Fuel Pellets in the Knockout (KO) Canister^a with Internals (Continued)

Radial Pitch, cm	Dimension-less Axial Pitch	Void Fraction, V _f	k _{eff} ± σ	k _{eff} + 2σ	AENCF, keV	H/X Ratio	File Name
1.4	1.5	0.733	0.9525 ± 0.0010	0.9544	128.6	265.6	wp1a_1.4+h.o
1.5	1.5	0.787	0.9216 ± 0.0010	0.9236	109.2	358.1	wp1a_1.5+h.o
1.2	2.0	0.567	0.9457 ± 0.0010	0.9477	205.7	125.6	wp1a_1.2+2h.o
1.3	2.0	0.676	0.9640 ± 0.0009	0.9658	152.7	203.0	wp1a_1.3+2h.o
1.4	2.0	0.754	0.9444 ± 0.0011	0.9465	121.3	296.3	wp1a_1.4+2h.o

NOTE: ^a Pellet stacks fill the entire length of the canister.

In summary, the intact cylindrical pellets are as reactive as the four spherical pellet types considered provided the pellet spacing is optimal. The most reactive cases occur for array void fractions of about 0.72 and 0.67 for canisters without and with internals, respectively, regardless of whether the pellets are cylindrical or spherical. This shows that this parameter is useful in characterizing the pellet array.

In the next table, Table 15, the TMI canister is dry (the fuel is still water saturated), the poison tube inserts are neglected and the canister contains one assembly's worth of fuel. (These are variations of cases in Table 13, but water in the canister is neglected.) In the first case, the pellets are touching in the axial and radial directions, while in the rest of the cases the pellets are separated in either the axial or radial directions. Any increase in spacing between pellets is seen to decrease k_{eff}, though there are no criticality concerns for any of these cases.

Table 15. Spherical TMI Fuel Pellets in Dry Knockout (KO) Canister^a without Internals

Radial Pitch, cm/ Void Fraction	k _{eff} ± σ	k _{eff} + 2σ	AENCF, keV	H/X Ratio	Comment	File Name
No water in KO canister containing Spherical Pellets (R=0.56772 cm)						
1.136 / 0.462	0.3069 ± 0.0005	0.3079	1406.0	7.3	Variation of case wp1a-l_tt.o; pellets touching in radial and axial directions	wp1a-l_tt-w.o
1.136 / 0.543	0.2733 ± 0.0004	0.2741	1461.6	7.3	Axial gap between pellets is 0.2 cm; pellets touching in radial direction	wp1a-l_t+-2-w.o
1.2 / 0.519	0.2838 ± 0.0004	0.2847	1445.3	7.3	Variation of case wp1a-l_1.2t.o; pellets touching in axial direction	wp1a-l_1.2t-w.o
1.4 / 0.640	0.2283 ± 0.0004	0.2290	1531.1	7.3	Variation of case wp1a-l_1.4t.o; pellets touching in axial direction	wp1a-l_1.4t-w.o

NOTE: ^a Canister contains one assembly's worth of pellets.

The results in Table 16 are variations of cases in the previous tables and show the effects of different canister and/or pellet configurations and loadings. In the first four sets of the table, approximately one assembly's worth of fuel pellets are loaded in the KO canister with poison tube inserts. For cases where the entire canister length is not filled with pellets and the poison tube inserts are present, the fuel always fills the upper (open) portion of the canister, unless noted

otherwise. Values of k_{eff} for these cases are 0.9637, 0.9608, 0.9616 and 0.9605 for each of the four different radii. The difference between the most reactive of these cases and that for the canister completely filled with fuel is not statistically significant, indicating that an assembly's worth of fuel in the canister is neutronically infinitely long. Also in the first set are cases where the canister contains an entire assembly's worth of pellets, but fills only 90% and 80% of the canister's cross-section. This is done by reducing the number of pellet stacks. For a horizontally positioned canister it would appear more likely that the cross-section would be partially rather than completely filled with fuel. Each reduction in cross-section decreases k_{eff} by 0.026 and 0.031. Cases where the canister is rotated 45° are included since this gives a different pellet array configuration with respect to the outer poison tubes, see Figure 7. This effect on k_{eff} is insignificant.

Table 16. Variations of Cases with Spherical Fuel Pellets in the Knockout (KO) Canister

Radial Pitch, cm / Void Fraction	$k_{eff} \pm \sigma$	$k_{eff} + 2\sigma$	AEN CF, keV	H/X Ratio	Comment ^a	File Name
Cross-sectional Area Varies for Array of Spherical Pellets (R=0.4699 cm) (Internals Modeled)						
1.2 / 0.704	0.9616 ± 0.0010	0.9637	139.0	231.7	Case wp1ae_1.2h.o but contains one assembly's worth of pellets	wae_1.2hL1as.o
1.2 / 0.704	0.9360 ± 0.0010	0.9379	138.2	231.7	Case wae_1.2hL1as.o but only 90% as many pellet stacks (607/674)	wae_1.2hL1_9.o
1.2 / 0.704	0.9359 ± 0.0009	0.9378	137.6	231.7	Previous case but canister rotated 45°	wae_1.2hL1_9a.o
1.2 / 0.703	0.9047 ± 0.0010	0.9067	141.2	231.7	Case wae_1.2hL1as.o but only 80% as many pellet stacks (539/674)	wae_1.2hL1_8.o
1.2 / 0.703	0.9061 ± 0.0009	0.9079	140.0	231.7	Previous case but canister rotated 45°	wae_1.2hL1_8a.o
Spherical Pellets (R=0.520 cm) in Canister with Internals						
1.3 / 0.688	0.9588 ± 0.0010	0.9608	146.5	214.6	Case wp1ac_1.3h.o but contains one assembly's worth of pellets	wac_1.3h1as.o
1.3 / 0.688	0.9378 ± 0.0010	0.9398	149.0	214.6	Case wp1ac_1.3h.o but water between SNF and KO canisters	wac_1.3h+w.o
Spherical Pellets (R=0.5450 cm) in Canister with Internals						
1.3 / 0.677	0.9596 ± 0.0010	0.9616	151.7	204.0	Case wp1ab_1.3.o but contains one assembly's worth of pellets	wab_1.3as.o
Spherical Pellets (R=0.56772 cm), Cases are Variations of Case wp1a_1.3+h.o						
1.3 / 0.657	0.9586 ± 0.0009	0.9605	163.0	186.6	Contains one assembly's worth of pellets	wL1asa.o
1.3 / 0.657	0.9574 ± 0.0009	0.9592	162.3	186.6	Case wL1asa.o but KO canister moved to top of SNF canister, which in turn is moved to top (right) of waste package	wL1asaR.o
1.3 / 0.657	0.9568 ± 0.0010	0.9587	161.2	186.6	Case wL1asa.o but KO canister filled from bottom end up	wL1Lasa.o
1.3 / 0.657	0.9593 ± 0.0010	0.9613	162.4	186.6	Thickness of sleeve reduced by 1/2 (0.25" thick)	hslv.o
1.3 / 0.657	0.9549 ± 0.0009	0.9568	163.0	186.6	Sleeve is neglected	noslv.o
1.3 / 0.657	0.9650 ± 0.0010	0.9670	160.4	186.6	Stainless steel sleeve replaced with carbon steel sleeve	cstl.o
1.3 / 0.657	0.9557 ± 0.0010	0.9577	165.9	179.3	Case cstl.o but fuel voids contain no water (fuel completely dry)	cstl-sat.o

Table 16. Variations of Cases with Spherical Fuel Pellets in the Knockout (KO) Canister (Continued)

Radial Pitch, cm / Void Fraction	$k_{eff} \pm \sigma$	$k_{eff} + 2\sigma$	AEN CF, keV	H/X Ratio	Comment ^a	File Name
1.3 / 0.657	0.9639 ± 0.0010	0.9659	161.8	186.6	Pellets fill 87.5% of KO canister length	wL-1.o
1.3 / 0.657	0.9620 ± 0.0011	0.9641	162.0	186.6	Pellets fill 75% of KO canister length	wL-2.o
1.3 / 0.657	0.9615 ± 0.0010	0.9636	161.4	186.6	Pellets fill 62.5% of KO canister length	wL-3.o
1.3 / 0.657	0.9550 ± 0.0010	0.9569	161.7	186.6	Pellets fill 50% of KO canister length	wL-4.o
1.3 / 0.657	0.9534 ± 0.0010	0.9555	162.4	186.6	Contains 84.2% of an assembly's worth	wL.842.o
1.3 / 0.657	0.9485 ± 0.0011	0.9506	165.2	186.6	Contains 68.7% of an assembly's worth	wL.687.o
1.3 / 0.657	0.9586 ± 0.0009	0.9604	162.5	186.6	HLW canisters in gravity position	grav1.o
1.3 / 0.657	0.9609 ± 0.0010	0.9629	161.8	186.6	HLW canisters in gravity position, sleeve collapsed	grav2.o
1.3 / 0.657	0.9613 ± 0.0010	0.9634	162.9	186.6	Previous case, but earlier waste package design dimensions used	grav2wp.o
Spherical Pellets (R=0.56772 cm), Cases are Variants of Case wL1asa.o						
1.3 / 0.657	0.9844 ± 0.0010	0.9863	164.0	176.5	Fuel enrichment is 2.96 wt% and contains one kg of Pu-239 per canister	wL1asa+Pu.o
1.3 / 0.657	0.9248 ± 0.0010	0.9267	167.2	212.0	Fuel enrichment is 2.64 wt% (intermediate enrichment)	wL1asaiE.o
1.3 / 0.657	0.9602 ± 0.0010	0.9622	167.9	196.3	Fuel enrichment is 2.64 wt% and contains one kg of Pu-239 per canister	wL1asaiE+Pu.o
Spherical Pellets (R=0.56772 cm), Variants of Case wp1a-l_1.4+h.o (without Internals)						
1.4 / 0.733	1.0803 ± 0.0009	1.0821	123.5	265.6	Entire length of canister filled with pellets	wa-l_1.4+hal.o
1.4 / 0.733	1.0797 ± 0.0010	1.0817	124.4	265.6	Previous case but earlier waste package design dimensions are used	wa-l_1.4+halwp.o
1.4 / 0.733	1.0522 ± 0.0010	1.0542	123.9	265.6	Canister contains one assembly's worth of pellets with 90% as many pellet stacks (444/493)	wa-l_1.4+h_.9.o
1.4 / 0.732	1.0212 ± 0.0010	1.0232	124.6	265.6	Case wa-l_1.4+h_.9.o but 80% as many pellet stacks (394/493)	wa-l_1.4+h_.8.o
1.4 / 0.732	0.9868 ± 0.0010	0.9889	126.3	265.6	Case wa-l_1.4+h_.9.o but 70% as many pellet stacks (345/493)	wa-l_1.4+h_.7.o
1.4 / 0.731	0.9407 ± 0.0010	0.9426	128.8	265.6	Case wa-l_1.4+h_.9.o but 60% as many pellet stacks (296/493); entire length filled	wa-l_1.4+h_.6.o

NOTE: ^a Ratio in parentheses is the reduced number to the original number of pellets stacks.

In the second set, a case is included where the entire SNF canister (outside the TMI canister) is water flooded. This reduces k_{eff} by 0.027.

In the second case of the fourth set of Table 16, the top of the KO canister is positioned next to the top of the SNF canister, which in turn is moved laterally to the top of the waste package. In the

third case of this same set, the KO canister is filled from the bottom up with an assembly's worth of pellets so that the upper (open) portion of the canister does not contain any fuel. Both of these effects are negligible. In the next three cases of the set the stainless steel sleeve is reduced in thickness, neglected and replaced with a carbon steel sleeve of the same dimensions. Neglecting the sleeve reduces k_{eff} by about 0.01, reducing the sleeve thickness by half has the same proportional effect, and replacing the stainless steel with carbon steel has no (statistical) effect. In the next case of the set, any water content in the fuel voids is neglected (for the case with the carbon steel sleeve), reducing k_{eff} by 0.009. In the next 6 cases of the set, the length (and amount) of fuel in the KO canister is reduced until the canister contains less than an assembly's worth of fuel. (Note that an assembly's worth of fuel fills about 51% of the length of the canister.) The difference in k_{eff} between a completely full canister and one containing 68.7% of an assembly's worth of fuel is only 0.016. Finally, in the second and third to the last cases of the set the KO, SNF and HLW canisters are positioned in what would be a gravity position for a horizontally oriented waste package. In the first of these cases, the sleeve is centered in the SNF canister, whereas in the second it is at the bottom of the SNF canister so as to simulate a collapsed sleeve, see Figure 9. The value of k_{eff} for the first of these cases is reduced by 0.006, whereas the second is statistically unchanged. The last case of the set compares the earlier waste package design to the previous case in the set and shows that the results are insensitive to these dimensional changes.

In the fifth set of Table 16, variations in fuel enrichment and plutonium content are investigated. These cases are variations of case wL1asa.o (base case) of the fourth set and contain an assembly's worth of fuel pellets. In the first case, the enrichment is reduced slightly to 2.96 wt% (actual value) and one kg of Pu-239 is added to the fuel. This increases k_{eff} by 0.026 from the base case and exceeds the ICL, though this combination of enrichment and plutonium content is unrealistic. In the next two cases the enrichment is further reduced to that of the intermediate value (2.64 wt%) and one of the cases also contains one kg of Pu-239. The value of k_{eff} for the case without plutonium is reduced by 0.034 as compared to the base case, whereas k_{eff} for the case with plutonium is statistically identical. This demonstrates that the fuel composition modeled here is conservative since the enrichment, U-235 content and plutonium content for this latter case exceeds that of any TMI canister.

In the last set of Table 16 the fuel loading is investigated for a KO canister that does not include the poison tube inserts. The base case for this set is case wp1a-I_1.4+h.o of Table 13. In the first case of the set the canister is completely filled with fuel. This slightly increases k_{eff} by a few σ further indicating that an assembly's worth of fuel is neutronically infinitely long. The next case is a variation of the first case but uses the earlier waste package design dimensions. Results for these cases are statistically identical. For the rest of the cases of this set the canister contains an assembly's worth of fuel, but the fuel array fills only a portion, as indicated in the table, of the canister's cross-section. As the cross-section of the array decreases its length increases thus keeping the amount of fuel constant until the length of the canister is filled (this occurs at a cross-section of 60%) The ICL is only satisfied when the array occupies less than 70% of the canister's cross-section.

Before proceeding with further analysis of the TMI fuel, it is necessary to evaluate TMI fuel in the D-type fuel canister to ensure that it is not more reactive than the KO canister. As such the KO canister has been replaced with a fuel canister, and the reactivity of the system is evaluated. The

fuel is modeled as intact cylindrical fuel pellets that are axially aligned to form pellet stacks that are positioned in a hexagonal array. No axial gap between pellets is considered since it was shown in the first set of Table 12 that a most reactive configuration can be achieved with axially touching pellets as long as the radial pitch is optimal. The fuel canister is water filled, and the empty space in the SNF canister (outside the fuel canister) is modeled as void.

Results are given in Table 17 for the fuel canister (D-type). In the first set of the table, the cross-section of the fuel canister is best filled with whole pellets in stacks, and the length of the stacks is chosen to give one assembly's worth of pellets. In the second set, partial pellet stacks are included around the perimeter of the fuel array. These stacks are where the fuel and inside wall of the canister intersect and this contributes fuel in addition to one assembly's worth. (All cases in the second set contain more than one assembly's worth of fuel.) The pitch of the stacks is varied for both sets. The most reactive case occurs for a pitch of 1.6 cm and an array void fraction of 0.69. These cases are seen to be less reactive than those for the KO canister. Thus the KO canister is used for evaluating the TMI fuel.

Table 17. Cylindrical TMI Fuel Pellets in the Fuel Canister (D-type)

Radial Pitch, cm	Axial Pellet Gap, cm	Void Fraction, V_f	$k_{eff} \pm \sigma$	$k_{eff} + 2\sigma$	AENCF, keV	H/X Ratio	File Name
(Whole) Cylindrical Pellets (R = 0.4699 cm)							
1.4	0.	0.608	0.9048 ± 0.0011	0.9069	195.7	148.0	fh_1.4.o
1.5	0.	0.651	0.9239 ± 0.0010	0.9259	171.8	183.2	fh_1.5.o
1.6	0.	0.693	0.9298 ± 0.0010	0.9318	151.0	220.8	fh_1.6.o
1.7	0.	0.721	0.9331 ± 0.0010	0.9351	137.3	260.9	fh_1.7.o
1.8	0.	0.759	0.9216 ± 0.0010	0.9237	125.0	303.4	fh_1.8.o
(Whole and Partial) Cylindrical Pellets (R = 0.4699 cm)							
1.4	0.	0.608	0.9087 ± 0.0010	0.9107	197.8	148.0	fh_1.4a.o
1.5	0.	0.651	0.9278 ± 0.0011	0.9300	169.9	183.2	fh_1.5a.o
1.6	0.	0.693	0.9366 ± 0.0011	0.9387	151.5	220.8	fh_1.6a.o
1.7	0.	0.721	0.9355 ± 0.0010	0.9375	137.5	260.9	fh_1.7a.o
1.8	0.	0.759	0.9285 ± 0.0010	0.9306	124.3	303.4	fh_1.8a.o

The final results in this section, see Table 18, are for homogenized TMI fuel in the KO canister that neglects the canister internals. For these cases, one assembly's worth of fuel is mixed with various amounts of water as listed in the "comment" column of the table. The remainder of the canister not occupied by the fuel mixture is water filled unless noted otherwise. Comparison of the result for the most reactive water moderated case here with those for the heterogeneous cases, Tables 12 and 13, shows that homogeneous fuel is less reactive.

Table 18. Homogenized TMI Fuel in the Knockout (KO) Canister (without Internals)

$k_{eff} \pm \sigma$	$k_{eff} + 2\sigma$	AEN CF, keV	H/X Ratio	Comment ^a	File Name
0.3403 ± 0.0004	0.3411	1787.3	0.0	No water in fuel or TMI canister; compare to case wp1a-l tt-w.o of Table 15	hom_w0.o
0.4476 ± 0.0006	0.4488	1219.8	7.3	Voids in fuel are water saturated; remainder of TMI canister is dry	hom_sat-w.o
0.4763 ± 0.0007	0.4776	1064.7	7.3	Voids in fuel are water saturated	hom_sat.o
0.6732 ± 0.0009	0.6750	593.3	31.6	Fuel has 20% wvf	hom_w.2.o
0.8514 ± 0.0010	0.8534	339.9	72.1	Fuel has 40% wvf	hom_w.4.o
0.9806 ± 0.0011	0.9828	191.1	153.2	Fuel has 60% wvf	hom_w.6.o
1.0169 ± 0.0010	1.0190	135.8	234.2	Fuel has 70% wvf	hom_w.7.o
1.0140 ± 0.0010	1.0159	89.6	396.3	Fuel has 80% wvf	hom_w.8.o
0.9826 ± 0.0012	0.9849	69.6	558.4	Fuel has 85% wvf	hom_w.85.o
0.9024 ± 0.0013	0.9051	50.1	882.5	Fuel has 90% wvf	hom_w.9.o

NOTE: ^a Water volume fraction (wvf) listed is in addition to the water in the fuel voids; canister contains one assembly's worth of fuel; unless noted otherwise, remainder of TMI canister is water flooded

6.2 DEGRADED MODE

This section gives the results of the calculations described in Section 5.5. Section 6.2.1 presents the results of the calculation where the inner component of the SNF canister degrades before the high-level waste canisters, the SNF canister, and the waste package basket (see Sections 5.5.1). Section 6.2.2 gives the results for the calculation where the internal components of the waste package (but external to the DOE SNF canister) degrade first (see Section 5.5.2). Section 6.2.3 presents the results for a waste package with its internal components fully degraded (see Section 5.5.3).

The results in the previous tables show that TMI fuel modeled as intact cylindrical pellets is just as reactive as any of the spherical pellets that are considered. Thus cylindrical pellets with a diameter and length of 0.9398 cm and 1.1049 cm, respectively, are used for much of the degraded mode analysis. Typical degraded analysis would assume little if any axial redistribution of fuel. Unfortunately, the initial axial distribution of the fuel is unspecified being somewhat random since it depends on the initial loading and subsequent handling of the TMI canister. As such the TMI fuel is assumed to have been in KO canisters because the unoccupied (open) volume above the poison tubes at the top of the canister has a larger cross-sectional area than that available in the fuel canisters. It was empirically determined that 1083 touching pellet stacks could fit into this open cross-section. Thus no more than 1083 pellet stacks are ever present in any degraded analysis. A larger number would only be possible if there were axial redistribution of fuel after the breach of the TMI canister which is not considered here. The length of the stacks is chosen to give one assembly's worth of fuel pellets. This choice for the maximum number of pellet stacks is very

conservative as illustrated by the following considerations. If this limit were determined by assuming the pellets uniformly filled the entire axial length of the KO canister, then the number of pellet stacks could be as small as 214 for a canister that contained one assembly's worth of pellets. This would reduce the fissile linear loading by more than a factor of five leading to a much less reactive configuration. The number of pellet stacks could easily be determined from a realistic, though conservative, estimate of the void fraction in the TMI canister. This is easily done with the expression for the array void fraction, V_f , given in Section 5.4.2. For intact, axially touching cylindrical pellets in the KO canister, 1083 pellets stacks corresponds to a void fraction of 18.6%. Considering that the pellets are randomly packed and the canister contains other inert materials, e.g., zirconium cladding, this value seems unrealistically small.

Since a maximum of just less than 700 pellet stacks fit in the square box structure of the fuel canister, the results for the KO canister easily bound those for the fuel canister.

6.2.1 Inner Components of the SNF Canister Degrade First

This section presents the results of the calculation described in Section 5.5.1. Here the KO canister and sleeve have degraded leaving degradation products and fuel in the SNF canister. Unless noted otherwise, there are 1083 pellet stacks in the canister and the sleeve was stainless steel. The iron components of the KO canister and sleeve degrade to goethite, though the degradation products from the nonferrous components have been released from the waste package and are neglected. The SNF canister is flooded with water, unless noted otherwise, and the other waste package components external to the SNF canister are intact. The HLW canisters are positioned at closest approach to the SNF canister in a non-gravity position, though this detail is unimportant to the criticality of the waste package.

Also listed in the results of this section is the height of the pellet array, H . This is defined as the distance from the inside bottom of the SNF canister to the top of the pellet array. If the array fills the entire cross-section of the canister, then this height is simply equal to the inside diameter of the canister, 43.8 cm. If there is no plausible mechanism to raise pellets against gravity, then the maximum values for H would be 36.2 cm and 37.8 cm for a collapsed and centered sleeve, respectively. Arrays with heights greater than these values are unrealistic since some of the pellets have been raised against gravity. This in effect places an upper limit on the maximum radial pitch for an array with a given number of pellet stacks. Nevertheless, results for such arrays are listed and are shown to be among the most reactive for this scenario.

In the first set of Table 19, the goethite is neglected leaving only fuel surrounded by water in the SNF canister. The first three cases have radially touching pellet stacks and varying axial separation between pellets. For a sufficiently large gap, k_{eff} is greater than critical. In the next case, k_{eff} is also greater than critical for a radial pitch of 1.6 cm and axially touching pellets. In the final case of the set, water is neglected in the canister and the pellets are touching in the radial and axial directions, showing that there are no criticality concerns for a dry canister.

Table 19. TMI Fuel Pellets in SNF Canister (Degraded Sleeve and KO Canister)

Radial Pitch × Axial Gap (cm)/ Void Fraction	$k_{eff} \pm \sigma$	$k_{eff} + 2\sigma$	AEN CF, keV	H/X Ratio ^a	Comment ^b	File Name
Water in SNF Canister; Goethite from Degraded KO Canister and Sleeve is Neglected						
0.94 x 0 / 0.183	0.7000 ± 0.0009	0.7018	550.2	25.6	H=25.7	sn_94_0.o
0.94 x 1 / 0.571	1.0104 ± 0.0010	1.0123	205.3	130.2	H=25.7	sn_94_1.o
0.94 x 1.5 / 0.654	1.0343 ± 0.0011	1.0365	167.3	182.5	H=25.7	sn_94_1.5.o
1.6 x 0 / 0.710	1.1524 ± 0.0009	1.1542	132.6	244.9	Canister contains 631 pellet stacks; H=43.8	sn_1.6_0.o
0.94 x 0 / 0.183	0.3727 ± 0.0005	0.3737	1341. 8	7.3	Void in SNF canister (water is neglected); H=25.7	sn_d_94_0.o
Dry Goethite (from Degraded KO Canister and Sleeve) and Water Surround Fuel						
0.94 x 0 / 0.183	0.5450 ± 0.0007	0.5465	766.3	15.2	H=25.7	sn_g_94_0.o
0.94 x 1 / 0.571	0.7282 ± 0.0009	0.7301	293.6	60.5 130.2	H=25.7	sn_g_94_1.o
0.94 x 1.5 / 0.654	0.7761 ± 0.0009	0.7779	228.5	83.1 156.4	H=25.7	sn_g_94_1.5.o
0.94 x 2.0 / 0.709	0.7877 ± 0.0009	0.7896	196.6	105.8 182.5	H=25.7	sn_g_94_2.o
0.94 x 2.5 / 0.750	0.7760 ± 0.0009	0.7778	177.8	128.4 234.8	H=25.7	sn_g_94_2.5.o
1 x 0 / 0.275	0.5924 ± 0.0007	0.5938	637.2	21.8	H=28.5	sn_g_1_0.o
1.2 x 0 / 0.494	0.8973 ± 0.0010	0.8993	291.4	46.7 98.4	H=41.9	sn_g_1.2_0.o
1.4 x 0 / 0.625	1.0305 ± 0.0010	1.0324	191.9	76.2 166.4	Canister contains 816 pellet stacks; H=43.8	sn_g_1.4_0.o
1.6 x 0 / 0.710	1.0636 ± 0.0010	1.0656	147.0	110.1 244.9	Canister contains 631 pellet stacks; H=43.8	sn_g_1.6_0.o
1.7 x 0 / 0.742	1.0718 ± 0.0010	1.0737	131.2	128.8 288.0	Canister contains 560 pellet stacks; H=43.8	sn_g_1.7_0.o
1.8 x 0 / 0.768	1.0639 ± 0.0009	1.0657	121.4	148.6 333.8	Canister contains 505 pellet stacks; H=43.8	sn_g_1.8_0.o
1.6 x 0 / 0.710	0.7313 ± 0.0008	0.7329	234.4	110.1	Case sn_g_1.6_0.o but canister filled with dry goethite; H=43.8	sn_g+_1.6_0.o
1.6 x 0 / 0.710	1.0132 ± 0.0010	1.0152	154.1	110.1 244.9	Case sn_g_1.6_0.o but canister contained carbon steel sleeve; H=43.8	Sn_gcs_1.6_0.o
Cross-sectional Area of the Pellet Array is Reduced for Some of the Cases in the Previous Set						
1.7 x 0 / 0.746	1.0490 ± 0.0009	1.0509	131.7	128.8 288.0	Canister contains 527 pellet stacks (527/560); H=39.9	sn_g_1.7b_0.o
1.7 x 0 / 0.746	1.0331 ± 0.0010	1.0350	132.8	128.8 288.0	Canister contains 508 pellet stacks (508/560); H=37.9	sn_g_1.7c_0.o
1.6 x 0 / 0.713	0.9599 ± 0.0010	0.9619	157.3	110.1 244.9	Canister contains 573 pellet stacks (573/631); canister contained carbon steel sleeve; H=37.9	sn_gcs_1.6c_0.o

Table 19. TMI Fuel Pellets in SNF Canister (Degraded Sleeve and KO Canister) (Continued)

Radial Pitch × Axial Gap (cm)/ Void Fraction	$k_{eff} \pm \sigma$	$k_{eff} + 2\sigma$	AEN CF, keV	H/X Ratio ^a	Comment ^b	File Name
1.7 x 0 / 0.746	0.9661 ± 0.0010	0.9680	141.1	128.8 288.0	Canister contains 508 pellet stacks (508/560); canister contained carbon steel sleeve; H=37.9	sn_gcs_1.7c_0.o
1.8 x 0 / 0.771	0.9656 ± 0.0010	0.9675	130.1	148.6 333.8	Canister contains 458 pellet stacks (458/505); canister contained carbon steel sleeve; H=37.9	Sn_gcs_1.8c_0.o
Goethite from KO Canister and Sleeve (carbon steel) is Mixed with Water^c						
1 x 0 / 0.275	0.7118 ± 0.0009	0.7135	505.9	32.9	H=28.5	sn_g.42_1_0.o
1 x 1 / 0.620	0.8979 ± 0.0010	0.8999	217.8	123.3	H=28.5	sn_g.42_1_1.o
1 x 1.2 / 0.653	0.8946 ± 0.0009	0.8965	202.1	141.4	H=28.5	sn_g.42_1_1.2.o
1 x 1.4 / 0.680	0.8903 ± 0.0009	0.8922	189.5	159.4	H=28.5	sn_g.42_1_1.4.o
1.2 x 0 / 0.494	0.9066 ± 0.0010	0.9086	293.6	76.8	H=41.9	sn_g.42_1.2_0.o
1.4 x 0 / 0.625	0.9683 ± 0.0010	0.9702	208.0	128.8	Canister contains 816 pellet stacks; H=43.8	sn_g.42_1.4_0.o
1.5 x 0 / 0.671	0.9739 ± 0.0009	0.9757	183.2	157.7	Canister contains 716 pellet stacks; H=43.8	sn_g.42_1.5_0.o
1.6 x 0 / 0.710	0.9673 ± 0.0009	0.9691	162.6	188.7	Canister contains 631 pellet stacks; H=43.8	sn_g.42_1.6_0.o
1.8 x 0 / 0.768	0.9308 ± 0.0008	0.9323	139.7	256.6	Canister contains 505 pellet stacks; H=43.8	sn_g.42_1.8_0.o
1.6 x 0 / 0.710	0.9107 ± 0.0009	0.9125	176.0	170.2	Canister contains 631 pellet stacks; 44.6% wvf; H=43.8	sn_g.55_1.6_0.o
Cross-sectional Area of the Pellets is Reduced for Some of the Cases in the Previous Set						
1.4 x 0 / 0.625	0.9704 ± 0.0010	0.9724	207.3	128.8	Canister contains 802 pellet stacks (802/816); H=41.9	sn_g.42_1.4a_0.o
1.4 x 0 / 0.626	0.9643 ± 0.0009	0.9661	205.3	128.8	Canister contains 777 pellet stacks (777/816); H=39.9	sn_g.42_1.4b_0.o
1.4 x 0 / 0.626	0.9597 ± 0.0009	0.9614	206.5	128.8	Canister contains 747 pellet stacks (747/816); H=37.9	sn_g.42_1.4c_0.o
1.4 x 0.2 / 0.684	0.9596 ± 0.0009	0.9614	175.4	164.2	Canister contains 747 pellet stacks (747/816); H=37.9	sn_g.42_1.4c_2.o
1.4 x 0.4 / 0.726	0.9518 ± 0.0009	0.9535	155.1	199.6	Canister contains 747 pellet stacks (747/816); H=37.9	sn_g.42_1.4c_4.o
1.5 x 0 / 0.672	0.9603 ± 0.0010	0.9623	182.1	157.7	Canister contains 656 pellet stacks (656/716); H=37.9	sn_g.42_1.5c_0.o
1.5 x 0.2 / 0.722	0.9500 ± 0.0009	0.9517	156.9	198.4	Canister contains 656 pellet stacks (656/716); H=37.9	sn_g.42_1.5c_2.o
1.5 x 0.4 / 0.759	0.9321 ± 0.0009	0.9338	140.2	239.1	Canister contains 656 pellet stacks (656/716); H=37.9	sn_g.42_1.5c_4.o

NOTES: ^a Second value of H/X (if given) is for the pellet stacks surrounded by water.

^b Unless noted otherwise, the SNF canister contains 1083 pellet stacks and contained a stainless steel sleeve; ratio in parentheses is the reduced number to the original number of pellets stacks; H is the height (cm) of the pellet array.

^c Water volume fraction (wvf) of mixture is 58.3% which just fills the entire SNF canister.

In the next set of results, dry goethite in the canister is covered by water. Cases investigate varying radial pitch and axial separation. The level of goethite in the canister is determined from the number of fuel pellets submerged in it and the amount produced from degradation. In the first five cases of the set the fuel pellets are touching in the radial direction and are completely submerged in the dry goethite. For these cases an increasing axial gap causes k_{eff} to increase and then reach a maximum value that is much less than the ICL. In the next six cases of the set, an increasing radial pitch places more of the pellets in the water causing k_{eff} to increase. The most reactive of these cases is much greater than critical and occurs at a pitch of 1.7 cm. In the next to the last case of the set, dry goethite replaces all the water in the canister for the case with a pitch of 1.6 cm. This greatly reduces k_{eff} by 0.333, showing that dry goethite is a worse moderator than water though it does have some moderating properties (compare to the last case of the first set of this table). In the last case of the set, the effect of replacing the stainless steel sleeve with a carbon steel sleeve is investigated. This increases the goethite in the canister since carbon steel has a higher iron content than stainless steel. This reduces k_{eff} by 0.050.

In the third set of the table, the cross-sectional area that the fuel array occupies (and thus the number of pellet stacks) is reduced for some of the more reactive cases of the second set. The stainless steel sleeve is also replaced by carbon steel for some of the cases. As seen, this is particularly effective in reducing the system reactivity below the ICL.

In the next to the last set of Table 19, the fuel is surrounded by a mixture of goethite and water. The amount of goethite is based on the canister having contained a carbon steel sleeve, and the volume fraction of water is chosen to be 58.3%. This is the maximum water volume fraction possible because the corresponding mixture volume when combined with the fuel pellet volume just fills the entire SNF canister. The cases in this set examine different combinations of radial pitch and axial separation. A few cases are found that violate the ICL. In the last case of the set, the wvf is reduced to 45% for one of the more reactive cases, and k_{eff} decreases by 0.057 showing that any decrease in wvf also decreases k_{eff} .

Finally in the last set of Table 19, the number of pellet stacks is reduced for some of the more reactive cases of the previous set. A decreasing number of pellet stacks and hence a decreasing linear loading produces a decreasing k_{eff} .

6.2.2 Outer Components of the Waste Package are Degraded (Outside SNF Canister)

This section gives the results of the calculations described in Section 5.5.2. In the configurations studied in this section, the high-level waste canisters and the waste package basket degrade before the inner components of the SNF canister. The results in this section are divided depending upon whether the SNF canister is intact or degraded and are given in Sections 6.2.2.1 and 6.2.2.2, respectively.

6.2.2.1 Intact SNF Canister with Contents Either Intact or Degraded Surrounded by Pre-breach Clay in the Waste Package

The description of the cases evaluated in this section is given in Section 5.5.2.1. The results are for an intact SNF canister whose contents are also intact (case wp1a_1.3+h.o of Table 14 is used as the base case with $k_{\text{eff}} = 0.9665$), and the canister is surrounded by pre-breach clay. The rest of the waste package is water flooded. The results in Table 20 investigate the positioning of the canister in the clay, the effect of water content in the pre-breach clay and the effect of the SNF canister containing clay and/or water. In the first three cases of the first set, the waste package contains dry clay and the location of the canister is positioned just under the surface of the clay, in the center of the clay, and at the bottom of the clay positioned on the waste package bottom. Values of k_{eff} for these cases only differ from the base case value when the canister is just below the surface of the clay, reducing k_{eff} by 0.010. The next case of the set is a comparison with the SNF canister resting on the waste package bottom and the earlier design dimensions used for the waste package. The results are insensitive to this change. In the next four cases, voids in the SNF canister are replaced with clay and/or water. Dry clay between the KO and SNF canisters increases the base case value of k_{eff} by 0.013, but as the water volume fraction of the clay increases k_{eff} decreases until the canister contains only water, where k_{eff} is reduced by 0.028 (relative to the base case). In the last case, dry goethite from the degraded carbon steel sleeve fills the SNF canister, reducing k_{eff} by 0.011. In the second set, the canister is located in the center of the clay, and the volume percent of water in the clay is increased until the waste package is completely filled. For an increasing wvf, k_{eff} decreases demonstrating that dry clay is a more reactive reflector. This occurs because the water 'thermalizes' neutrons away from the canister increasing the probability of capture in the pre-breach clay.

Table 20. TMI Fuel Pellets in Intact SNF and TMI Canisters Surrounded by Pre-breach Clay

$k_{eff} \pm \sigma$	$k_{eff} + 2\sigma$	AEN CF, keV	H/X Ratio	Comment	File Name
Following Cases are Variations of Case wp1a_1.3+h.o^a (R = 0.56772 cm)					
0.9540 ± 0.0011	0.9562	162.2	186.6	Top of SNF canister just below surface of dry clay	w_1.3+h_cla.o
0.9628 ± 0.0010	0.9647	160.9	186.6	SNF canister centered in dry clay	w_1.3+h_clb.o
0.9657 ± 0.0009	0.9675	159.8	186.6	SNF canister at bottom of waste package below dry clay	w_1.3+h_clc.o
0.9645 ± 0.0010	0.9665	160.1	186.6	Previous case but waste package uses earlier design dimensions	w_1.3+h_clcwp.o
0.9778 ± 0.0010	0.9799	158.5	186.6	Case w_1.3+h_clb.o, but SNF canister contains dry clay	w_1.3+h_clb+c.o
0.9709 ± 0.0010	0.9729	158.8	186.6	Case w_1.3+h_clb.o, but SNF canister contains clay with a 10% water volume fraction	w_1.3+h_clb+c.1.o
0.9655 ± 0.0010	0.9674	159.7	186.6	Case w_1.3+h_clb.o, but SNF canister contains clay with a 20% water volume fraction	w_1.3+h_clb+c.2.o
0.9367 ± 0.0009	0.9386	164.0	186.6	Case w_1.3+h_clb.o, but SNF canister contains water	w_1.3+h_clb+w.o
0.9535 ± 0.0010	0.9554	161.9	186.6	Case w_1.3+h_clb.o, but SNF canister contains dry goethite from degraded carbon steel sleeve	w_1.3+h_clb+g.o
Following Cases are Variations of Case w_1.3+h_clb.o^{a, b}					
0.9431 ± 0.0010	0.9451	163.4	186.6	Clay contains 20% water by volume	w_1.3+h_clb.2.o
0.9277 ± 0.0009	0.9296	166.5	186.6	Clay contains 40% water by volume	w_1.3+h_clb.4.o
0.9214 ± 0.0011	0.9235	169.1	186.6	Clay contains 55% water by volume (waste package is full)	w_1.3+h_clb.55.o

NOTES: ^a The radial pitch is 1.3 cm, the dimensionless axial pitch is 1.5 and the void fraction, V_r , is 0.790.

^b The SNF canister is centered in the clay mixture.

For the results in Table 21 the KO canister and sleeve have degraded leaving degradation products and fuel in the intact SNF canister. The outer waste package components have degraded to pre-breach clay leaving the SNF canister centered in dry pre-breach clay. These results closely parallel those in Table 19 of Section 6.2.1. Unless noted otherwise, there are 1083 pellet stacks in the canister, the sleeve was stainless steel and the SNF canister is flooded with water.

Table 21. TMI Fuel Pellets in Intact SNF Canister Surrounded by Dry Pre-breach Clay (Degraded TMI Canister and Sleeve)

Radial Pitch × Axial Gap (cm) / Void Fraction	$k_{eff} \pm \sigma$	$k_{eff} + 2\sigma$	AEN CF, keV	H/X Ratio ^a	Comment ^b	File Name
Water in SNF Canister; Goethite (from Degradation of TMI Canister and Sleeve) is neglected						
0.94 x 0 / 0.183	0.7152 ± 0.0009	0.7171	526.4	25.6	H=25.7	sc_94_0.o
0.94 x 1 / 0.571	1.0142 ± 0.0010	1.0163	204.8	130.2	H=25.7	sc_94_1.o
0.94 x 1.5 / 0.654	1.0365 ± 0.0010	1.0385	165.9	182.5	H=25.7	sc_94_1.5.o
1.6 x 0 / 0.710	1.1568 ± 0.0011	1.1589	130.7	244.9	Canister contains 631 pellet stacks; H=43.8	sc_1.6_0.o
0.94 x 0 / 0.183	0.4290 ± 0.0006	0.4302	1060.5	7.3	Void in SNF canister (water is neglected); H=25.7	sc_d_94_0.o
Dry Goethite (from Degraded KO Canister and Sleeve) and Water Surround Fuel						
0.94 x 0 / 0.183	0.5682 ± 0.0008	0.5697	717.0	15.2	H=25.7	sc_g_94_0.o
0.94 x 1 / 0.571	0.7373 ± 0.0009	0.7391	287.8	60.5 130.2	H=25.7	sc_g_94_1.o
0.94 x 1.5 / 0.654	0.7826 ± 0.0009	0.7844	221.9	83.1 156.4	H=25.7	sc_g_94_1.5.o
0.94 x 2.0 / 0.709	0.7895 ± 0.0008	0.7912	192.6	105.8 182.5	H=25.7	sc_g_94_2.o
0.94 x 2.5 / 0.750	0.7789 ± 0.0009	0.7807	175.8	128.4 234.8	H=25.7	sc_g_94_2.5.o
1 x 0 / 0.275	0.6126 ± 0.0008	0.6142	602.6	21.8	H=28.5	sc_g_1_0.o
1.2 x 0 / 0.494	0.9200 ± 0.0010	0.9219	280.8	46.7 98.4	H=41.9	sc_g_1.2_0.o
1.4 x 0 / 0.625	1.0416 ± 0.0010	1.0435	188.0	76.2 166.4	Canister contains 816 pellet stacks; H=43.8	sc_g_1.4_0.o
1.6 x 0 / 0.710	1.0778 ± 0.0010	1.0797	143.8	110.1 244.9	Canister contains 631 pellet stacks; H=43.8	Sc_g_1.6_0.o
1.6 x 0 / 0.710	1.0749 ± 0.0009	1.0767	144.2	110.1 244.9	Previous case but earlier waste package design dimensions are used	sc_g_1.6_0wp.o
1.7 x 0 / 0.742	1.0776 ± 0.0009	1.0794	129.6	128.8 288.0	Canister contains 560 pellet stacks; H=43.8	sc_g_1.7_0.o
1.8 x 0 / 0.768	1.0692 ± 0.0009	1.0710	119.3	148.6 333.8	Canister contains 505 pellet stacks; H=43.8	sc_g_1.8_0.o
1.6 x 0 / 0.710	0.7422 ± 0.0008	0.7438	226.0	110.1	Case sc_g_1.6_0.o but canister filled with dry goethite; H=43.8	sc_g+_1.6_0.o
1.6 x 0 / 0.710	1.0248 ± 0.0009	1.0266	151.4	110.1 244.9	Case sc_g_1.6_0.o but canister contained carbon steel sleeve; H=43.8	sc_gcs_1.6_0.o
Cross-sectional Area of the Pellet Array is Reduced for Some of the Cases in the Previous Set						
1.7 x 0 / 0.746	1.0530 ± 0.0010	1.0549	130.3	128.8 288.0	Canister contains 527 pellet stacks (527/560); H=39.9	sc_g_1.7b_0.o
1.7 x 0 / 0.746	1.0366 ± 0.0009	1.0384	131.8	128.8 288.0	Canister contains 508 pellet stacks (508/560); H=37.9	sc_g_1.7c_0.o

Table 21. TMI Fuel Pellets in Intact SNF Canister Surrounded by Dry Pre-breach Clay (Degraded TMI Canister and Sleeve) (Continued)

Radial Pitch × Axial Gap (cm) / Void Fraction	$k_{eff} \pm \sigma$	$k_{eff} + 2\sigma$	AEN CF, keV	H/X Ratio ^a	Comment ^b	File Name
1.6 x 0 / 0.713	0.9672 ± 0.0010	0.969 2	156.4	110.1 244.9	Canister contains 573 pellet stacks (573/631) and canister contained carbon steel sleeve; H=37.9	sc_gcs_1.6c_0.o
1.7 x 0 / 0.746	0.9717 ± 0.0009	0.973 6	140.6	128.8 288.0	Canister contains 508 pellet stacks (508/560) and canister contained carbon steel sleeve; H=37.9	sc_gcs_1.7c_0.o
1.8 x 0 / 0.771	0.9709 ± 0.0009	0.972 7	128.4	148.6 333.8	Canister contains 458 pellet stacks (458/505) and canister contained carbon steel sleeve; H=37.9	sc_gcs_1.8c_0.o

NOTES: ^a Second value of H/X (if given) is for the pellet stacks surrounded by water.

^b Unless noted otherwise, the SNF canister contains 1083 pellet stacks and contained a stainless steel sleeve; ratio in parentheses is the reduced number to the original number of pellets stacks; H is the height (cm) of the pellet array, see Section 6.2.1.

In the first set, the goethite from degradation of the KO canister and sleeve is neglected and the pellets are surrounded by water. The SNF canister details for this set are identical to those of the first set of Table 19, and the results vary by only a few σ for the more thermalized cases (lower values of AENCF). For the least thermalized case (dry SNF canister), k_{eff} is 0.057 larger for the canister reflected by dry pre-breach clay.

Again the SNF canister details in the second and third sets are the same as those used in Table 19, i.e., dry goethite covered by water is in the SNF canister, and a variety of pellet array spacings and configurations are examined. The results are roughly 0.005 larger than those of Table 19. A case is also given in the second set of the table comparing the earlier waste package design, showing that the results are insensitive to this design change.

The results in the next table, Table 22, are a continuation of the same configurations as in the previous table, Table 21, except the goethite from the degradation of the KO canister and sleeve is mixed with sufficient water (58.3% wvf) to completely fill the rest of the SNF canister (unless noted otherwise). These results parallel those of the last two sets of Table 19, except the waste package internals are degraded rather than being intact. As indicated by the results in the previous table, the dry pre-breach clay is seen to be a better reflector than the intact waste package internals with the most reactive case of this set being 0.01 larger than the equivalent case of Table 19.

Table 22. TMI Fuel in Intact SNF Canister Containing Goethite Mixed with Water Surrounded by Dry Pre-breach Clay

Radial Pitch × Axial Gap (cm) / Void Fraction	$k_{eff} \pm \sigma$	$k_{eff} + 2\sigma$	AEN CF, keV	H/X Ratio	Comment ^a	File Name
Goethite from KO Canister and Sleeve (Carbon Steel) is Mixed with Water^b						
1 x 0 / 0.275	0.7259 ± 0.0009	0.7276	485.9	32.9	H=28.5	sc_g.42_1_0.o
1 x 0.8 / 0.580	0.8978 ± 0.0009	0.8996	236.0	105.2	H=28.5	sc_g.42_1_8.o
1 x 1 / 0.620	0.9037 ± 0.0010	0.9056	216.1	123.3	H=28.5	sc_g.42_1_1.o
1 x 1.2 / 0.653	0.9002 ± 0.0009	0.9020	200.1	141.4	H=28.5	sc_g.42_1_1.2.o
1 x 1.4 / 0.680	0.8946 ± 0.0009	0.8965	187.3	159.4	H=28.5	sc_g.42_1_1.4.o
1 x 1.6 / 0.704	0.8851 ± 0.0009	0.8869	177.8	177.5	H=28.5	sc_g.42_1_1.6.o
1 x 1.8 / 0.724	0.8693 ± 0.0009	0.8710	171.5	195.6	H=28.5	sc_g.42_1_1.8.o
1.2 x 0 / 0.494	0.9209 ± 0.0009	0.9228	284.5	76.8	H=41.9	sc_g.42_1.2_0.o
1.4 x 0 / 0.625	0.9800 ± 0.0010	0.9819	203.1	128.8	Canister contains 816 pellet stacks; H=43.8	sc_g.42_1.4_0.o
1.5 x 0 / 0.671	0.9822 ± 0.0009	0.9839	179.4	157.7	Canister contains 716 pellet stacks; H=43.8	sc_g.42_1.5_0.o
1.6 x 0 / 0.710	0.9734 ± 0.0008	0.9750	161.4	188.7	Canister contains 631 pellet stacks; H=43.8	sc_g.42_1.6_0.o
1.8 x 0 / 0.768	0.9356 ± 0.0009	0.9373	138.0	256.6	Canister contains 505 pellet stacks; H=43.8	sc_g.42_1.8_0.o
1.6 x 0 / 0.710	0.9174 ± 0.0009	0.9192	174.2	170.2	Canister contains 631 pellet stacks; 44.6% water volume fraction; H=43.8	sc_g.55_1.6_0.o
Cross-sectional Area of Pellet Array is Reduced for Most Reactive Cases of Previous Set						
1.4 x 0 / 0.625	0.9779 ± 0.0009	0.9797	202.2	128.8	Canister contains 802 pellet stacks (802/816); H=41.9	sc_g.42_1.4a_0.o
1.4 x 0 / 0.626	0.9703 ± 0.0010	0.9722	202.6	128.8	Canister contains 777 pellet stacks (777/816); H=39.9	sc_g.42_1.4b_0.o
1.4 x 0 / 0.626	0.9629 ± 0.0009	0.9648	202.7	128.8	Canister contains 747 pellet stacks (747/816); H=37.9	sc_g.42_1.4c_0.o
1.4 x 0.2 / 0.684	0.9615 ± 0.0009	0.9633	172.8	164.2	Canister contains 747 pellet stacks (747/816); H=37.9	sc_g.42_1.4c_2.o
1.4 x 0.4 / 0.726	0.9551 ± 0.0009	0.9569	153.9	199.6	Canister contains 747 pellet stacks (747/816); H=37.9	sc_g.42_1.4c_4.o
1.5 x 0 / 0.672	0.9647 ± 0.0009	0.9664	179.0	157.7	Canister contains 656 pellet stacks (656/716); H=37.9	sc_g.42_1.5c_0.o
1.5 x 0.2 / 0.722	0.9565 ± 0.0010	0.9584	155.5	198.4	Canister contains 656 pellet stacks (656/716); H=37.9	sc_g.42_1.5c_2.o
1.5 x 0.4 / 0.759	0.9365 ± 0.0008	0.9382	139.4	239.1	Canister contains 656 pellet stacks (656/716); H=37.9	sc_g.42_1.5c_4.o
1.6 x 0 / 0.684	0.9654 ± 0.0009	0.9671	161.3	188.7	Canister contains 597 pellet stacks (597/613); H=39.9	Sc_g.42_1.6b_0.o

NOTES: ^a The SNF canister contained a carbon steel sleeve and, unless noted otherwise, 1083 pellet stacks; ratio in parentheses is the reduced number to the original number of pellets stacks; H is the height (cm) of the pellet array, see Section 6.2.1.

^b Water volume fraction (wvf) of mixture is 58.3% which just fills the entire SNF canister.

In the next set, the number of pellet stacks is reduced so that only a portion of the cross-sectional area of the SNF canister is filled for those cases in the previous set that exceed the ICL. For a reduction in the number of stacks, the number of pellets per stack is appropriately increased to maintain an assembly's worth of pellets per canister. The results show that an 8.4% reduction in the number of pellet stacks is sufficient to meet the ICL for the most reactive case of the first set. Additional cases are included for this configuration to show that increasing axial gap further decreases k_{eff} .

6.2.2.2 TMI Fuel Surrounded by Degradation Products with (Non-reacted) Pre-breach Clay

In this section the SNF canister and sleeve have degraded to goethite that has mixed, but not chemically reacted, with the pre-breach clay formed from the degradation of the outer components of the waste package. These cases are described in Section 5.5.2.2, and the results are presented in Sections 6.2.2.2.1 (intact TMI canister) and 6.2.2.2.2 (degraded TMI canister).

6.2.2.2.1 Intact KO Canister Surrounded by Degradation Products from the SNF Canister and Sleeve Mixed with Pre-breach Clay

The results in this section are for the KO canister and its contents intact and the rest of the components in the waste package degraded as described in Section 5.5.2.2.1. The cases considered are based on some of the more reactive cases of Table 14 with the description of the KO canister and its contents being identical. Unless noted otherwise, the canister is centered in dry pre-breach clay. The results for these cases are given in Table 23. In the first set of the table, the goethite from the degraded SNF canister and sleeve is neglected. The first two cases demonstrate that a canister containing one assembly's worth of fuel is no more reactive than a canister completely filled with fuel. Values of k_{eff} for these cases are 0.014 larger than the base case value ($k_{\text{eff}} = 0.9660$), showing that dry pre-breach clay in the waste package is more reactive than intact internals. In the last two cases of the set the number of pellet stacks is reduced filling a smaller portion of the canister cross-section (as indicated in the table). The ICL is satisfied for even a 10% reduction in the number of stacks.

Table 23. TMI Fuel in Intact KO Canister with Degraded SNF Canister Surrounded by Pre-breach Clay

$k_{eff} \pm \sigma$	$k_{eff} + 2\sigma$	AEN CF, keV	H/X Ratio	Comment	File Name
Variations of Case wp1ae_1.2h.o^a (R = 0.4699 cm) of Table 14 and Goethite Neglected					
0.9780 ± 0.0010	0.9800	135.3	231.7	Spherical pellets fill canister	wae-s_clb.o
0.9747 ± 0.0009	0.9765	137.7	231.7	Canister contains one assembly's worth of fuel pellets	wae-s_1.2has_clb.o
0.9450 ± 0.0010	0.9470	137.1	231.7	Previous case, but pellet array fills 90% of canister cross-section	wae-sas_clb_.9.o
0.9135 ± 0.0009	0.9154	139.7	231.7	Previous case, but pellet array fills 80% of canister cross-section	wae-sas_clb_.8.o
Following Cases are Variations of Case wp1a_1.3+h.o^b (R = 0.56772 cm) of Table 14					
0.9767 ± 0.0010	0.9788	158.0	186.6	Canister centered in clay; goethite neglected	w-s_clb.o
0.9782 ± 0.0010	0.9802	158.1	186.6	Previous case, but canister at bottom of WP	w-s_clc.o
0.9519 ± 0.0010	0.9539	161.6	186.6	Case w-s_clb.o, but 20% (by volume) water in clay	w-s_clb.2.o
0.9381 ± 0.0010	0.9401	163.1	186.6	Case w-s_clb.o, but 40% (by volume) water in clay	w-s_clb.4.o
0.9499 ± 0.0010	0.9520	161.8	186.6	Canister surrounded by dry goethite centered in dry clay	w-s_g_clb.o
0.9405 ± 0.0010	0.9425	162.4	186.6	Previous case, but 20% (by volume) water in goethite	w-s_g.8_clb.o
0.9311 ± 0.0011	0.9332	164.2	186.6	Previous case, but 40% (by volume) water in goethite	w-s_g.6_clb.o
0.9459 ± 0.0010	0.9478	163.4	186.6	Case w-s_g_clb.o, but SNF canister contained a carbon steel sleeve	w-s_gcs_clb.o
0.9582 ± 0.0009	0.9600	162.4	178.5	Case w-s_clb.o but 5% (by volume) clay mixed with water in TMI canister	w-s_clb+c.05i.o
0.9491 ± 0.0009	0.9509	165.7	174.5	Case w-s_clb.o but 7.5% (by volume) clay mixed with water in TMI canister	w-s_clb+c.075i.o

NOTES: ^a Void fraction is 0.704.^b Void fraction is 0.657.

In the first four cases of the second set, the goethite is again neglected and the positioning of the canister and the water content of the pre-breach clay are varied. The addition of water to the clay decreases k_{eff} , but the reactivity is unchanged for the canister at the center or bottom of the dry clay. For the rest of the cases of the set the canister is centered in dry clay since this is most reactive. In the next four cases of the set, the goethite mixed with varying amounts of water (as indicated in the table) forms an annulus around the canister. The amount of goethite is based on a stainless steel sleeve, though one case considers an increased amount of goethite based on a carbon steel sleeve. Results for these cases show that an increase in either goethite or water in the goethite decreases k_{eff} . In the last two cases of the set, the goethite is neglected, the canister is centered in the dry pre-breach clay layer (shown to be the most reactive configuration) and a small amount of pre-breach clay is homogeneously mixed with the water inside the KO canister. The results for these cases show that an increase in the amount of clay inside the canister causes a decrease in k_{eff} .

6.2.2.2.2 Degraded SNF Canister, TMI Canister and Sleeve Mixed with Pre-breach Clay Surround TMI Fuel

The results in this section are for cases described in Section 5.5.2.2.2 where pre-breach clay and goethite from the degraded SNF canister, sleeve (carbon steel) and TMI canister surround the TMI fuel pellets at the bottom of the waste package. These materials are assumed to form separate layers that may also contain water and/or fuel. In general, some of the pellets are in each of the different layers depending on the volume of each material, the order in which the materials are layered and the height of the pellet stack. In determining the height of each layer the displacement of pellets is considered. Pellet stacks of cylindrical pellets with no axial gap between pellets are modeled for these cases. The composition of each layer is given in the table as well as the volume fraction of water in the materials. These results are given in Table 24. The values of H/X listed in the table are an average of the values for square and triangular lattices and are also weighted by the number of pellet stacks in each layer (for those cases where the stacks are in different layers).

Table 24. TMI Fuel Pellets Form Array Surrounded by Layers of Goethite and Pre-breach Clay in the Waste Package

Bottom Layer Contents by Volume (%)	Next Layer Contents by Volume (%)	Radial Pitch (cm) ^a / Comment / Void Fraction ^b	$k_{\text{eff}} \pm \sigma$	$k_{\text{eff}} + 2\sigma$	AENCF (keV)	H/X Ratio	File Name
The Following Cases Have 1083 Pellet Stacks (Unless Noted Otherwise)							
Goethite 100	Clay 100	1.0	0.5673 ± 0.0007	0.5687	692.3	21.8 10.6	wp_1a_g_c.o
Water 100	Clay 100	1 / Previous case but water replaces goethite (goethite neglected)	0.7119 ± 0.0009	0.7138	512.9	40.8 10.6	wp_1a_w_c.o
Goethite 40 water 60	Clay 100	1.2	0.8759 ± 0.0009	0.8777	308.4	77.7 16.3	wp_1.2a_g.4_c.o
Goethite 40 water 60	Clay 100	1.2 / Previous case but different pellet stack configuration	0.9039 ± 0.0009	0.9057	290.2	77.7 16.3	wp_1.2b_g.4_c.o
Goethite 40 water 60	Clay 100	1.4	0.9459 ± 0.0009	0.9476	220.4	130.3 23.1	wp_1.4a_g.4_c.o
Goethite 40 water 60	Clay 100	1.4 / Previous case but different pellet stack configuration	0.9707 ± 0.0010	0.9726	205.7	130.3 23.1	wp_1.4b_g.4_c.o
Goethite 40 water 60	Clay 80 water 20	1.4 / Same configuration as case wp_1.4b_g.4_c.o	0.9720 ± 0.0010	0.9739	205.2	130.3 51.7	wp_1.4b_g.4_c.8.o
Goethite 40 water 60	Clay 100	1.4 / Similar configuration as case wp_1.4b_g.4_c.o but only 946 stacks	0.9723 ± 0.0009	0.9742	197.9	130.3 23.1	wp_1.4bL_g.4_c.o
Goethite 40 water 60	Clay 100	1.5	0.9584 ± 0.0009	0.9602	194.2	159.6 26.8	wp_1.5a_g.4_c.o
Goethite 40 water 60	Clay 100	1.5 / Previous case but different pellet stack configuration	0.9783 ± 0.0009	0.9802	180.0	159.6 26.8	wp_1.5b_g.4_c.o
Goethite 40 water 60	Clay 80 water 20	1.5 / Same configuration as case wp_1.5b_g.4_c.o	0.9768 ± 0.0009	0.9786	180.6	159.6 62.3	wp_1.5b_g.4_c.8.o

Table 24. TMI Fuel Pellets Form Array Surrounded by Layers of Goethite and Pre-breach Clay in the Waste Package (Continued)

Bottom Layer Contents by Volume (%)	Next Layer Contents by Volume (%)	Radial Pitch (cm) ^a / Comment / Void Fraction ^b	$k_{eff} \pm \sigma$	$k_{eff} + 2\sigma$	AENCF (keV)	H/X Ratio	File Name
Goethite 40 water 60	Clay 60 water 40	1.5 / Same configuration as case wp_1.5b_g.4_c.o	0.9798 ± 0.0009	0.9816	176.5	159.6 97.8	wp_1.5b_g.4_c.6.o
Goethite 40 water 60	Clay 47 water 53	1.5 / Same configuration as case wp_1.5b_g.4_c.o ^c	0.9813 ± 0.0010	0.9833	176.7	159.6 120.7	wp_1.5b_g.4_c.47.o
Goethite 40 water 60	Clay 47 water 53	Previous case but earlier WP design dimensions used	0.9817 ± 0.0008	0.9834	175.9	159.6 120.7	wp_1.5b_g.4_c.47p.o
Goethite 60 water 40	Clay 46 water 54	1.5 / Same configuration as case wp_1.5b_g.4_c.o ^c	0.9136 ± 0.0009	0.9155	195.3	137.3 122.8	wp_1.5b_g.6_c.46.o
Goethite 80 water 20	Clay 45 water 55	1.5 / Same configuration as case wp_1.5b_g.4_c.o ^c	0.8787 ± 0.0009	0.8805	206.3	114.9 123.8	wp_1.5b_g.8_c.45.o
Goethite 100	Clay 45 water 55	1.5 / Same configuration as case wp_1.5b_g.4_c.o ^c	0.8696 ± 0.0009	0.8714	212.5	92.6 124.3	Wp_1.5b_g_c.45.o
Goethite 100	Clay 100	1.5 / Same configuration as case wp_1.5b_g.4_c.o	0.6713 ± 0.0008	0.6729	301.9	92.6 26.8	wp_1.5b_g_c.o
Goethite 40 water 60	Clay 100	1.5 / Similar configuration as case wp_1.5b_g.4_c.o but only 954 stacks	0.9738 ± 0.0009	0.9756	174.6	159.6 26.8	wp_1.5bL_g.4_c.o
Goethite 40 water 60	Clay 100	1.6	0.9578 ± 0.0009	0.9596	174.9	191.0 30.9	wp_1.6a_g.4_c.o
Goethite 40 water 60	Clay 80 water 20	1.6 / Same configuration as case wp_1.6a_g.4_c.o	0.9665 ± 0.0008	0.9682	172.3	191.0 73.7	wp_1.6a_g.4_c.8.o
Goethite 40 water 60	Clay 100	1.6 / Similar configuration as case wp_1.6a_g.4_c.o but only 729 stacks	0.9615 ± 0.0009	0.9634	161.3	191.0 30.9	wp_1.6aL_g.4_c.o
Goethite 40 water 60	Clay 100	1.6 / Case wp_1.6a_g.4_c.o but different configuration	0.9688 ± 0.0009	0.9706	163.9	191.0 30.9	wp_1.6b_g.4_c.o
Goethite 40 water 60	Clay 47 water 53	1.6 / Same configuration as case wp_1.6b_g.4_c.o	0.9738 ± 0.0009	0.9755	158.3	191.0 144.0	wp_1.6b_g.4_c.47.o
Goethite 40 water 60	Clay 100	1.8	0.9316 ± 0.0009	0.9333	149.8	259.7 39.7	wp_1.8a_g.4_c.o
Goethite 40 water 60	Clay 100	1.8 / Previous case but different pellet stack configuration	0.9338 ± 0.0008	0.9354	141.5	259.7 39.7	wp_1.8b_g.4_c.o
Variations of Cases in the Previous Set but with Number of Pellet Stacks Reduced (less than 1083)							
Goethite 40 water 60	Clay 47 water 53	1.5 / Case wp_1.5b_g.4_c.47.o but 998 pellet stacks (998/1083)	0.9728 ± 0.0009	0.9747	175.6	159.6 120.7	wp_1.5bb_g.4_c.47.o

Table 24. TMI Fuel Pellets Form Array Surrounded by Layers of Goethite and Pre-breach Clay in the Waste Pckage (Continued)

Bottom Layer Contents by Volume (%)	Next Layer Contents by Volume (%)	Radial Pitch (cm) ^a / Comment / Void Fraction ^b	$k_{eff} \pm \sigma$	$k_{eff} + 2\sigma$	AENCF (keV)	H/X Ratio	File Name
Goethite 40 water 60	Clay 47 water 53	1.5 / Case wp_1.5b_g.4_c.47.o but 932 pellet stacks (932/1083)	0.9615 ± 0.0009	0.9632	175.1	159.6 120.7	wp_1.5bc_g.4_c.47.o
Goethite 40 water 60	Clay 47 water 53	1.6 / Case wp_1.6b_g.4_c.47.o but 1065 pellet stacks (1065/1083)	0.9729 ± 0.0008	0.9746	158.7	191.0 144.0	wp_1.6ba_g.4_c.47.o
Goethite 40 water 60	Clay 47 water 53	1.6 / Case wp_1.6b_g.4_c.47.o but 998 pellet stacks (998/1083)	0.9651 ± 0.0009	0.9670	157.8	191.0 144.0	wp_1.6bb_g.4_c.47.o

NOTES: ^a Cylindrical pellets with no axial gap; ratio in parentheses is the reduced number to the original number of pellets stacks.

^b Void fractions are equal to the simple average of the void fractions for a square and hexagonal unit cell; values are: 0.253, 0.481, 0.619, 0.668, 0.708 and 0.769 for pitches of 1.0 cm, 1.2 cm, 1.4 cm, 1.5 cm, 1.6 cm and 1.8 cm, respectively.

^c The waste package is completely filled by fuel and layers of degraded materials.

In the first set of results in the table, there are 1083 pellet stacks, unless noted otherwise, this being the maximum number of axially aligned stacks that fit in a KO canister. The results are arranged in order of increasing radial pitch. For each value of pitch the water volume fractions of the layers are varied and/or different pellet configurations are investigated. The bottom layer is composed of goethite and/or water, and this layer is covered by a layer of pre-breach clay and water. Any remaining space in the waste package is water flooded. A case in this set using the earlier waste package design dimensions shows that the results are insensitive to this change.

Examination of the results in this set shows that the reactivity for each case is dependent on the pellet array configuration, pitch and water content of the material. The configurations can be categorized according to the surface to volume (S/V) ratios of the entire pellet array with a more compacted array having a smaller S/V ratio than an array where the pins are spread out. For all else being equal (fuel, pitch and composition of material), the larger S/V ratios promote more neutron leakage and a decreased k_{eff} . Smaller S/V ratio configurations would appear to be less probable since any disturbance of the waste package would tend to spread out the pins increasing the S/V ratio, increasing leakage and decreasing k_{eff} . For increasing pitch, the results show that k_{eff} initially increases, reaches a maximum value and then decreases. An increasing water content in the degradation materials has the greatest effect when applied to the bottom layer where a significant amount of the fuel is found. This is further illustrated by those cases where decreasing the number of pellet stacks either has no effect on or slightly increases the reactivity. This illustrates the interplay between the pitch, fuel pellet configuration and water content of the materials.

In the second set of the table, the number of pellet stacks for some of the more reactive cases of the first set is sufficiently reduced so that the ICL is satisfied.

6.2.3 TMI Fuel Surrounded by Post-breach Clay in the Waste Package

This section presents the results of the calculations described in Section 5.5.3. Table 25 gives the values of k_{eff} for these calculations where the waste package containing post-breach clay (composition given in Table 10 at 72689 years) surrounds the TMI fuel pellets. For most of the cases in the table, the post-breach clay is mixed with sufficient water to completely fill the waste package. The radial pitch of the pellet stack is varied, and the largest value of k_{eff} occurs at a pitch of 1.6 cm. For this most reactive case, the volume fraction of water is decreased until the post-breach clay is dry. Decreasing the amount of water in the clay is seen to decrease k_{eff} . Other cases investigate a different pellet configuration and reducing the number of pellet stacks for this most reactive case, these reduce k_{eff} below the ICL. A case is also included showing that the earlier waste package design dimensions produces statistically identical results.

Table 25. TMI Fuel Pellets are Surrounded with the Post-breach Clay
(Clay Composition is for 72689 years after emplacement, see Table 10)

Content of Fuel Layer by Volume (%)	$k_{eff} \pm \sigma$	$k_{eff} + 2\sigma$	AENCF (keV)	H/X Ratio	Radial Pitch (cm) / Comment ^a / Void Fraction ^b	File Name
Clay 43.4 Water 56.6	0.6812 ± 0.0009	0.6829	537.5	27.7	1 ^c	psa.43_1.o
Clay 43.4 Water 56.6	0.8473 ± 0.0010	0.8492	322.2	62.8	1.2 ^c	psa.43_1.2.o
Clay 43.4 Water 56.6	0.9411 ± 0.0010	0.9432	228.1	104.2	1.4 ^c	psa.43_1.4.o
Clay 43.4 Water 56.6	0.9639 ± 0.0009	0.9656	196.8	127.3	1.5 ^c	psa.43_1.5.o
Clay 43.4 Water 56.6	0.9759 ± 0.0010	0.9778	176.1	152.0	1.6 ^c	psa.43_1.6.o
Clay 43.4 Water 56.6	0.9787 ± 0.0010	0.9807	173.5	152.0	Previous case but earlier waste package design dimensions are used	psa.43_1.6wp.o
Clay 43.4 Water 56.6	0.9461 ± 0.0009	0.9479	176.2	152.0	1.6 ^c / Previous case but different pellet stack configuration	psa.43_1.6b.o
Clay 43.4 Water 56.6	0.9654 ± 0.0009	0.9673	177.8	152.0	1.6 ^c / case psa.43_1.6.o but 998 pellet stacks (998/1083)	psa.43_1.6ab.o
Clay 60 Water 40	0.8774 ± 0.0009	0.8791	207.3	115.9	1.6	psa.6_1.6.o
Clay 80 Water 20	0.7305 ± 0.0009	0.7322	270.1	72.9	1.6	psa.8_1.6.o
Clay 100	0.5182 ± 0.0007	0.5195	419.2	30.0	1.6	psa_1.6.o
Clay 43.4 Water 56.6	0.9399 ± 0.0009	0.9417	161.2	178.3	1.7 ^c	psa.43_1.7.o
Clay 43.4 Water 56.6	0.9659 ± 0.0009	0.9677	147.7	206.1	1.8 ^c	psa.43_1.8.o

NOTES: ^a The waste package contains cylindrical pellets with no axial gap in 1083 pellet stacks, unless noted otherwise; ratio in parentheses is the reduced number to the original number of pellets stacks.

^b Void fractions are equal to the simple average of the void fractions for a square and hexagonal unit cell; values are: 0.253, 0.481, 0.619, 0.668, 0.708, 0.741 and 0.769 for pitches of 1 cm, 1.2 cm, 1.4 cm, 1.5 cm, 1.6 cm, 1.7 cm and 1.8 cm, respectively.

^c The waste package is completely filled by fuel and post-breach clay mixture.

For the results in Table 26, an assembly's worth of TMI pellets are assumed to be completely degraded and homogeneously mixed with the post-breach clay compositions given in Tables 10 and 11. The first three cases of Table 26 are for each of the compositions given in these tables. For these cases the clay layers are dry though water fills the rest of the waste package. Clearly, there are no criticality concerns for any of these cases. The water volume fraction is increased in the next three cases, showing a slightly peak in reactivity for a 20% wvf, though k_{eff} is so small that it is of no concern. In the last case, the U-238 content of the TMI fuel is neglected for the 20% wvf case. This increases k_{eff} though its value is still too small to be of any concern.

Table 26. Degraded TMI Fuel Mixed with Post-breach Clay

Content of Fuel Layer by Volume (%)	$k_{\text{eff}} \pm \sigma$	$k_{\text{eff}} + 2\sigma$	AENCF (keV)	H/X Ratio	Comment ^a	File Name
Clay 100	0.1200 ± 0.0001	0.1202	73.4	997.5	Post-breach clay at 72689 years, see Table 10	psa.o
Clay 100	0.0890 ± 0.0001	0.0892	81.8	1020.5	Post-breach clay at 378240 years, see Table 10	psb.o
Clay 100	0.1191 ± 0.0001	0.1193	73.9	997.4	Post-breach clay at 74818 years, see Table 11	psc.o
Clay 80 Water 20	0.1264 ± 0.0001	0.1266	45.7	3610.9	Post-breach clay at 72689 years, see Table 10	psa.8.o
Clay 60 Water 40	0.1167 ± 0.0001	0.1169	33.4	7966.8	Post-breach clay at 72689 years, see Table 10	psa.6.o
Clay 43.4 Water 56.6	0.1010 ± 0.0001	0.1011	24.9	14728.1	Post-breach clay at 72689 years, see Table 10; waste package complete filled	psa.43.o
Clay 80 Water 20	0.1321 ± 0.0001	0.1323	5.6	3610.9	Case psa.8.o, but U-238 content of fuel is neglected	psa.8-U.o

6.3 SUMMARY

The results throughout Sections 6.1 and 6.2 present a large number of parametric evaluations for intact configurations and a wide range of degraded configurations for the codisposal of TMI-2 SNF. All outputs are reasonable compared to the inputs and the results of this calculation are suitable for their intended use.

7. REFERENCES

7.1 DOCUMENTS CITED

Audi, G. and Wapstra, A.H. 1995, *Atomic Mass Adjustment, Mass List for Analysis*. Upton, New York: Brookhaven National Laboratory, National Nuclear Data Center. TIC: 242718.

Beyer, W.H., ed. 1987. *CRC Standard Mathematical Tables*. 28th Edition. 3rd Printing 1988. Boca Raton, Florida: CRC Press. TIC: 240507

BSC (Bechtel SAIC Company) 2001a. *EQ6 Calculation for Chemical Degradation of Fort Saint Vrain (Th/U Carbide) Waste Packages*. CAL-EDC-MD-000011 REV 00. Las Vegas, Nevada: Bechtel SAIC Company. ACC: MOL.20010831.0300.

CRWMS M&O 1998a. *Software Qualification Report for MCNP Version 4B2, A General Monte Carlo N-Particle Transport Code*. CSCI: 30033 V4B2LV. DI: 30033-2003, Rev. 01. Las Vegas, Nevada: CRWMS M&O. ACC: MOL.19980622.0637.

CRWMS M&O 1998b. *Software Code: MCNP. V 4B2LV. HP, HPUX 9.07 and 10.20; PC, Windows 95; Sun, Solaris 2.6*. 30033 V4B2LV.

CRWMS M&O 1999a. *DOE SRS HLW Glass Chemical Composition*. BBA000000-01717-0210-00038 REV 00. Las Vegas, Nevada: CRWMS M&O. ACC: MOL.19990215.0397.

CRWMS M&O 1999b. *Generic Degradation Scenario and Configuration Analysis for DOE Codisposal Waste Package*. BBA000000-01717-0200-00071 REV 00. Las Vegas, Nevada: CRWMS M&O. ACC: MOL.19991118.0180.

CRWMS M&O 2000a. *EQ6 Calculation for Chemical Degradation of Shippingport LWBR (Th/U Oxide) Spent Nuclear Fuel Waste Packages*. CAL-EDC-MD-000008 REV 00. Las Vegas, Nevada: CRWMS M&O. ACC: MOL.20000926.0295.

CRWMS M&O 2000b. *Design Analysis for the Defense High-Level Waste Disposal Container*, ANL-DDC-ME-000001 Rev 00. Las Vegas, Nevada: CRWMS M&O. ACC: MOL.20000627.0254.

CRWMS M&O 2001. *Evaluation of Codisposal Viability for U-Metal (N-Reactor) DOE-Owned Fuel*. TDR-EDC-NU-000004 REV 00. Las Vegas, Nevada: CRWMS M&O. ACC: MOL.20010314.0004.

DOE (U.S. Department of Energy) 1999. *Design Specification. Volume 1 of Preliminary Design Specification for Department of Energy Standardized Spent Nuclear Fuel Canisters*. DOE/SNF/REP-011, Rev. 3. Washington, D.C.: U.S. Department of Energy, Office of Spent Fuel Management and Special Projects. TIC: 246602.

DOE 2002. *Criticality Scoping Analysis of a Dual Canister/Waste Package Disposal Strategy*. DOE/SNF/REP-080, Rev. 0. Idaho Falls, Idaho: U.S. Department of Energy, Idaho Operations Office. ACC: MOL.20031014.0018.

DOE 2003a. *Quality Assurance Requirements and Description*. DOE/RW-0333P, Rev. 13. Washington, D.C.: U.S. Department of Energy, Office of Civilian Radioactive Waste Management. ACC: DOC.20030422.0003.

DOE 2003b. *TMI Fuel Characteristics for Disposal Criticality Analysis*. DOE/SNF/REP-084, Rev. 0. Idaho Falls, Idaho: U.S. Department of Energy, Idaho Operations Office. ACC: MOL.20031013.0388

Parrington, J.R.; Knox, H.D.; Breneman, S.L.; Baum, E.M.; and Feiner, F. 1996. *Nuclides and Isotopes, Chart of the Nuclides*. 15th Edition. San Jose, California: General Electric Company and KAPL, Inc. TIC: 233705.

Stout, R.B. and Leider, H.R., eds. 1991. *Preliminary Waste Form Characteristics Report*. Version 1.0. Livermore, California: Lawrence Livermore National Laboratory. ACC: MOL.19940726.0118.

Taylor, W.J. 1997. "Incorporating Hanford 15 Foot (4.5 Meter) Canister into Civilian Radioactive Waste Management System (CRWMS) Baseline." Memorandum from W.J. Taylor (DOE) to J. Williams (Office of Waste Acceptance Storage and Transportation), April 2, 1997. ACC: HQP.19970609.0014.

YMP (Yucca Mountain Site Characterization Project) 2000. *Disposal Criticality Analysis Methodology Topical Report*. YMP/TR-004Q, Rev. 01. Las Vegas, Nevada: Yucca Mountain Site Characterization Office. ACC: MOL.20001214.0001.

7.2 CODES, STANDARDS, REGULATIONS, AND PROCEDURES

AP-3.12Q, Rev. 2, ICN 2. *Design Calculation and Analyses*. Washington, D.C.: U.S. Department of Energy, Office of Civilian Radioactive Waste Management. ACC: DOC.20040318.0002.

AP-3.15Q, Rev. 4, ICN 2. *Managing Technical Product Inputs*. Washington, D.C.: U.S. Department of Energy, Office of Civilian Radioactive Waste Management. ACC: DOC.20030627.0002.

ASTM (American Society for Testing and Materials) A 240/ A 240M-99b. 2000. *Standard Specification for Heat-Resisting Chromium and Chromium-Nickel Stainless Steel Plate, Sheet, and Strip for Pressure Vessels*. West Conshohocken, Pennsylvania: American Society for Testing and Materials. TIC: 248529.

ASTM A 276-91a. 1991. *Standard Specification for Stainless and Heat-Resisting Steel Bars and Shapes*. Philadelphia, Pennsylvania: American Society for Testing and Materials. TIC: 240022.

ASTM A 516/A 516M-90. 1991. *Standard Specification for Pressure Vessel Plates, Carbon Steel, for Moderate-and Lower-Temperature Service*. West Conshohocken, Pennsylvania: American Society for Testing and Materials. TIC: 240032.

ASTM G 1-90 (Reapproved 1999). 1999. *Standard Practice for Preparing, Cleaning, and Evaluating Corrosion Test Specimens*. West Conshohocken, Pennsylvania: American Society for Testing and Materials. TIC: 238771.

LP-SI.11Q-BSC, Rev.0. *Software Management*. Las Vegas, NV: BSC. ACC: DOC.20040225.0007.

7.3 SOURCE DATA

MO0003RIB00071.000. Physical and Chemical Characteristics of Alloy 22. Submittal date: 03/13/2000.

MO0003RIB00072.000. Physical and Chemical Characteristics of Steel, A 516. Submittal date: 03/13/2000.

8. ATTACHMENTS

Attachment I: One Compact Disk (CD) containing MCNP input and output files and the EXCEL spreadsheet used in the calculation process.

Attachment II: Description of file contained in Attachment I (1 page).

ATTACHMENT II

This attachment contains a listing and description of the zip file contained on the attachment CD of this calculation. The zip archive was created using WinZip 8.1. The zip file attributes are:

<u>Archive File Name</u>	<u>File Size (bytes)</u>	<u>FileDate</u>	<u>File Time</u>
TMI.zip	75,224,537	10/15/2003	12:58 PM

There are 871 total files contained in a unique directory structure. Upon file extraction, 870 MCNP input and output files along with one Excel spreadsheet will be found.